(12)

DTNSRDC/SPD-1138-01

DAVID W. TAYLOR NAVAL SHIP RESEARCH AND DEVELOPMENT CENTER

Bethesda, Maryland 20084

AD-A160 803

RO/RO-CAUSEWAY PLATFORM FACILITY OFF-LOADING PERFORMANCE IN SEA STATE 3

Charles R. Turner

APPROVED FOR PUBLIC RELEASE: DISTRIBUTION UNLIMITED

DTIC FILE COPY

DTIC ELECTE OCT 3 1 1985 S D A

Ship Performance Department

June 1985

DTNSRDC/SPD-1138-01

RO/RO-CAUSEWAY PLATFORM FACILITY OFF-LOADING PERFORMANCE IN SEA STATE 3

NDW-DTNSRDC 5602/30 (2-80)
(supersedes 3960/46)

MAJOR DTNSRDC ORGANIZATIONAL COMPONENTS

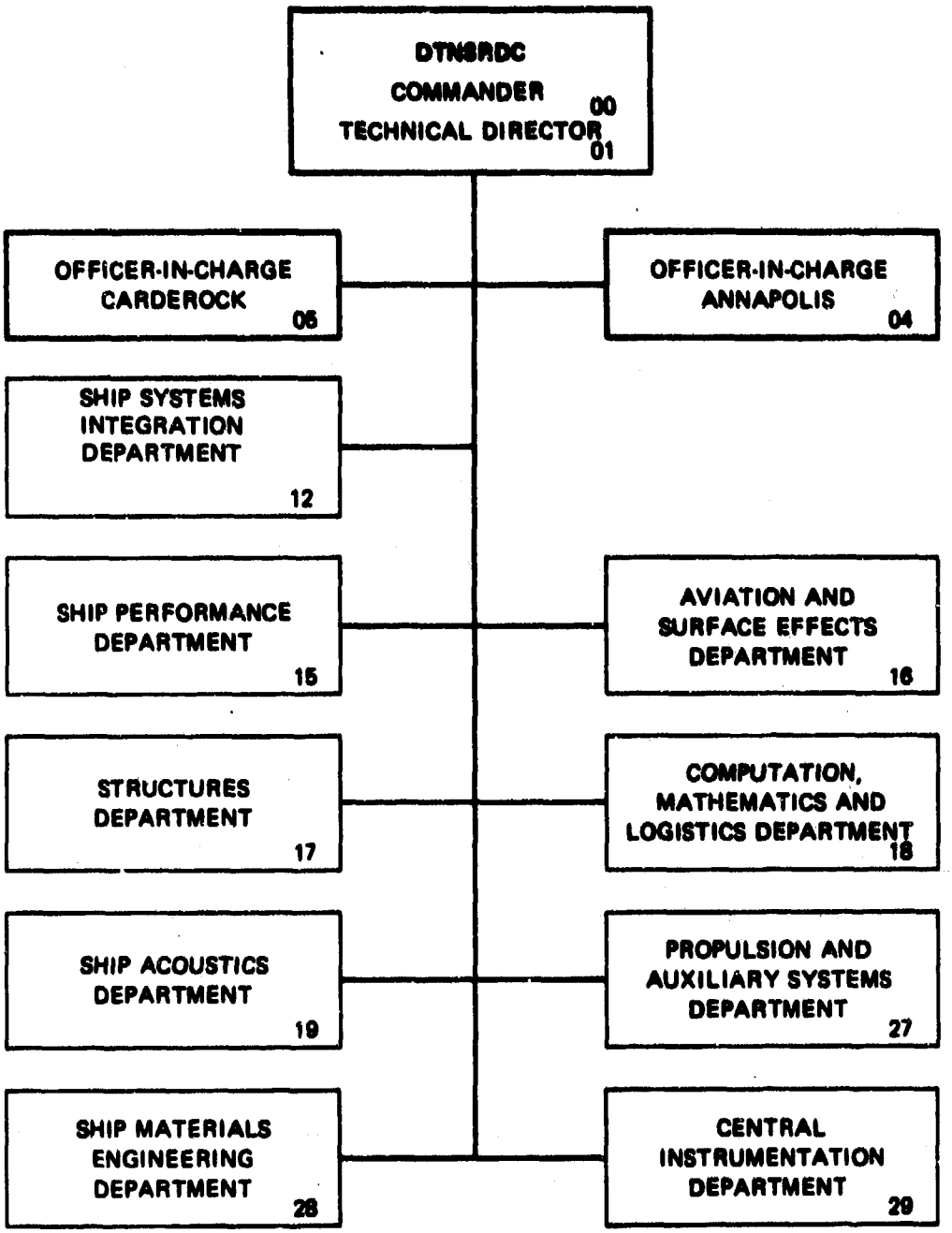

GPO 866 987

DEPARTMENT OF THE NAVY
DAVID W. TAYLOR NAVAL SHIP RESEARCH
AND DEVELOPMENT CENTER
HEADQUARTERS
BETHESDA, MARYLAND 20084

ANNAPOLIS LABORATORY
ANNAPOLIS, MD 21402
CARDEROCK LABORATORY
BETHESDA, MD 20084

IN REPLY REFER TO:
4082
1250AR
9 OCT 1985

From: Commander, David Taylor Naval Ship R&D Center

Subj: UNLOADING RO/RO SHIPS OFFSHORE, FLEET LOGISTICS READINESS TECHNOLOGY (FLRT) (SEA) PROGRAM

Encl: (1) RO/RO Discharge Facility Information Photo
(2) DTNSRDC rept SPD-1138-01 of Jun 1985

1. In 1979 the Naval Facilities Engineering Command (NAVFAC), as the Developing Activity for the Container Offloading and Transfer System (COTS) program, assigned the David W. Taylor Naval Ship R&D Center (DTNSRDC) as the Technical Manager and Test Director for the calm water Roll-On/Roll-Off (RO/RO) Discharge Facility, enclosure (1). DTNSRDC was responsible for the design, development, and testing of the Facility. The final Development and Operation Tests were highly successful and led to the completion of the Operational Evaluation (OPEVAL) in September 1983. The Facility received complete approval for Service use as a result of the successful OPEVAL and is now being procured by both the Navy and the Army.

2. An operational need exists to be able to offload (i.e., drive-off) military vehicles from all U.S. flag RO/RO vessels in up to sea state 3 conditions (3.5 - 5 ft significant wave heights). It was recognized that the technology and test experience gained in the Calm Water RO/RO Discharge Facility development would be essential and serve as a baseline to expand the operational capability of the calm water system to achieve a full sea state 3 drive-off system. The subject project will determine the feasibility and design of a system that will provide the required sea state 3 capability with minimum complexity, cost, and manpower.

3. Enclosure (2) is forwarded for your information. The model test results indicate that:

a. The causeway platform will experience little wetness during Sea State 3 operations.

b. At low wave frequencies Causeway Platform Facilities roll and pitch values are greatest and severe ship roll can occur in beam waves.

c. Ship heading control would significantly reduce roll and relative angular displacement.

Subj: UNLOADING RO/RO SHIPS OFFSHORE, FLEET LOGISTICS READINESS TECHNOLOGY (FLRT) (SEA) PROGRAM

4. Comments concerning enclosure (2) are welcome and should be forwarded to:

Commander
David W. Taylor Naval Ship R&D Center
(Code 1250, A. Rausch)
Annapolis Laboratory
Annapolis, Maryland 21402-5067
Telephone (301)267-2261, Autovon 281-2261, or FTS 980-2261

B. W. BENSON
By direction

Distribution:
MSC (M4E2a, M&X) (2)
COMNAVSEASYSTCOM (05R, 05R12, 56W21, PMS377) (4)
COMNAVFACENGCOM (032B)
NCEL (L65)
OPNAV (95, 372, 42) (3)
CMC (LME-1, LPJ, LPP, LMM) (4)
MCDEC
MTMC (TEA) (2)
USATSCH (MAJ J. Krobert)
USATCFE
USATRADOC (ATTE-R)
USATRANSCH (ATSP-CD-CS, ATSP-CD-TE) (2)
MERADCOM (DRDME-MD, DRDME-MRD) (2)
USCENTCOM MacDill AFB
MARAD (724, 743) (2)
USA DAMA-CSS
DTIC (w/o encl (1)) (12)

UNCLASSIFIED

SECURITY CLASSIFICATION OF THIS PAGE (When Data Entered)

REPORT DOCUMENTATION PAGE	READ INSTRUCTIONS BEFORE COMPLETING FORM
1. REPORT NUMBER: DTNSRDC/SPD-1138-01	2. GOVT ACCESSION NO: AD-A160803
	3. RECIPIENT'S CATALOG NUMBER
4. TITLE (and Subtitle): RO/RO-CAUSEWAY PLATFORM FACILITY OFF-LOADING PERFORMANCE IN SEA STATE 3	5. TYPE OF REPORT & PERIOD COVERED
	6. PERFORMING ORG. REPORT NUMBER
7. AUTHOR(s): Charles R. Turner	8. CONTRACT OR GRANT NUMBER(s)
9. PERFORMING ORGANIZATION NAME AND ADDRESS: David Taylor Naval Ship R&D Center, Ship Performance Department (Code 1562), Bethesda, Maryland 20084	10. PROGRAM ELEMENT, PROJECT, TASK AREA & WORK UNIT NUMBERS: Program Element 62760N, Sub Project SF 60-531, Work Unit No. 1190-400
11. CONTROLLING OFFICE NAME AND ADDRESS	12. REPORT DATE: June 1985
	13. NUMBER OF PAGES
14. MONITORING AGENCY NAME & ADDRESS(if different from Controlling Office)	15. SECURITY CLASS. (of this report): UNCLASSIFIED
	15a. DECLASSIFICATION/DOWNGRADING SCHEDULE

16. DISTRIBUTION STATEMENT (of this Report)

Unlimited Distribution

17. DISTRIBUTION STATEMENT (of the abstract entered in Block 20, if different from Report)

18. SUPPLEMENTARY NOTES

19. KEY WORDS (Continue on reverse side if necessary and identify by block number)

Causeway Platform Facility, Causeway Ferry, RO/RO Ship, Off-loading, Sea State 3, Logistics

20. ABSTRACT (Continue on reverse side if necessary and identify by block number)

Seakeeping experiments were conducted to evaluate the Sea State 3 capabilities of a roll-on/roll-off (RO/RO) ship offshore off-loading system intended for use in the logistical support of operations over beaches without developed port facilities. Two systems were tested to model the assembly and execution stages of the off-loading operation. The assembly stage consisted of a RO/RO ship to which was moored a causeway platform facility composed of six causeway sections; the latter were moored in a configuration of two connected end-to-end by

DD FORM 1 JAN 73 1473 EDITION OF 1 NOV 65 IS OBSOLETE

S/N 0102-LF-014-6601

UNCLASSIFIED

SECURITY CLASSIFICATION OF THIS PAGE (When Data Entered)

(Block 20 continued)

three abreast. The second stage modeled the complete setup used for off-loading operations. It employed, in addition to the above platform, a causeway ferry consisting of three pontoon sections in single file connected to the aft end of the platform, and a ramp installed from the ship to the platform. Measurements were made of the following in regular and random waves at several speeds and headings: i) absolute motions of the RO/RO ship, one platform section, and one section of the causeway ferry; ii) relative vertical displacement between the ship and platform, and; iii) relative angular displacements at the ramp ends and between individual causeway sections. Analysis of regular wave data yielded transfer functions of system responses. Values of significant double amplitude responses were determined from random wave data to investigate system performance in a realistic sea state. A significant result is that beam and head sea headings cause the excitation of two distinct modes of response. Specifically, angular displacements about longitudinal axes of the platform/causeway ferry system, as a group, demonstrate responses which are similar to each other, with response peaks occurring in beam seas. This is true also of angular responses about the transverse axes in head seas. In general, there is a large shift in the transfer function peaks of angular responses about the longitudinal axes from high to low encounter frequencies when the ramp and causeway ferry are added. This would tend to make the full-scale responses very sensitive to the particular frequency distribution of the wave spectral energy existing during actual off-loading operations.

Accesion For
NTIS CRA&I ☒
DTIC TAB ☐
Unannounced ☐
Justification .....
By .....
Distribution /
Availability Codes
Dist | Avail and / or Special
A-1
QUALITY INSPECTED 5

TABLE OF CONTENTS

LIST OF TABLES

LIST OF FIGURES

ABSTRACT

Seakeeping experiments were conducted to evaluate the Sea State 3 capabilities of a roll-on/roll-off (RO/RO) ship offshore off-loading system intended for use in the logistical support of operations over beaches without developed port facilities. Two systems were tested to model the assembly and execution stages of the off-loading operation. The assembly stage consisted of a RO/RO ship to which was moored a causeway platform facility composed of six causeway sections; the latter were moored in a configuration of two connected end-to-end by three abreast. The second stage modeled the complete setup used for off-loading operations. It employed, in addition to the above platform, a causeway ferry consisting of three pontoon sections in single file connected to the aft end of the platform, and a ramp installed from the ship to the platform. Measurements were made of the following in regular and random waves at several speeds and headings: i) absolute motions of the RO/RO ship, one platform section, and one section of the causeway ferry; ii) relative vertical displacement between the ship and platform, and; iii) relative angular displacements at the ramp ends and between individual causeway sections. Analysis of regular wave data yielded transfer functions of system responses. Values of significant double amplitude responses were determined from random wave data to investigate system performance in a realistic sea state. A significant result is that beam and head sea headings cause the excitation of two distinct modes of response. Specifically, angular displacements about longitudinal axes of the platform/causeway ferry system, as a group, demonstrate responses which are similar to each other, with response peaks occurring in beam seas. This is true also of angular responses about the transverse axes in head seas. In general, there is a large shift in the transfer function peaks of angular responses about the longitudinal axes from high to low encounter frequencies when the ramp and causeway ferry are added. This would tend to make the full-scale responses very sensitive to the particular frequency distribution of the wave spectral energy existing during actual off-loading operations.

PREVIOUS PAGE IS BLANK

ADMINISTRATIVE INFORMATION

The seakeeping model experiments conducted are an integral part of the Naval Sea Systems Command (NAVSEA) program to develop new technology that will enable all U.S. Flag ~~RO/RO~~ roll-on/roll-off vessels to be safely off-loaded offshore in rough seas (Sea State 3 conditions - 5 ft significant wave height). This task is an element of the Fleet Logistics Readiness Technology Program, Program Element 62760N, Sub Project SF 60-531. The Program Manager is NAVSEA 05R12. Technical program development and management were provided by the David Taylor Naval Ship Research and Development Center (DTNSRDC) Mobile Support Systems Office, Code 125, Task Area SF60531001 and Work Unit 1-1190-400.

INTRODUCTION

The offshore off-loading system currently under investigation employs standard Navy causeway sections which would be transported to the off-loading site on ships. A platform capable of supporting the lower end of an off-loading ramp would be assembled by interconnecting several causeway sections and mooring them to the ship. Vehicles would be driven from the ship onto the platform via the ramp. Self-propelled causeway ferries consisting of several other standard sections driven by a powered causeway section would then ferry the equipment from the platform to the beach.

Seakeeping dynamics of the causeway platform and the causeway ferry have been investigated previously and are documented in References 1 and 2*. The experiment described in this report was conducted in the Maneuvering and Seakeeping Facility at the David Taylor Naval Ship Research and Development Center (DTNSRDC). In this experiment, motions were measured at several headings and speeds in regular and random waves for two model configurations. The first configuration consisted of a self-sustaining RO/RO ship with the platform moored aft; the second configuration included, in addition to the above, the off-loading ramp from the ship to the platform and a causeway ferry connected to the aft end of the platform. Transfer functions from analysis of regular wave

*References are listed on page 18.

Keywords: charts; experimental data; transfer functions.

data and significant double amplitudes of the motions of the model system in random waves are presented and discussed in this report.

DESCRIPTION OF THE MODEL SYSTEM AND INERTIAL CHARACTERISTICS

The full-scale causeway sections planned for use in RO/RO off-loading operations are stock Navy items composed of standard Navy Lighter (NL) flotation cans. These watertight cans are constructed of 3/16 in. (4.76 mm) thick plate steel with internal reinforcing ribs. Standard cans (as opposed to the bow/stern modules) have planform dimensions of 5 ft by 7 ft (1.52 m by 2.13 m) and a depth of 5 ft (1.52 m). The bow/stern units are not rectangular in cross section, but have one inclined side and planform dimensions of 7 ft by 7 ft (2.13 m by 2.13 m). In the assembled barges, the inclined side faces outward toward the bow or stern to aid in movement through the water. These steel cans are bolted together along steel angle sections and may be assembled to form various sizes of causeway sections. A 3 by 15 can arrangement, which forms an individual pontoon 21 ft (6.40 m) wide by 90 ft (27.43 m) long, is used in the proposed RO/RO off-loading system.

The models used were constructed for previous experiments of 1/4 in. (6.35 mm) plywood on wooden frames to a scale of 1/15 as shown in Figure 1. No attempt was made in the construction of the models to duplicate the spaces between the individual cans since it was decided that this would not influence model motions significantly and the cost of constructing new models was far beyond the experiment's budget. The models for the standard and powered pontoons were of identical construction. Differences in mass and inertial characteristics were provided during the ballasting operation. Mass and inertial characteristics were adjusted to model the full-scale values by addition of ballast weight. By swinging each model as a compound pendulum and moving the ballast weights to change the periods of oscillation, the moments of inertia of the models were adjusted through an iterative process to correctly scaled values. For this experiment, all pontoons but one were ballasted to simulate standard unloaded causeway sections; the exception was ballasted to represent a powered causeway section. Inertial characteristics are listed in Table 1.

At a scale ratio of 15, the RO/RO ship model would have been on the order of 50 ft (15.24 m) in length. Since a model of this size did not exist at DTNSRDC and would have been prohibitively expensive to build, the largest RO/RO model available was used instead. This was a 30.6 ft (9.33 m) long RO/RO ship model with a beam of 43.9 in. (1.12 m). Even though this was smaller than ideal, it nonetheless represents (at a scale ratio of 15) a ship length of 459 ft (139.9 m), which is still a reasonable size for a ship. Nominal values for the inertial characteristics of the ship were estimated from actual stability calculation forms for a Ponce de Leon class RO/RO ship in a partially loaded condition. The model was ballasted to be dynamically similar to the 700 ft (213 m) ship at a displacement of 17,801 long tons (L-T) (18,087 tonnes) by oscillation as a bifilar pendulum and adjusting ballast weight locations to obtain the moments of inertia shown in Table 1 (i.e., radii of gyration/length and mass/length^3 ratios were the same as for the Ponce de Leon class ship).

The ramp model was constructed as a simple wooden frame, shown in Figure 2, and ballast was added to produce realistic inertial characteristics. In this case, due to the simplicity of the ramp model, the required locations of the ballast were determined analytically rather than by oscillation. Since a variety of different ramps may be used during actual off-loading operations, the length and mass of a representative specimen were used and nominal values for the moments of inertia were computed by assuming that the ramp could be approximated as a homogeneous rectangular bar of the same overall dimensions as the specimen; that is, as a rectangular prism with dimensions of 5 ft deep × 24 ft wide × 110 ft long (1.5 m × 7.3 m × 33.5 m) and a weight of 171 L-T (174 tonnes).

In full-scale off-loading operations, the causeway sections are connected to each other along their sides and ends by steel and rubber composite connectors called flexors. These flexors allow the required amount of rotational freedom while maintaining the correct spacing between sections. For this investigation, no attempt was made to model the rigidity of the flexors; ordinary door hinges were used instead.

Experiments were conducted with two model variations to investigate different phases in the RO/RO off-loading operation. The first, Configuration 1, represented the assembly phase and consisted of only the Causeway Platform

Facility (CPF) moored aft of the RO/RO model. The CPF consisted of six standard causeway sections connected two long by three abreast. A photograph of this configuration and a dimensioned sketch are shown in Figures 3 and 4, respectively. The standoff moor shown was adjusted for a full scale spacing of 40 ft (12.2 m) between the ship and CPF. This closely approximates the mooring arrangement used in off-loading a RO/RO ship with a stern type off-loading ramp (e.g. a ship such as MV CYGNUS).

The other arrangement tested, Configuration 2, included in addition to the above setup, an off-loading ramp resting on the platform and a causeway ferry consisting of 1 powered and 2 standard causeway sections. The powered causeway section was stern-connected to the CPF. A photograph of Configuration 2 and a dimensioned sketch are shown in Figures 5 and 6, respectively. The upper ramp end was hinged to the stern of the ship with the lower end resting on the CPF. Although free to slide, adequate restraint was provided by the ramp to maintain alignment of the ship and CPF for the conditions tested. The point of contact of the lower end was near the transverse junction of the CPF.

INSTRUMENTATION AND DATA COLLECTION

The system of coordinate axes chosen for the model experiment was a standard right-handed system with directions of the positive x, y, and z axes being forward, starboard, and downward, respectively. Measured quantities consisted of absolute and relative linear and angular displacements. Linear displacements were measured with ultrasonic transducers. Pitch and roll of the RO/RO ship and selected sections of the CPF and causeway ferry were measured with vertical plane gyroscopes. Relative angular displacements at hinged junctions between the causeway sections and at the ends of the off-loading ramp were measured with potentiometers. Locations of all transducers mounted on the model are shown in Figure 7. Definitions of the specific measurements and the channel abbreviations are presented in Table 2.

Ultrasonic transducers were used to measure wave height, heave of the RO/RO ship, and the relative vertical displacement between the stern of the ship and bow of the CPF. For wave height, ultrasonic transducers mounted on the towing

carriage gave a direct measurement of the distance to the water surface. Two transducers were required to measure heave of the RO/RO. One was mounted near the bow of the ship and the other near the stern. Both were aimed vertically at reflecting targets mounted on the carriage above. By specifying the geometric location of each, an algorithm in the data processing computer program combined the output of both transducers to yield heave at the center of gravity (CG) of the RO/RO ship. Relative vertical displacement between the stern of the ship and the CPF was obtained with an ultrasonic transducer attached to a boom aft of the stern of the ship and aimed toward the deck of the CPF. By a procedure analogous to that used to determine heave, the computer program in the post-test analysis accounted for heave and pitch of the RO/RO and the overhang distance of the transducer to calculate a corrected value of relative vertical displacement.

Vertical plane gyroscopes were mounted on the RO/RO ship, the center-forward causeway section of the CPF, and the section of the causeway ferry connected to the CPF. These measured the absolute angular displacements in pitch and roll of the models on which they were mounted.

Relative angle potentiometers were used to measure angular displacements between pontoon sections and at the ramp ends. Each transducer consisted of a high resolution potentiometer mounted on a bracket so that the axis of the potentiometer shaft coincided with a hinge axis. One end of a lightweight high tensile strength aluminum tube was attached perpendicularly to the potentiometer shaft and the other end was held by an elastic band against the adjacent pontoon or ramp surface. For angular measurements at longitudinal junctions of the CPF, the length of the tube was limited to 1.5 ft (0.457 m). For all other locations, the tubes were approximately 3 ft (0.914 m) long. By having a lever arm of this length, the effect on the relative angle measurement due to minor vertical play which existed in the hinges and also at the lower ramp end became insignificant. The polarity of relative angular displacement was chosen so that an angle between two adjacent surfaces which tended to form them into the shape of a V was positive.

Data collection and analysis were performed during the test with a Perkin Elmer Model 7/16 minicomputer. Pertinent statistical values and calculated results were provided after each run to yield valuable feedback for test plan optimization during the experiment. Prior to digital processing, signals from all

of the transducers were passed through 6 pole Butterworth low pass filters which provided an attenuation of 3dB at a frequency of 5 Hz. These filters prevented aliasing and eliminated high frequency noise on the data signals. Data were recorded at a sample rate of 30 samples per second for each channel and stored on magnetic tape in both digital and unfiltered analog form for future use.

OVERVIEW OF TEST PROGRAM

The model test was designed to evaluate the performance capabilities of a RO/RO ship off-loading system in a State 3 Sea. This involved conducting regular wave runs for a range of wave frequencies to determine motion transfer functions (TF's) and the frequencies causing the greatest excitation of the various system motions. Model motions were also measured in random waves to determine responses in a realistic seaway.

When waves of moderate slope are used, system responses are approximately linear. In this usage, linearity refers to conditions where the motion responses are proportional to wave amplitude or wave slope. In the linear range, nondimensional transfer functions at a given frequency are relatively invariant with small changes in wave amplitude or wave slope. Transfer functions tend to show the sensitivity of the various system responses as a function of encounter frequency, and therefore, can be used to make comparisons of system responses among various combinations of current, heading, and wave frequency.

Transfer functions are nondimensional system responses per unit wave amplitude or wave slope as a function of encounter frequency and are defined as follows:

$$\text{transfer function for angular response} = \frac{\text{amplitude of angular response}}{\text{maximum wave slope}}$$

$$\text{transfer function for displacement response} = \frac{\text{amplitude of displacement response}}{\text{wave amplitude}}$$

where:

wave amplitude = a = H/2

maximum wave slope = $\pi H/\lambda$

H = double amplitude of wave or wave height

λ = wavelength

To determine TF's in regular waves, waves of approximately sinusoidal profile were generated so that only one frequency component of excitation was present. Harmonic analyses of the data were performed to determine the amplitude and frequency of the fundamental harmonic and its ratio to the measured signal. All runs were checked to ensure that the energy content of the fundamental harmonic was a sufficiently high percentage of the total wave energy based upon the standard deviation (i.e. to make sure the waves were sufficiently sinusoidal).

Irregular waves approximating a Pierson-Moskowitz spectrum with a full scale significant wave height of 5 ft (1.52 m) and a modal period of 6.2 seconds were generated to model a realistic seaway. Conditions with swell superimposed on an irregular seaway are of practical importance and were also generated. For these, a regular wave frequency which produced a large excitation of some system component was chosen from plots of transfer functions and combined with the Pierson-Moskowitz spectrum to provide significant wave heights of about 5 ft (1.52 m). Directions of the swell and irregular waves were the same.

Run length times for random wave runs were approximately 10 minutes model scale which is equivalent to about 40 minutes full scale. This amount of data was required to ensure sufficiently high confidence in the statistical analyses. The data channels were sampled, and the values processed to obtain mean values, standard deviations (RMS about the mean), and significant double amplitudes (average of the highest one-third double amplitudes) of the system motions.

PRESENTATION AND DISCUSSION OF EXPERIMENTAL RESULTS

During the model experiments in head and quartering waves, the RO/RO ship and off-loading system were moored to the towing carriage by a steel cable attached to the bow of the RO/RO ship. This arrangement was used to simulate the anchor chain of the full scale ship to provide the most realistic motion responses possible. When being towed to simulate an offshore ocean current, the model system was free to swing and could therefore reach an equilibrium heading with respect to wave and current induced forces. The relationships between the current and wave directions and the model orientation for head and quartering waves are shown in Figures 8 and 9. For head seas, since there was symmetry of side forces from the waves, the heading of the model deviated very little from 180 degrees (head seas). In quartering waves, if the model system had remained parallel to the current, the heading with respect to the waves would have been 135 degrees. Wave forces, however, were large enough at this heading to cause the model system to swing by as much as 30 degrees from a bow into the current heading as shown in Figure 9. The heading changes decreased as current speed increased, but the effect of waves on heading was considerable; even at the highest speed tested. Except for the heave transducers, this caused no major problems with the test instrumentation. The change in heading with respect to the carriage was enough to move the ultrasonic transducers out of alignment with the overhead targets. Therefore, heave could be measured only in head seas.

Relative heading between the waves and the model in beam seas is shown in Figure 10. Based on the quartering sea results, the model system was restrained by lines to maintain the correct heading. These lines remained loose enough to have little apparent influence on the system motions.

STATIC OFFSETS

Periodically throughout the model test, zeros of the measurement transducers were checked. A record of static offsets was maintained and could be referenced to indicate and correct any unwarranted changes in the model system; e.g., a leak which may have altered the trim and draft of one of the causeway

sections. For values such as pitch and roll of the RO/RO ship and the angles at the ends of the off-loading ramp, the transducer voltage outputs were set to zero (or zeroed) as the model system lay in equilibrium in calm water. For angular measurements on the causeway sections, ballast weights were applied to level the models and the transducers were zeroed. In the case of pitch and roll of the CPF and causeway ferry, ballast was applied until the decks were level and then the outputs of the vertical plane gyros were zeroed. For relative angles between adjacent causeway sections, ballast weight was applied until the decks were coplanar and then the relative angle transducer was zeroed. When all ballast used for the zeroing procedures was removed and the system was allowed to reach equilibrium, static values of heel, trim, and relative angles were recorded. Table 3 lists values of these angles, obtained from averaging the results of several zero runs, for both model configurations. All subsequent experiments were conducted without the zeroing weights in place.

REGULAR WAVE RESULTS

Transfer functions, determined from regular wave runs, are shown in Figures 11 through 26. An attempt has been made to present these results in the most advantageous order possible for ease of study and visualization of trends. Each page has plots for all three headings tested and results for the two configurations are shown on opposing pages. Also, an attempt has been made to organize the discussion to include groups of channels which exhibit similar response trends. In general, there were two main groups — angular responses about axes parallel to the longitudinal axis (X-axis), and angular responses about axes parallel to the transverse direction (Y-axis). The first group includes roll of the RO/RO ship, CPF, and causeway ferry, and the relative angular displacements about the longitudinal axes of the CPF, designated as CPF RA1 and CPF RA2. The second group includes pitch of the RO/RO ship, CPF, and causeway ferry, and relative angular displacements about transverse axes of the CPF and causeway ferry. A detailed definition of each channel abbreviation is given in Table 2 and a sketch showing the transducer locations is shown in Figure 7.

Consider first roll transfer functions for Configuration 1. In beam seas, this TF for the RO/RO, shown in Figure 11, does not exhibit a peak, but increases steadily with wavelength (decreasing encounter frequency) to a maximum value of about 7.3 for the longest wavelength generated which was approximately equal to the length of the ship. This shows that the roll amplitude of the RO/RO ship was 7.3 times greater than the maximum wave slope at this encounter frequency. For the wavelength to wave height ratios generated (λ/H), which had nominal values of approximately 100, the maximum wave slope would be 1.8 degrees. This would give a maximum RO/RO roll amplitude of over 13 degrees for this particular wavelength and wave height. The maximum value of the RO/RO ship roll TF in bow quartering seas is only slightly less at a value of 5.8. Based on this information and also on observations made during the test, these conditions would be critical for off-loading operations.

Transfer functions for roll of the CPF and the relative angular displacements at the port and starboard junctions (CPF roll, CPF RA1, and CPF RA2, respectively) are shown in Figures 12, 13, and 14, respectively, and are quite similar to each other. In beam seas, without the ramp, each has a minor peak at an encounter frequency of 0.85 rps ($\lambda \approx 270$ ft = 82 m) and a second peak several times larger at an encounter frequency of 1.5 rps ($\lambda \approx 90$ ft = 27 m, which is the causeway section length). The maximum value of these TF's for CPF RA1 and CPF RA2 is about 1.5 times larger than for the CPF roll TF. As would be expected, the TF of the relative angular displacement was slightly larger for the starboard junction, CPF RA2, (which was on the side of the CPF toward the incoming wave) than for the port junction, CPF RA1. Magnitudes of these TF's at headings other than beam seas were small at all frequencies tested.

With the off-loading ramp installed (Configuration 2), the roll motions of all segments of the model system are coupled (i.e. the RO/RO ship and CPF interreact with each other through the ramp). For Configuration 2, there is a great deal of similarity between the TF's of roll of the RO/RO ship, roll of the CPF, CPF RA1, and CPF RA2. All of these exhibit peak values in beam seas at an encounter frequency of about 0.75 rps which corresponds to a wavelength of 360 ft (110 m). This indicates that the roll of the CPF, CPF RA1, and CPF RA2 are being driven by the roll motion of the RO/RO ship which exhibits response peaks in roll near this frequency for both configurations. The maximum value for the

roll TF of the RO/RO ship is reduced by a considerable amount with the ramp in place. The other TF's for angular motions of the CPF are reduced slightly.

The pitch TF of the RO/RO ship is shown in Figure 15. With maximum values of 0.5 in quartering waves and 0.8 in head waves, pitch motions of the ship will be minor. Presence of the ramp results in no significant change in pitch of the RO/RO.

Transfer functions for pitch of the CPF and for the relative angular displacement at the transverse junction of the CPF (CPF RA3) are very similar to each other as shown in Figures 16 and 17. Both demonstrate peaks at the same values of encounter frequency for the same headings, although the magnitude of the TF for CPF RA3 is about 1.5 times larger than for pitch of the CPF.

The transfer function for relative vertical displacement (RVD) between the ship and CPF is shown in Figure 18. In beam seas, this TF demonstrates the same trends with respect to frequency as does the roll TF of the CPF in beam seas for Configuration 1 (Figure 12A), although the magnitude of the RVD TF is much smaller. For Configuration 1, the TF for RVD at the beam sea heading reaches a peak value of 1.0 at a wavelength of 90 ft (27 m). With the ramp installed (Configuration 2), the peak still occurs at the same wavelength, but its magnitude is increased to 1.35. In head and quartering waves, the TF for RVD bears little resemblance to any of the other transfer functions. This is reasonable since the RVD is a combination of many other motions. Maximum values of this TF in head and quartering waves without the ramp installed (Configuration 1) are approximately 2.75. For Configuration 2, the maximum value is decreased to 2.0 in quartering waves, while in head seas, there is no appreciable decrease in magnitude due to presence of the ramp.

The heave transfer function for the RO/RO ship is shown in Figure 19 for head seas only. The maximum value is approximately 0.6 and there are no significant differences between the two configurations.

For all practical purposes, the roll transfer function of the causeway ferry, shown in Figure 20, is identical to the roll TF of the CPF in Configuration 2 (cf. Figure 12B). This is due to the fact that the CPF and causeway ferry were constrained against relative angular displacements about the longitudinal axis by the hinged connection (which had a transverse axis) between them.

Pitch responses for the causeway ferry, shown in Figure 21, are very similar to those of the CPF. At all headings, the response peaks of pitch for the causeway ferry and CPF when the ramp is installed (Configuration 2) occur near the same frequencies. In quartering waves, the magnitudes of the response peaks are approximately equal. In head seas, the magnitude of the peak is slightly higher for the pitch TF of the causeway ferry than for that of the CPF.

Transfer functions for the relative angular displacements at the junctions of the causeway ferry are shown in Figures 22, 23, and 24. All are very similar to one another and to the TF's of CPF pitch and CPF RA3. In quartering waves, all three exhibit peaks at frequencies of encounter slightly greater than 1.0 rps which corresponds to a wavelength approximately twice the causeway section length. For head sea conditions the peaks occur at encounter frequencies near 0.9 rps ($\lambda \approx 270$ ft ≈ 82 m). Relative angular responses of the causeway ferry in quartering seas are close in magnitude to those of CPF RA3 throughout the range of frequencies tested. In head seas, the magnitudes are slightly greater than for CPF RA3.

Relative angular displacement TF's at the ends of the ramp are shown in Figures 25 and 26. At the upper end of the ramp, this TF increases steadily with wavelength to a maximum of about 2.9 in head seas at an encounter frequency of 0.75 rps ($\lambda \approx 359$ ft ≈ 110 m). The TF for relative angle at the bottom end of the ramp is much lower with maximum values of about 0.9 and 1.5 for quartering and head waves respectively.

RANDOM WAVE RESULTS WITHOUT SWELL SUPERIMPOSED

Random long-crested waves with energy distributed over a wide range of frequencies were generated to model a realistic sea state. An approximation of a Pierson-Moskowitz spectrum with a full scale significant wave height ($\overline{H}_{1/3}$) of 5 ft (1.52 m) and a modal period of 6.2 seconds was generated. This approximates a Sea State 3 (SS3) condition and a typical example of the spectral energy distribution is shown in Figure 27. The actual spectra obtained, however, vary somewhat from run to run. Data presented in this section are significant values (average of the highest one-third double amplitudes) of the measured responses.

All data have been normalized by multiplying by the ratio of the nominal significant wave height 5 ft (1.52 m) to the significant wave height actually obtained.

As shown in Figure 28, the significant roll of the RO/RO ship actually increased slightly with the ramp installed (Configuration 2). At a heading of 90 degrees, the significant roll was about 3.6 degrees for Configuration 1 and 5.3 degrees for Configuration 2. This can be explained by studying the roll transfer function of the RO/RO ship in figure 11 and considering the wave energy distribution shown in Figure 27. Peak wave energy occurred at frequencies of about 1.1 rps. Although the peak of the roll TF of the RO/RO ship is diminished with the ramp in place, the new peak shifted toward higher frequencies at which a higher percentage of the total energy existed in the irregular wave spectrum. For Configuration 2, the sensitivity of the roll of the RO/RO ship is actually increased at the frequencies at which most of the energy existed in the State 3 Seas generated during the test.

Conversely, significant values of roll of the CPF, CPF RA1, and CPF RA2, shown in Figures 29, 30, and 31, are decreased for Configuration 2 in beam seas where these responses are more pronounced. This is explained by the fact that addition of the ramp shifts the response peaks of these motions to lower wave frequencies (as can be seen in Figures 12 through 14) where a lower percentage of the total energy was present during the SS3 conditions. Significant angular response for CPF RA2 (the starboard longitudinal junction), which was on the side facing the incoming waves, was considerably larger than for CPF RA1 (the port longitudinal junction) -- especially for Configuration 2.

Significant pitch of the RO/RO ship, shown in Figure 32, is essentially constant for all combinations of speed and heading for both configurations. Reasons why pitch in beam seas is as large as at the other two headings are not apparent, but may be due to coupling of pitch with roll through heave. In any case, pitch motions of the RO/RO ship are small and should cause no problems.

Significant values of pitch of the CPF and relative angular displacements at the transverse junction of the CPF (CPF RA3) are shown in Figures 33 and 34. Both of these exhibit similar trends although significant values of CPF RA3 are somewhat larger than those of pitch. This result is consistent with the TF's

for these two motions as can be seen in Figures 16 and 17. Also, presence of the ramp tends to increase the significant values of both of these, with a larger change for CPF RA3.

Relative vertical displacement between the RO/RO ship and the CPF (RVD) for Configuration 2 shows only a slight increase in quartering seas over the results for Configuration 1, as indicated in Figure 35. Considering trends with respect to heading, there is a close resemblance between significant values of RVD and pitch of the CPF. Although it is not obvious from studying the TF's, this indicates that a predominant factor influencing RVD is pitch of the CPF.

Significant heave of the RO/RO ship is shown in Figure 36 for head seas only. There is inconsequential change due either to speed or presence of the ramp, and with significant values of less than 1.0 ft (0.30 m), there should be no problems due to this motion in SS3. Visual observations made during the test indicate this to be true at the other headings as well.

Significant roll of the causeway ferry, shown in Figure 37, is almost identical to significant roll of the CPF. A maximum value of 5.3 degrees occurs in beam seas. Any difference between roll values of the CPF and causeway ferry is due to torsional flexing of the models. Since no attempt was made to scale the torsional stiffness of the models or their connectors, these differences in roll cannot be applied to indicate full scale behavior.

Significant values of pitch of the causeway ferry and relative angular displacements at its junctions are shown in Figures 38 through 41. Trends were similar for all of these motions. All show the same changes with respect to heading, but relative angular motions at the junctions are about 1.5 times larger than the pitch of the causeway ferry. Significant responses of pitch of the CPF and causeway ferry are almost identical, as are the values of the significant relative angular motions at the causeway ferry junctions and CPF RA3.

Figures 42 and 43 show the significant relative angular motions at the upper and lower ramp ends, respectively. Significant angular response at the upper end is fairly low with a maximum value of 2.7 degrees in quartering seas, and varies only slightly with heading. At the lower end, the significant values of angular displacement are almost identical to significant pitch of the CPF, and have magnitudes approximately twice as large as the relative angles measured at the ramp's upper end.

SUMMARY AND CONCLUSIONS

Experiments were conducted in regular and random waves to investigate the Sea State 3 operational capabilities of a RO/RO ship off-loading system intended for use in support of operations where no port facilities exist. A Causeway Platform Facility (CPF) consisting of six causeway sections connected in two rows by three abreast was moored aft of the stern of a RO/RO ship model. This entire system was towed by a line from the ship's bow to simulate anchorage in a current. Current speeds of 0, 2, and 4 knots were evaluated in head, quartering, and beam waves for two different configurations. The first configuration consisted of the RO/RO ship with only the CPF moored aft. The second included, in addition to the CPF, an off-loading ramp from the ship to the CPF and a causeway ferry composed of three causeway sections connected in single file aft of the CPF.

Regular wave conditions were generated to define the nondimensional transfer functions (TF's) of the various system responses and the wave frequencies causing the greatest excitations. In general, angular displacements of the CPF/causeway ferry system about parallel axes exhibit quite similar response trends. There are two groups of parallel axes which consist of the axes parallel to the X-coordinate axis and those parallel to the Y-coordinate axis. The group of motions about axes parallel to the X-axis (the longitudinal group) is comprised of CPF RA1, CPF RA2, and roll of the RO/RO ship, CPF, and causeway ferry. The other group of motions, about axes parallel to the Y-axis (the transverse group), is comprised of CPF RA3, relative angular displacements about the junctions of the causeway ferry, and pitch of the RO/RO ship, CPF, and causeway ferry. Since the CPF and causeway ferry are constrained against relative angular displacements about the longitudinal axis, their roll transfer functions are forced to be similar. As would be expected, the largest excitation of angular responses about the longitudinal axes occurs in beam waves, but a more significant trend is the shift in the peaks of the corresponding TF's at this heading from approximately 1.5 rps to 0.75 rps when the causeway ferry and off-loading ramp are installed. Likewise, TF's of angular responses about transverse axes exhibit similar trends, but are not significantly influenced by the presence of the off-loading ramp. The greatest excitation to responses

about the transverse axes occurs in head and quartering waves, with TF's for both of these headings being approximately equal. The Relative Vertical Displacement (RVD) TF demonstrates characteristics which bear the closest similarity to that mode of angular motion which is being excited the most at the corresponding heading.

In random waves, it was observed that significant values of the motions of all components of the model system depend to a large extent on how the addition of the ramp and causeway ferry shifts the peaks of the TF's with respect to the frequency of peak energy (modal frequency) of the irregular wave spectrum. Since the TF's of angular responses about longitudinal axes were decreased at the modal frequency (approximately 1.1 rps) by adding the ramp and causeway ferry, the motions about these axes of the CPF were decreased considerably (as can be seen in Figures 29, 30, and 31) in beam seas. Although quite low in both head and quartering waves, there was little change in the significant values of the angular responses about longitudinal axes due to the presence of the ramp and causeway ferry (Configuration 2). Significant values of the angular responses about transverse axes were generally quite low in beam waves and reached a peak at the quartering sea heading as is shown in Figures 33, 34, and 38 through 43. Presence of the ramp and causeway ferry caused only minor changes in the TF's of the motions about the transverse axes, and likewise, there was essentially no difference in the significant values for the two model configurations. RVD, which is a very important motion, was lowest in beam waves. So, for heading changes from head to beam in Sea State 3 conditions, RVD and angular displacements about transverse axes decrease while angular motions about longitudinal axes increase. Magnitudes of the angular displacements about longitudinal axes are, in general, considerably larger than those about transverse axes. Determination of which motions affect the off-loading operations least adversely will help determine the best heading (e.g., whether pitch or roll motions present the greater difficulty to progression of vehicles down the causeway ferry, or whether pitch or relative roll causes the greater difficulty in docking the causeway ferry to the CPF). The actual seaway and its modal frequency will also influence the ratios of the motion magnitudes in the two response groups.

Results of swell superimposed on an irregular seaway are presented in Appendix A. These results are very specialized because adding swell is

equivalent to increasing the energy at one specific frequency. Here, specialized refers to the fact that each irregular wave/swell combination is unique and results would, therefore, be applicable only to that specific condition. Variation of the ratio of swell energy to the total spectral energy allows the generation of an unlimited number of unique seaways. Chances of ever encountering a specific condition again in full-scale operations are small. TF's, for example, can be used in theory to determine any responses in the linear range if the wave spectrum is known. The resultant shift in energy with respect to the peaks of the TF's will determine the effects on the individual motions. For example, if the frequency of the swell is near a peak in the TF for a specific motion (i.e., near a resonance point), the resultant increase in excitation to that motion will be large. Alternatively, if the swell is at a frequency where the TF for a specific motion is small, the resultant increase in excitation to that motion will be proportionately lower. Therefore, the specific spectral energy distribution for each test condition is presented since it is imperative to know the actual seaway for which the results were measured.

Except for a few isolated occurrences, the decks of the causeway sections experienced very little wetness. At low wave frequencies, severe roll of the RO/RO ship was excited which could cause problems (i.e., roll amplitudes of about 7.5 degrees per degree of maximum wave slope for regular wave frequencies of 0.65 rps). It appears as if roll and relative angles at the longitudinal junctions may be the limiting factors. Use of multipoint moorings or other means of heading control would have advantages. For instance, if roll posed the greatest threat to safe passage of vehicles, the ramp could be lowered in beam waves where RVD is lowest and then the entire system could be rotated to a head sea heading where roll and the significant longitudinal angular displacements are lower.

REFERENCES

1. Zarnick, E., C. Turner, and J. Hoyt, "Model Experiments of RO/RO Ships Off-Loading System in Waves and Current", Report DTNSRDC/SPD-1046-01 (Dec 1982).

2. Turner, C.R., "Zero Speed Seakeeping Characteristics of a Causeway Ferry Consisting of Four Pontoons Connected End-to-End", Report DTNSRDC/SPD-1075-01 (Jun 1983).

APPENDIX A

RANDOM WAVE RESULTS WITH SWELL SUPERIMPOSED

Since off-loading conditions with swell superimposed are of practical importance, they were a requested part of the test plan. Results of the experiments for these conditions have been placed in this Appendix because many of the motion responses are essentially identical to the SS3 results presented previously. Only those plots which show a notable difference will be discussed.

When considering these results, there are several important facts which must be remembered. First, superimposing a swell frequency amounts only to adding more energy to the spectrum at that frequency. Therefore, the modal period of the nominal SS3 Pierson-Moskowitz spectrum is shifted. Depending on how this alters the frequency distribution of energy with respect to the peaks of the transfer functions will determine the effect on the various motions. Some responses increase while others are reduced. Also, results of testing in this type of seaway are extremely specific, i.e., since there are an infinite number of unique spectra obtainable by superimposing varying amounts of energy at one swell frequency, there are an infinite number of unique results possible. For this reason, the plots of spectral energy distribution are included for each different wave spectrum generated. These are shown in Figures A.1, A.2, and A.3 for swell frequencies of 0.865, 1.060, and 1.498 rps, full scale. The headings and ramp configurations with which the various spectra were used are listed in Table A.1.

The superimposed swell frequencies were selected to be the frequencies at which large motion responses occurred in regular waves in some critical mode of motion (such as RVD). The modal period of the SS3 Pierson-Moskowitz spectrum is near 6.0 seconds which corresponds to a wave frequency of 1.05 rps. Considering Figure 27, the swell frequencies were chosen to add energy to the seaway such that the modal period of the wave spectrum was shifted toward frequencies at which peak values occur in the RVD TF's. For example, in beam seas, the peaks of the TF's for RVD were near frequencies of 1.5 rps which is the frequency chosen for the superimposed swell. In all cases, the significant wave height for these modified sea states was adjusted to be approximately 5 ft (1.52 m).

Significant pitch of the RO/RO, shown in Figure A.8, is not changed by the addition of the swell component (compared to the SS3 results in Figure 32) except in bow quartering seas at zero speed with the ramp and causeway ferry connected (Configuration 2). The reasons for this are not apparent. Although the swell added energy which shifted the wave spectral energy toward frequencies at which larger values occurred in the TF for pitch of the RO/RO ship, this was also true for the same configuration in head seas, but no change occurred for the latter.

Significant pitch of the CPF, relative angular displacement at the transverse junction of the CPF (CPF RA3), and relative vertical displacement, shown in Figures A.9 to A.11, increased with addition of swell in head and quartering seas. This result corresponds to a shift in the wave spectral energy toward higher values of the corresponding TF's, and indicates the relationship of pitch of the CPF to RVD and CPF RA3. There is also a similar increase in pitch of the causeway ferry and relative angular displacements at its junctions — especially in quartering seas.

TABLE 1 - FULL-SCALE CHARACTERISTICS		
RO/RO Ship - Partially Loaded		
Length Overall (LOA)	459.0 ft	139.9 m
Length Between Perpendiculars (LBP)	434.7 ft	132.5 m
Breadth Molded	54.8 ft	16.7 m
Displacement	5070.0 L-T	5151.4 tonnes
Longitudinal Center of Gravity (LCG) (Aft of Forward Perpendicular)	224.5 ft	68.4 m
Vertical Center of Gravity (VCG) (Above Baseline)	19.3 ft	5.9 m
Pitch Radius of Gyration (R_{yy})	0.249 × LOA	
Roll Radius of Gyration (R_{xx})	0.347 × Beam	

TABLE 1 (Continued)

3 × 15 Causeway Section		
	Standard	Powered
Length Overall (LOA)	90.0 ft 27.4 m	90.0 ft 27.4 m
Beam	21.0 ft 6.4 m	21.0 ft 6.4 m
Mean Draft[1]	1.25 ft 0.38 m	1.65 ft 0.50 m
Displacement	129,870 lb 58,908 kg	179,820 lb 81,565 kg
Trim[1]	0.0 deg	1.6 deg
Longitudinal Center of Gravity (LCG)[2]	45.0 ft 13.7 m	54.5 ft 16.6 m
Transverse Center of Gravity[3]	0.0 ft	0.0 ft
Vertical Center of Gravity (VCG)[4]	2.5 ft 0.76 m	2.6 ft 0.79 m
Pitch Radius of Gyration (R_{yy})	0.267 × LOA	0.282 × LOA
Roll Radius of Gyration (R_{xx})	0.325 × Beam	0.334 × Beam

1 - Calculated
2 - Measured from the causeway section bow
3 - Measured from the causeway section centerline
4 - Measured from the causeway section baseline

TABLE 2 - CHANNEL ABBREVIATIONS

ABBREVIATION	DESCRIPTION
RVD	Relative vertical displacement between the stern of the RO/RO Ship and the bow of the center-forward CPF section
CPF ROLL	Roll of the center-forward section of the CPF
CPF PITCH	Pitch of the center-forward section of the CPF
CPF RA1	Relative angle at the port longitudinal junction of the CPF
CPF RA2	Relative angle at the starboard longitudinal junction of the CPF
CPF RA3	Relative angle at the transverse junction of the CPF
CF ROLL	Roll of the first (powered) section of the causeway ferry
CF PITCH	Pitch of the first (powered) section of the causeway ferry
CF RA1	Relative angle at the junction between the CPF and first (powered) section of the causeway ferry
CF RA2	Relative angle at the junction between the first and second sections of the causeway ferry
CF RA3	Relative angle at the junction between the second and third sections of the causeway ferry
RAMP RA1	Relative angle between the off-loading ramp and the RO/RO Ship
RAMP RA2	Relative angle between the off-loading ramp and the center-forward CPF section

TABLE 3 - STATIC OFFSETS*

CHANNEL	CONFIGURATION 1 - Without Ramp and Causeway Ferry	CONFIGURATION 2 - With Ramp and Causeway Ferry
CPF ROLL	0.03 deg	-0.26 deg
CPF PITCH	0.05 deg	0.66 deg
CPF RA1	-0.05 deg	3.20 deg
CPF RA2	0.98 deg	3.30 deg
CPF RA3	0.39 deg	1.60 deg
CF ROLL		0.10 deg
CF PITCH		-0.25 deg
CF RA1		-1.02 deg
CF RA2		-0.07 deg
CF RA3		-0.17 deg

*For Roll and Pitch - Positive angular displacements are defined by the right-hand rule in the coordinate system described on page 5. Relative angular displacements are positive which form adjacent sections into the shape of a V.

	MODEL SCALE	FULL SCALE
Length:	6.0 ft (1.83 m)	90.0 ft (27.43 m)
Beam :	1.4 ft (0.43 m)	21.0 ft (6.40 m)
Depth :	4.0 in. (0.10 m)	5.0 ft (1.52 m)

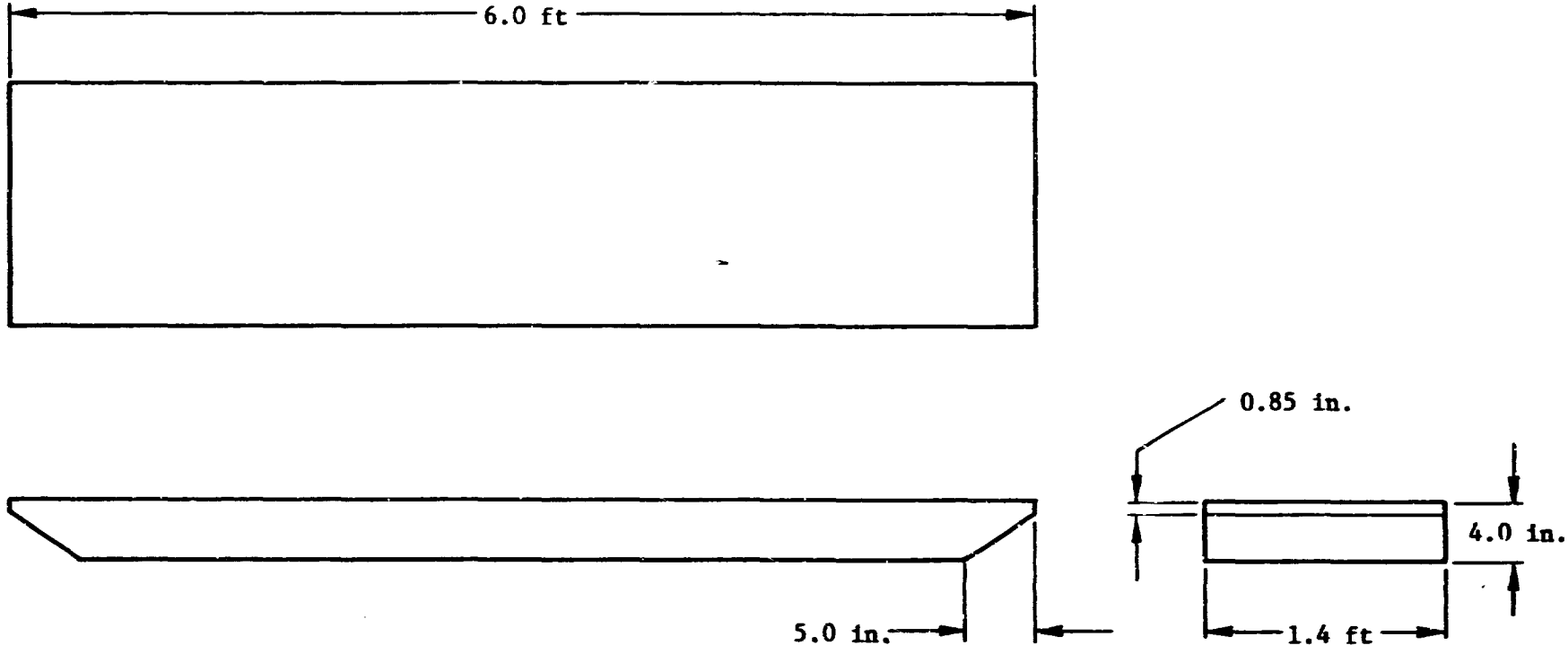

Figure 1 - Dimensions of a Causeway Section Model

	MODEL SCALE	FULL SCALE
Length:	88.0 in. (2.24 m)	110.0 ft (33.5 m)
Width :	22.4 in. (0.57 m)	28.0 ft (8.5 m)
Weight:	113.5 lb (51.5 kg)	171 L-T (173.7 tonnes)
Longitudinal Radius of Gyration	2.12 ft (0.65 m)	31.8 ft (9.7 m)

Scale Ratio 1/15

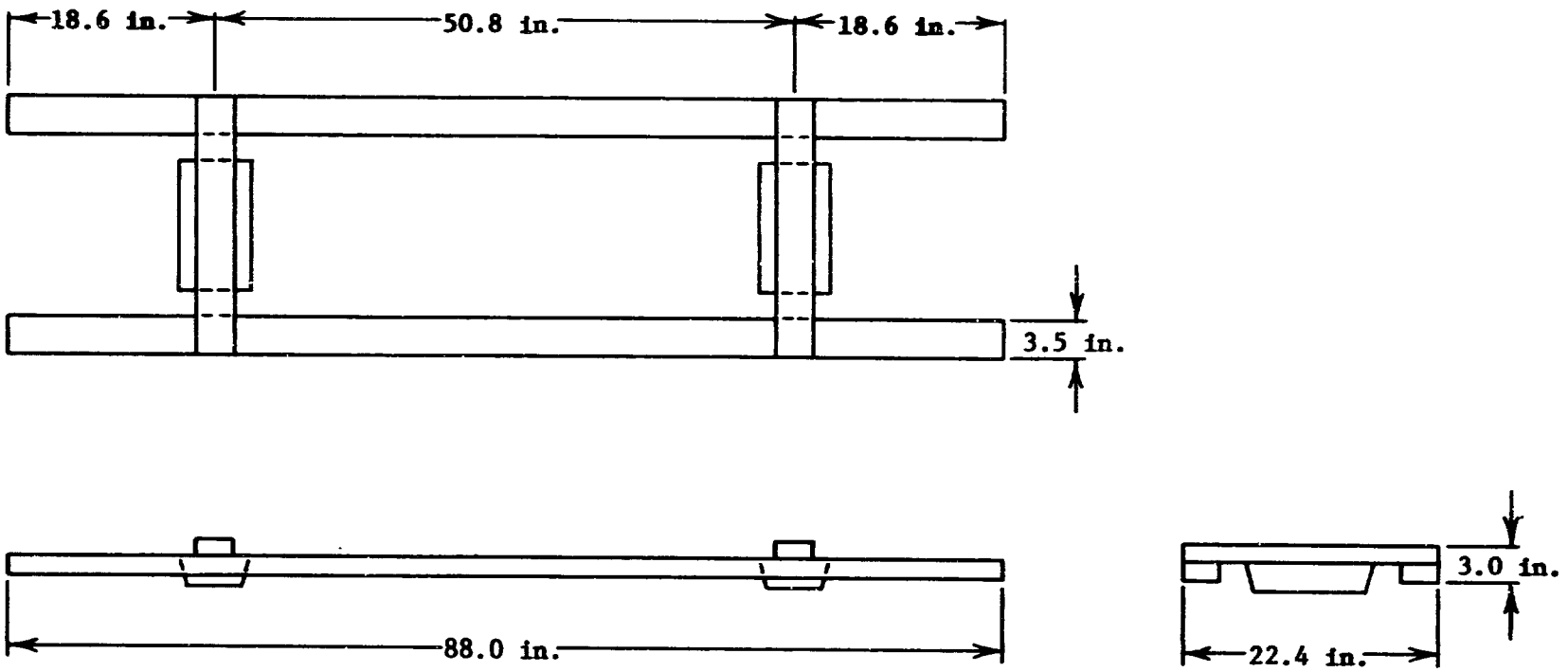

Figure 2 - Dimensions of the Off-loading Ramp

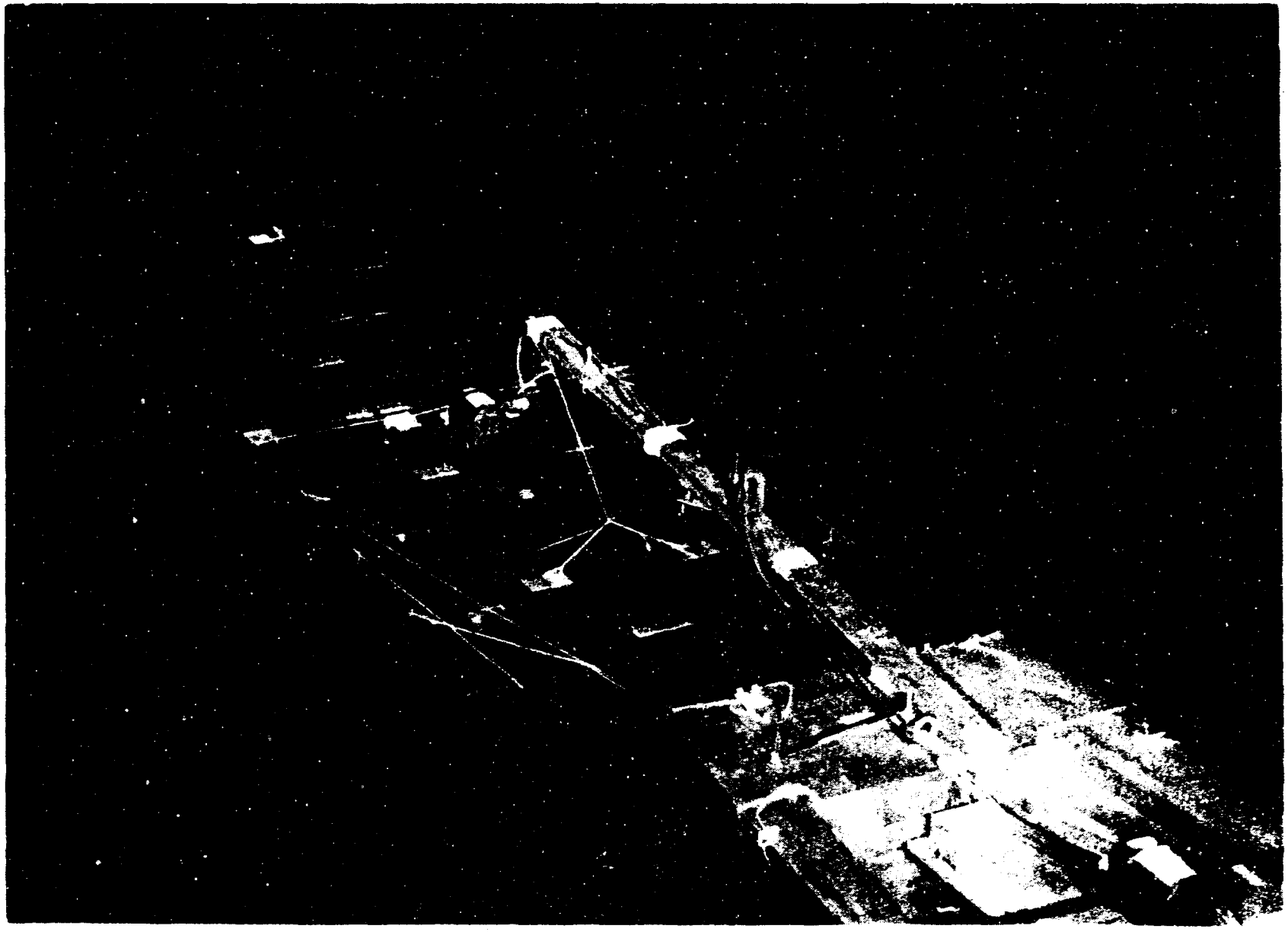

Figure 3 - Photograph of Configuration 1

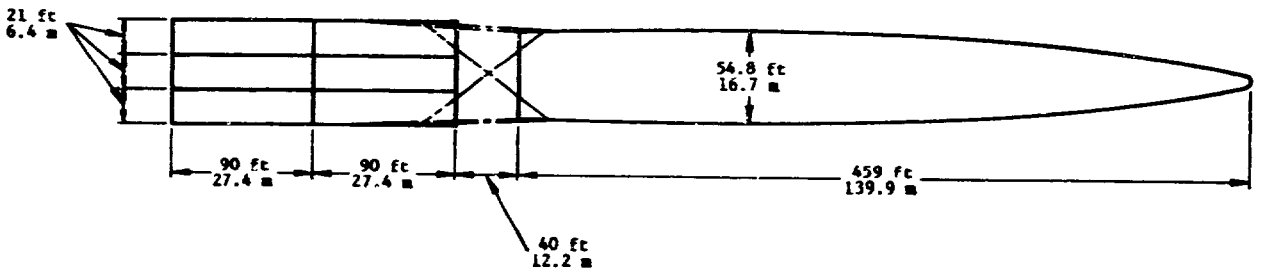

Figure 4 - Dimensioned Plan View of Configuration 1

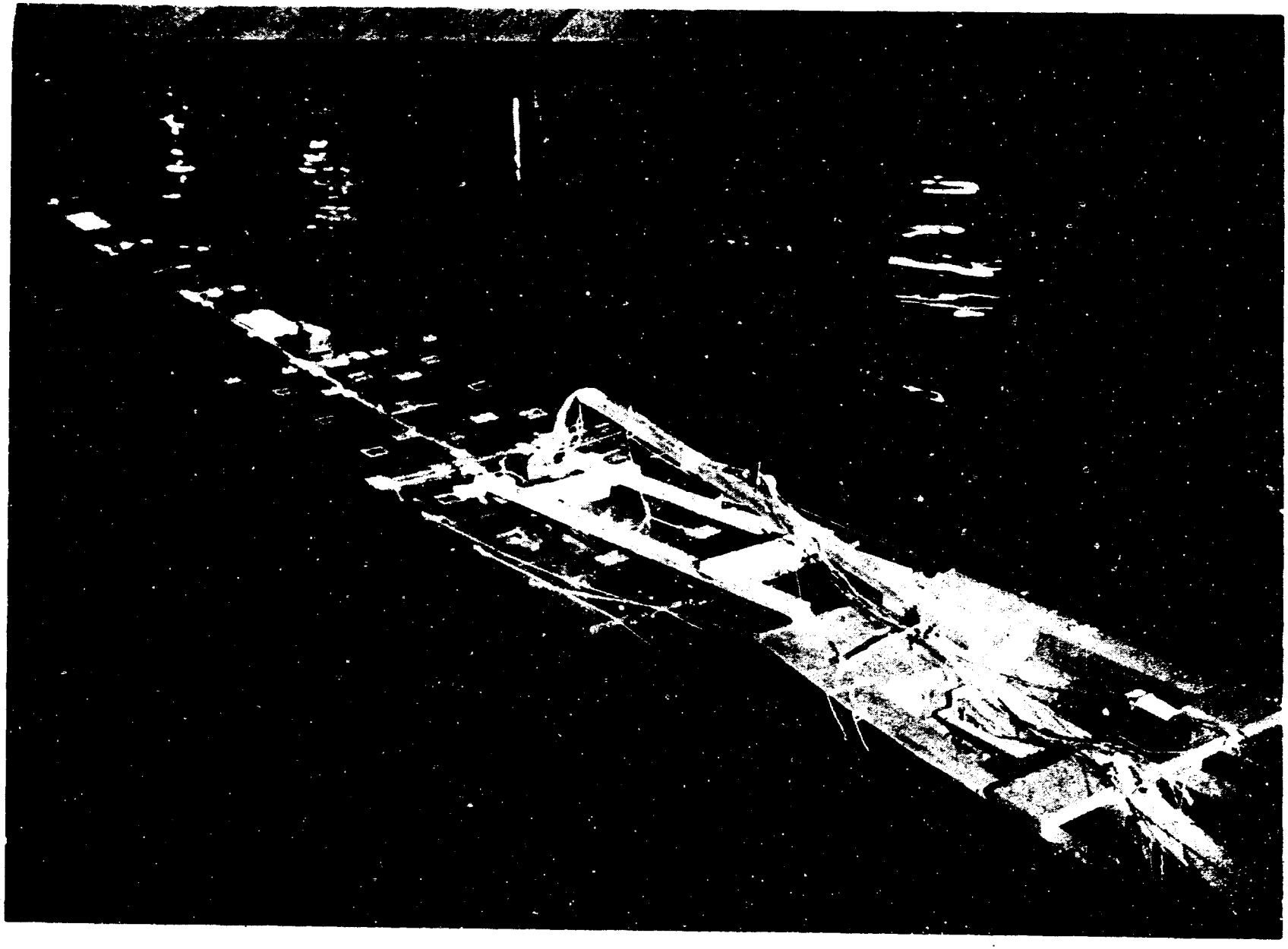

Figure 5 - Photograph of Configuration 2

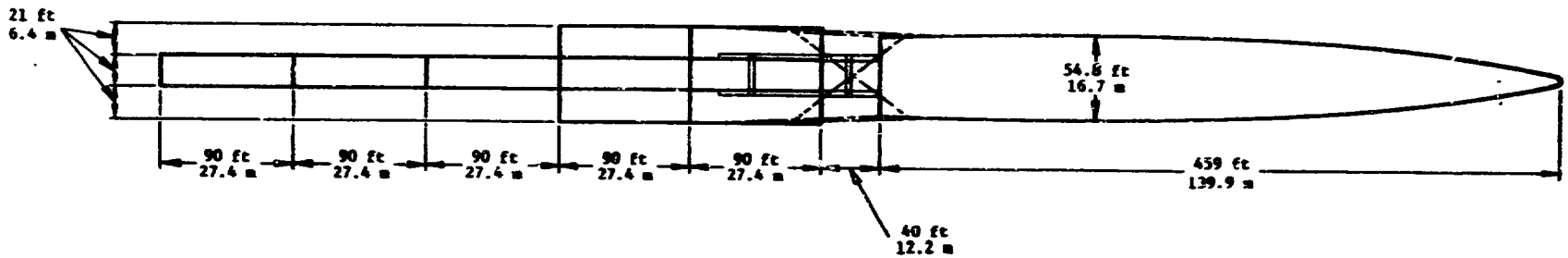

Figure 6 - Dimensioned Plan View of Configuration 2

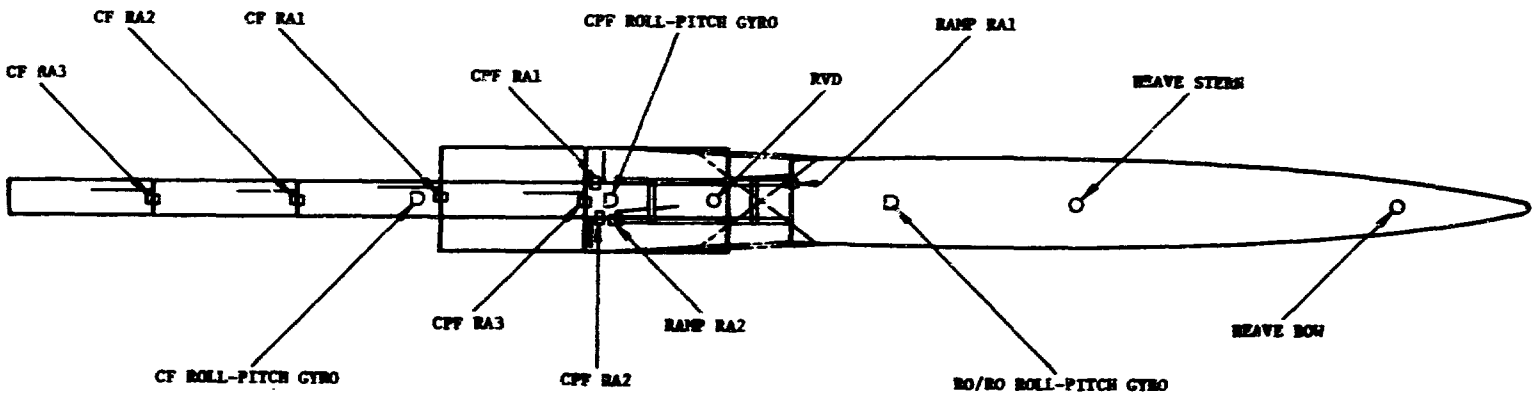

Figure 7 - Transducer Locations

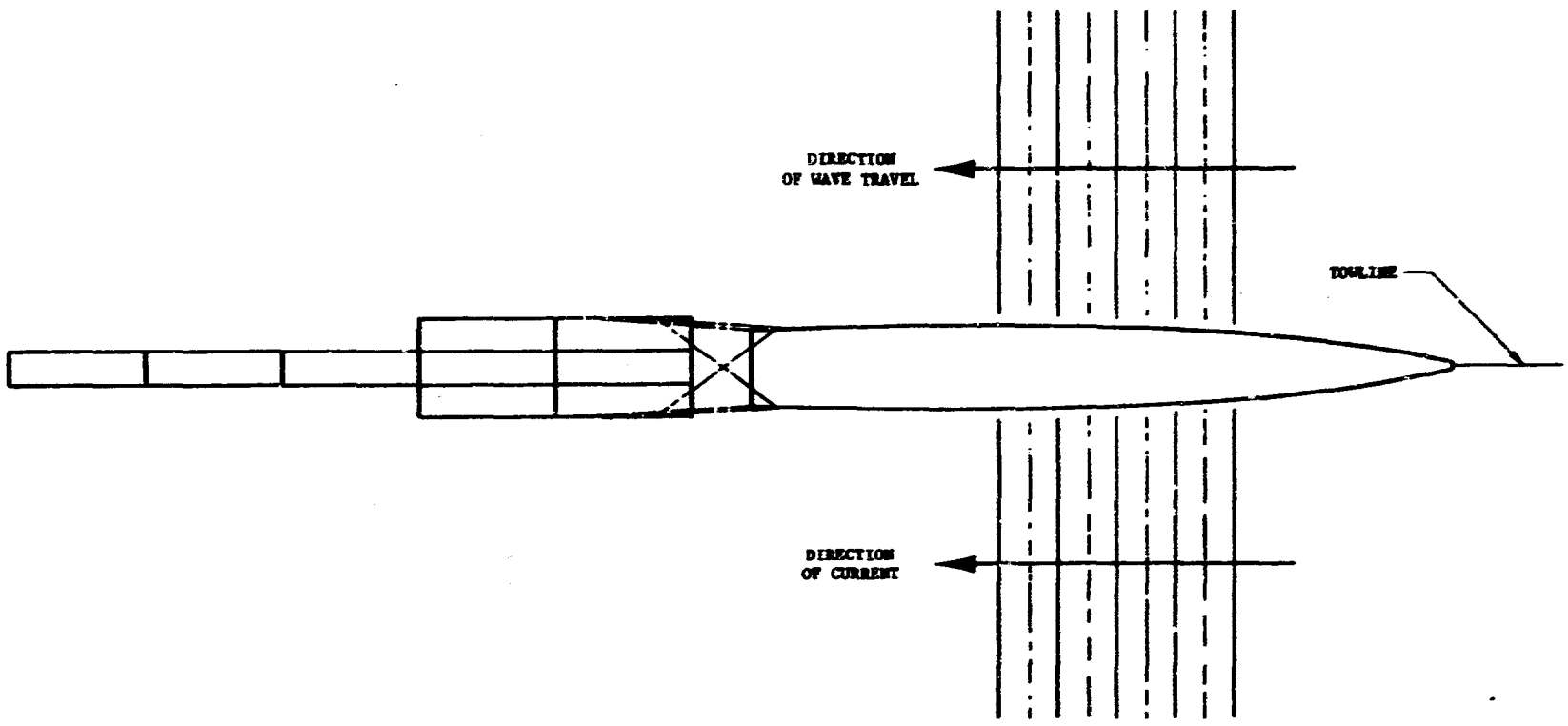

Figure 8 - Model Orientation in Head Waves

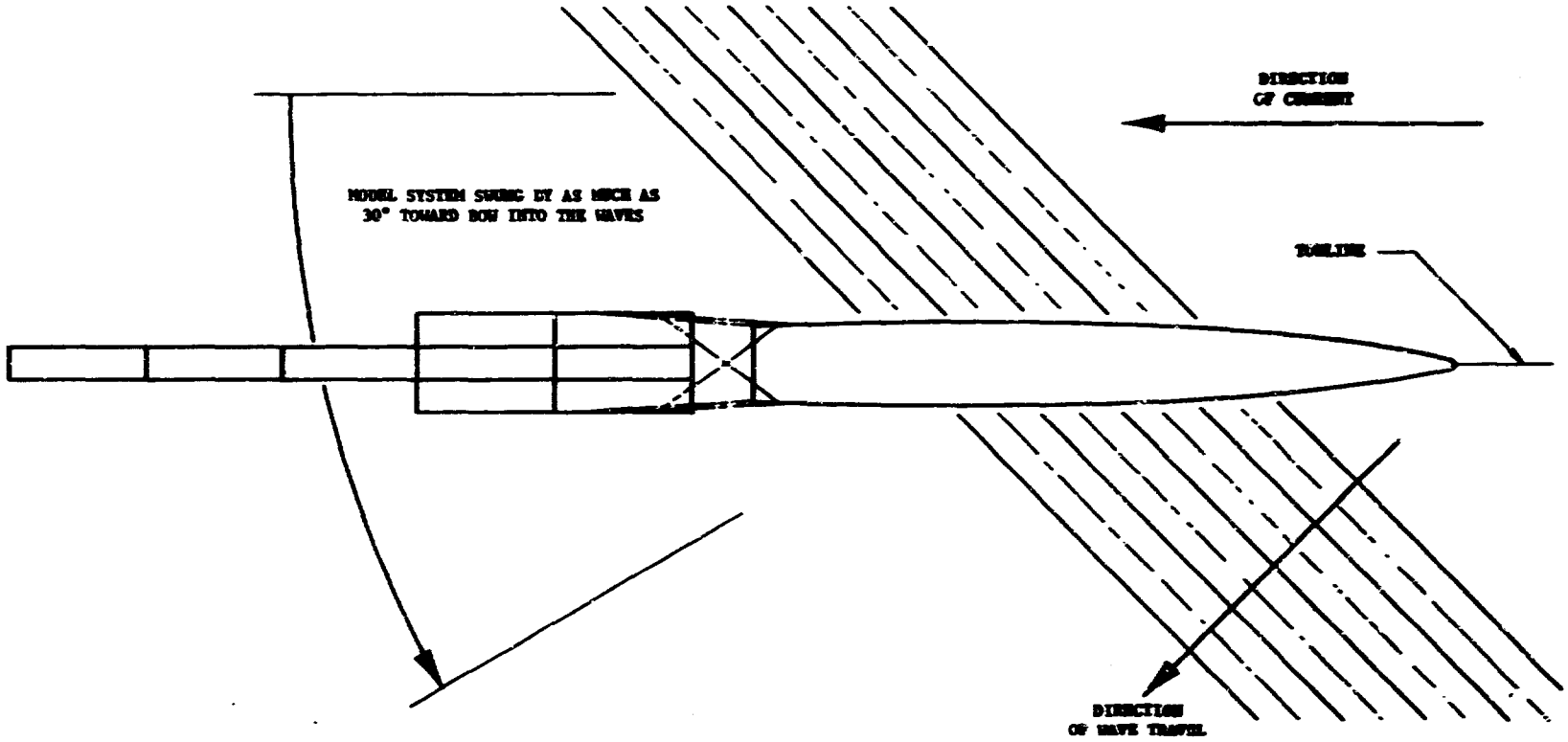

Figure 9 - Model Orientation in Quartering Waves

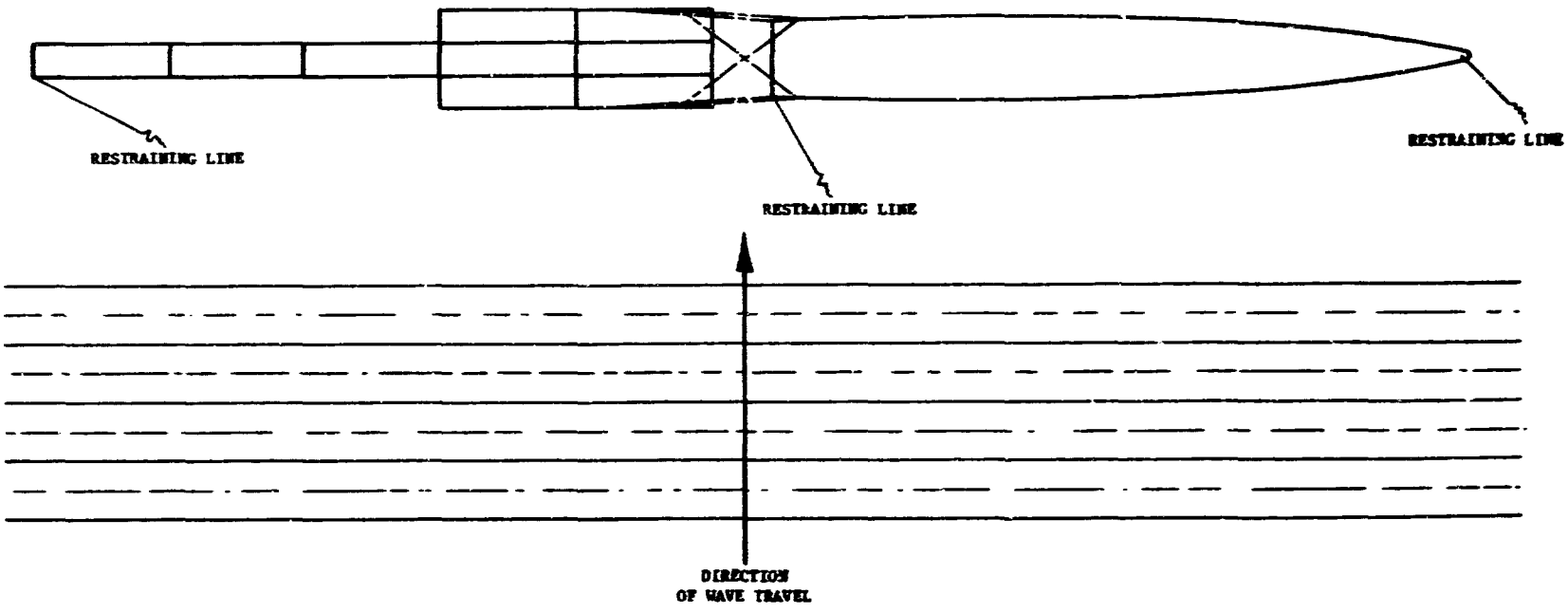

Figure 10 - Model Orientation in Beam Waves

THIS PAGE INTENTIONALLY LEFT BLANK

Figure 11 - Roll Transfer Function of the RO/RO Ship

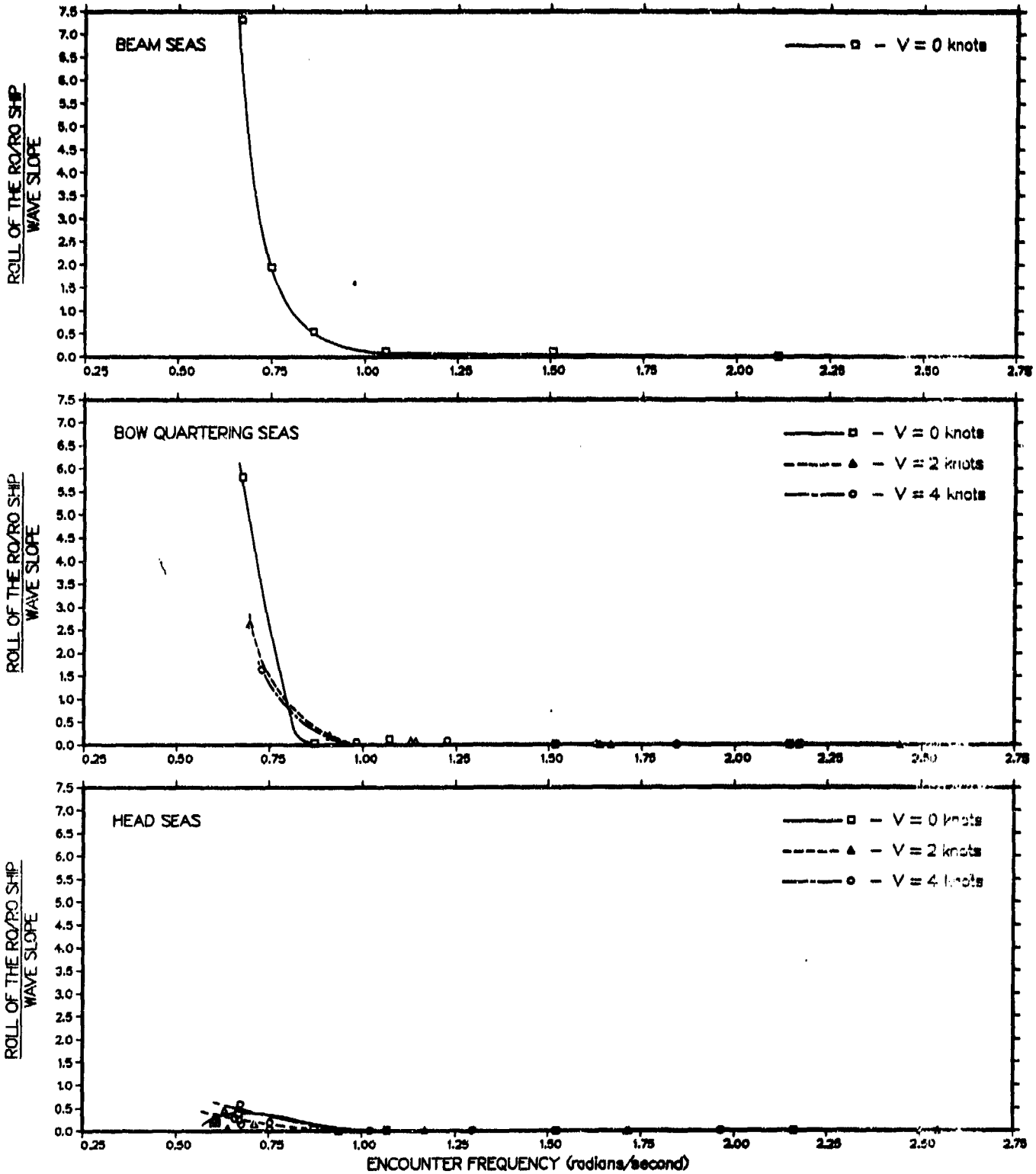

Figure 11A - Without Ramp and Causeway Ferry Connected

Figure 11 (Continued)

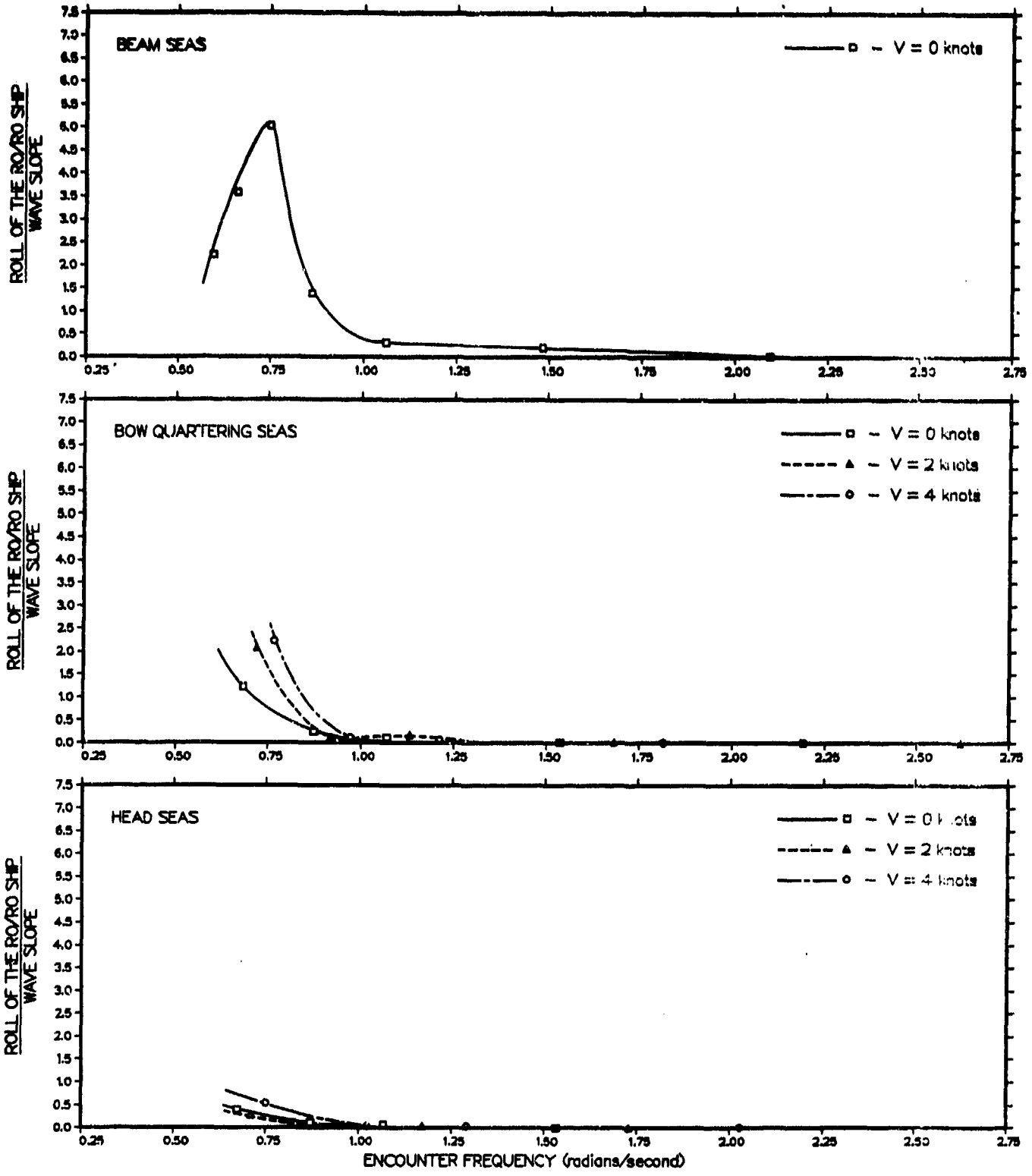

Figure 11B - With Ramp and Causeway Ferry Connected

Figure 12 - Roll Transfer Function of the Causeway Platform Facility

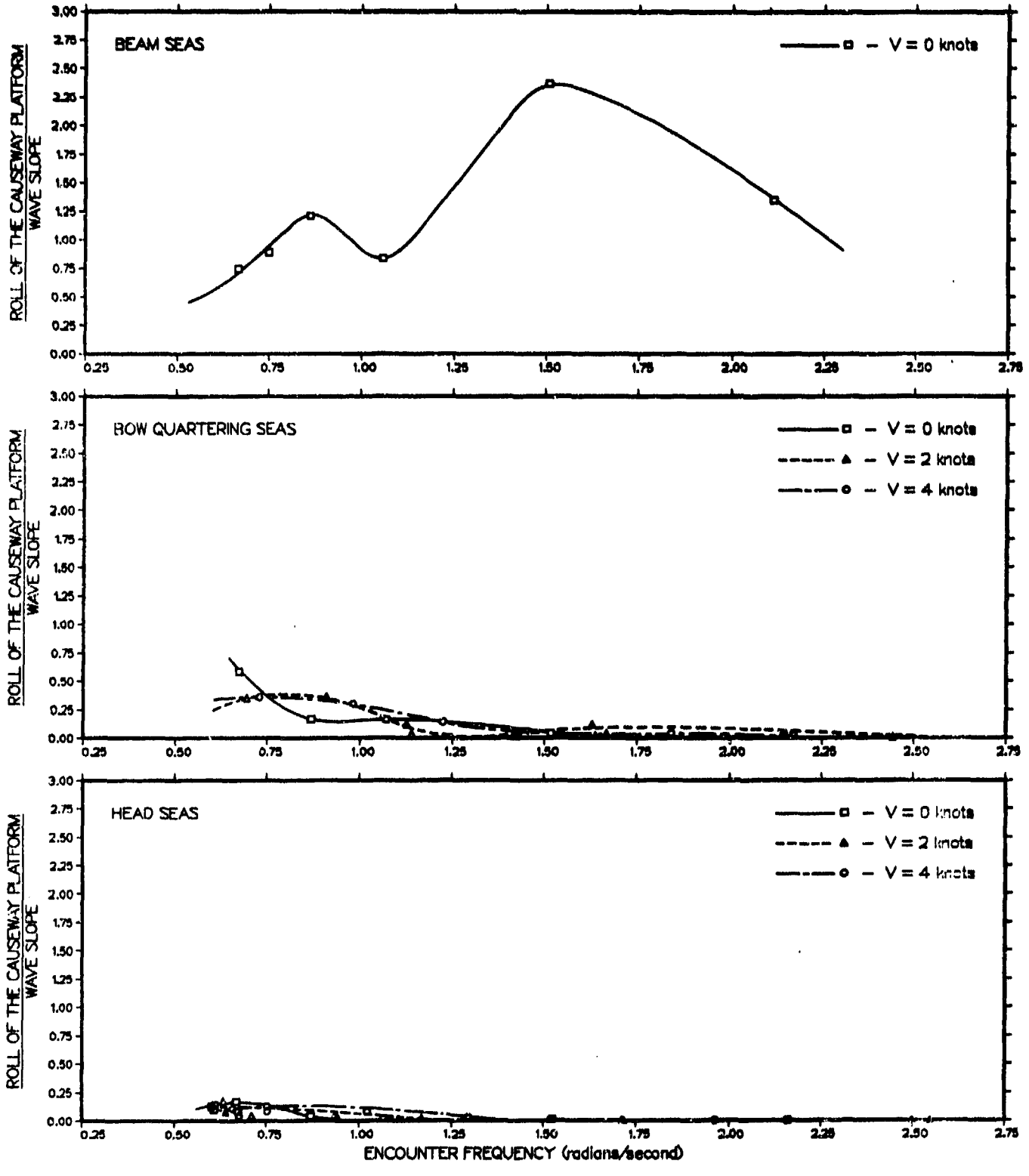

Figure 12A - Without Ramp and Causeway Ferry Connected

Figure 12 (Continued)

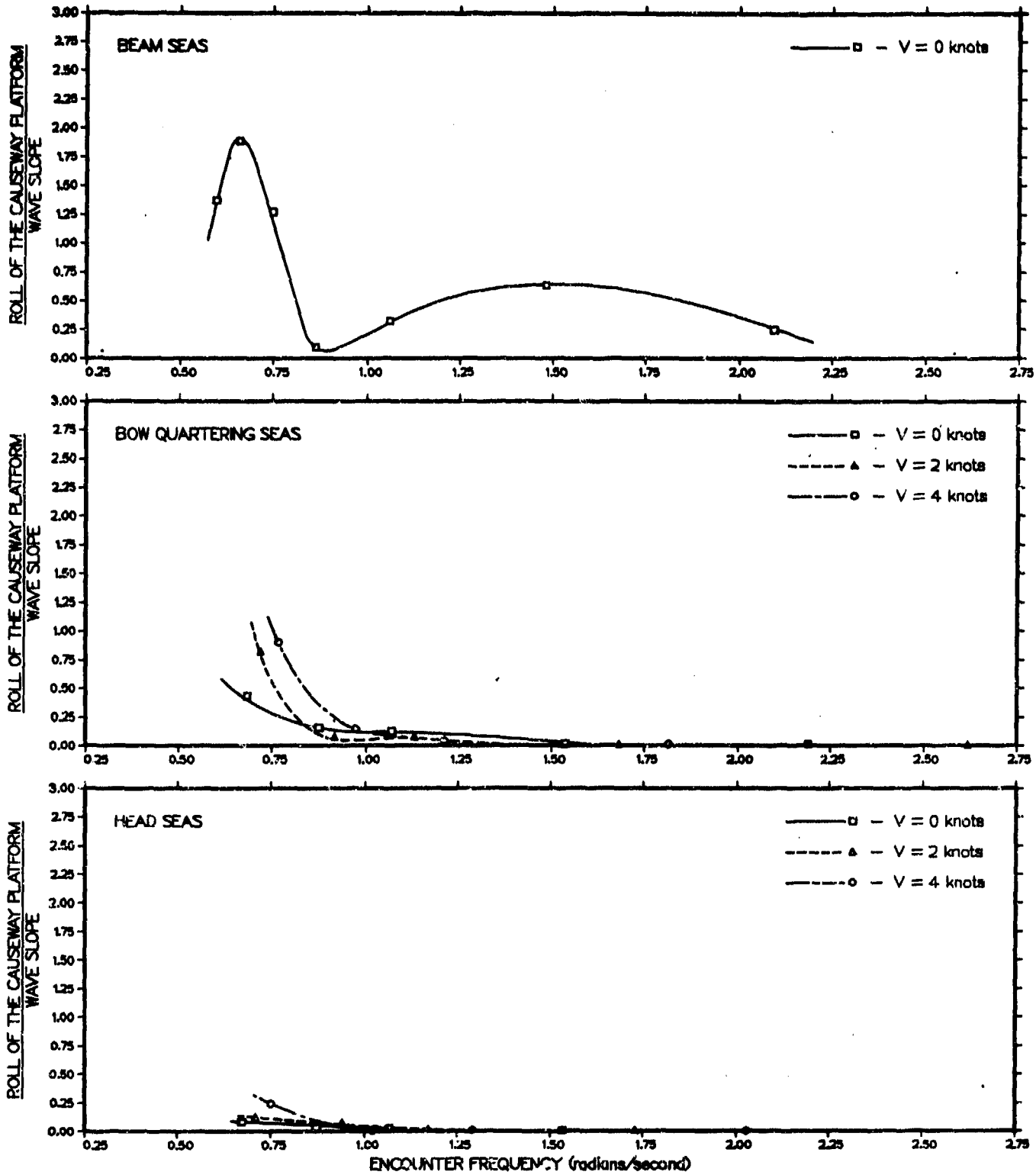

Figure 12B - With Ramp and Causeway Ferry Connected

Figure 13 - Transfer Function of the Relative Angular Displacement at the Port Junction of the Causeway Platform Facility

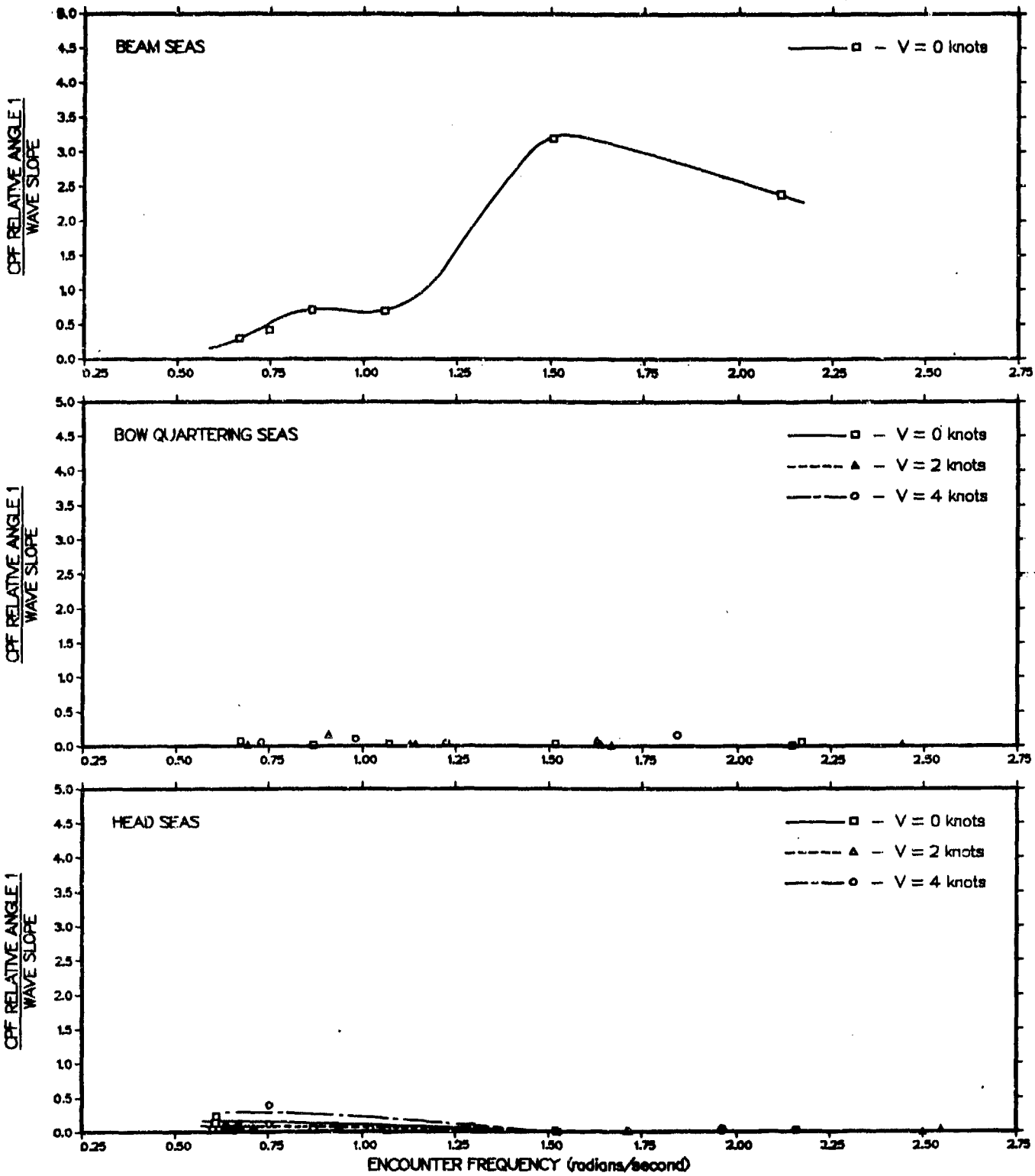

Figure 13A - Without Ramp and Causeway Ferry Connected

Figure 13 (Continued)

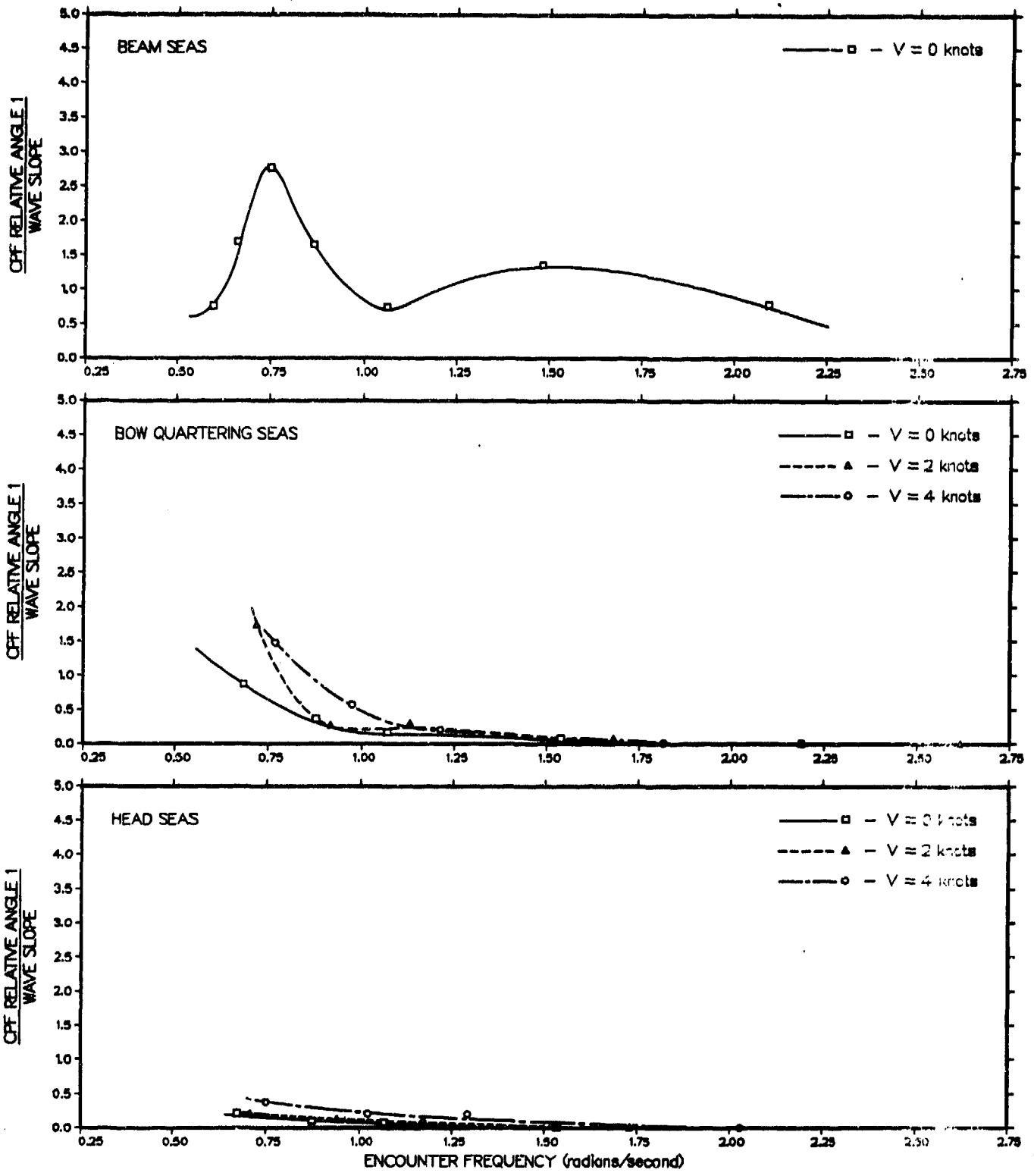

Figure 13B - With Ramp and Causeway Ferry Connected

Figure 14 - Transfer Function of the Relative Angular Displacement at the Starboard Junction of the Causeway Platform Facility

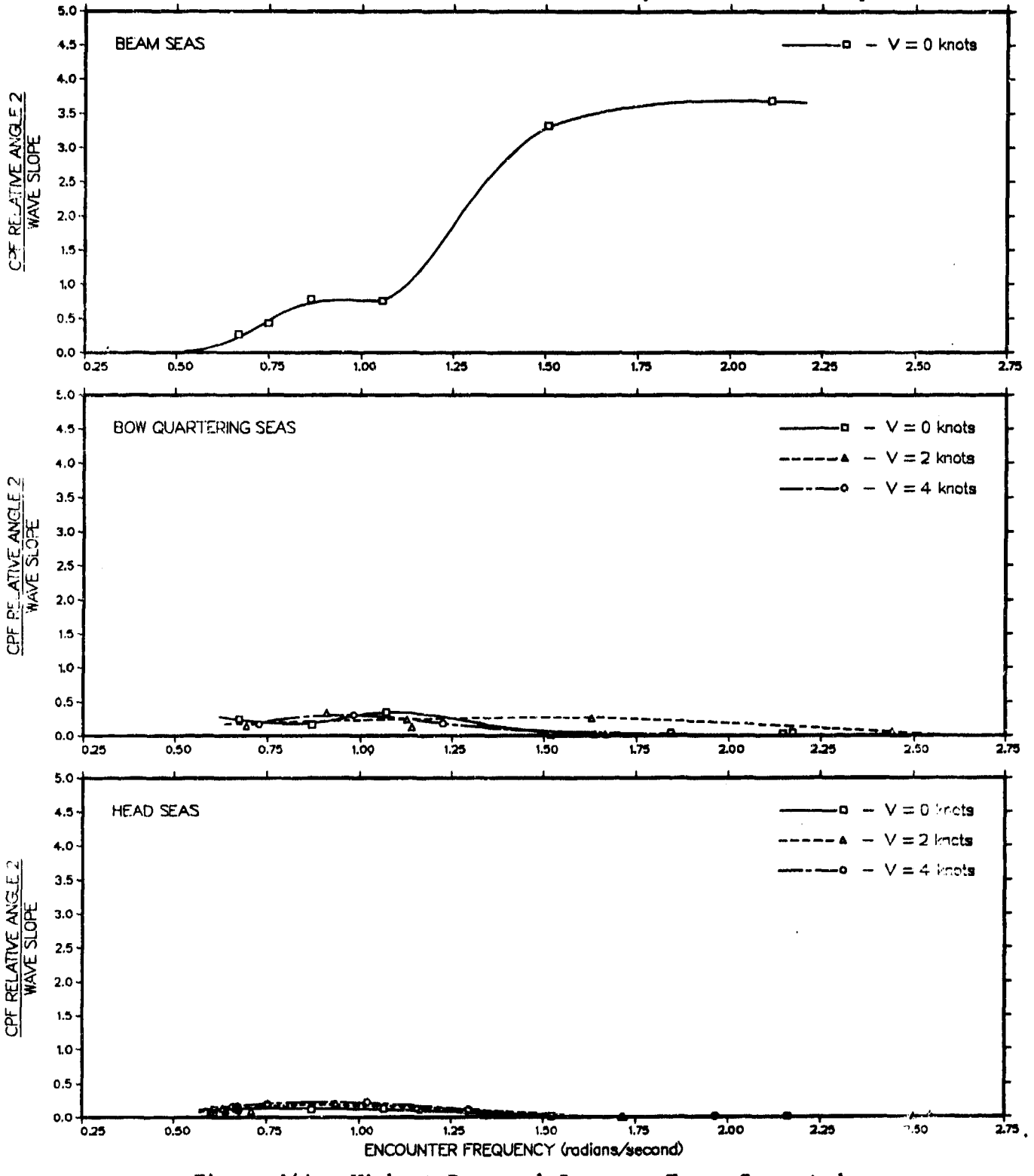

Figure 14A - Without Ramp and Causeway Ferry Connected

Figure 14 (Continued)

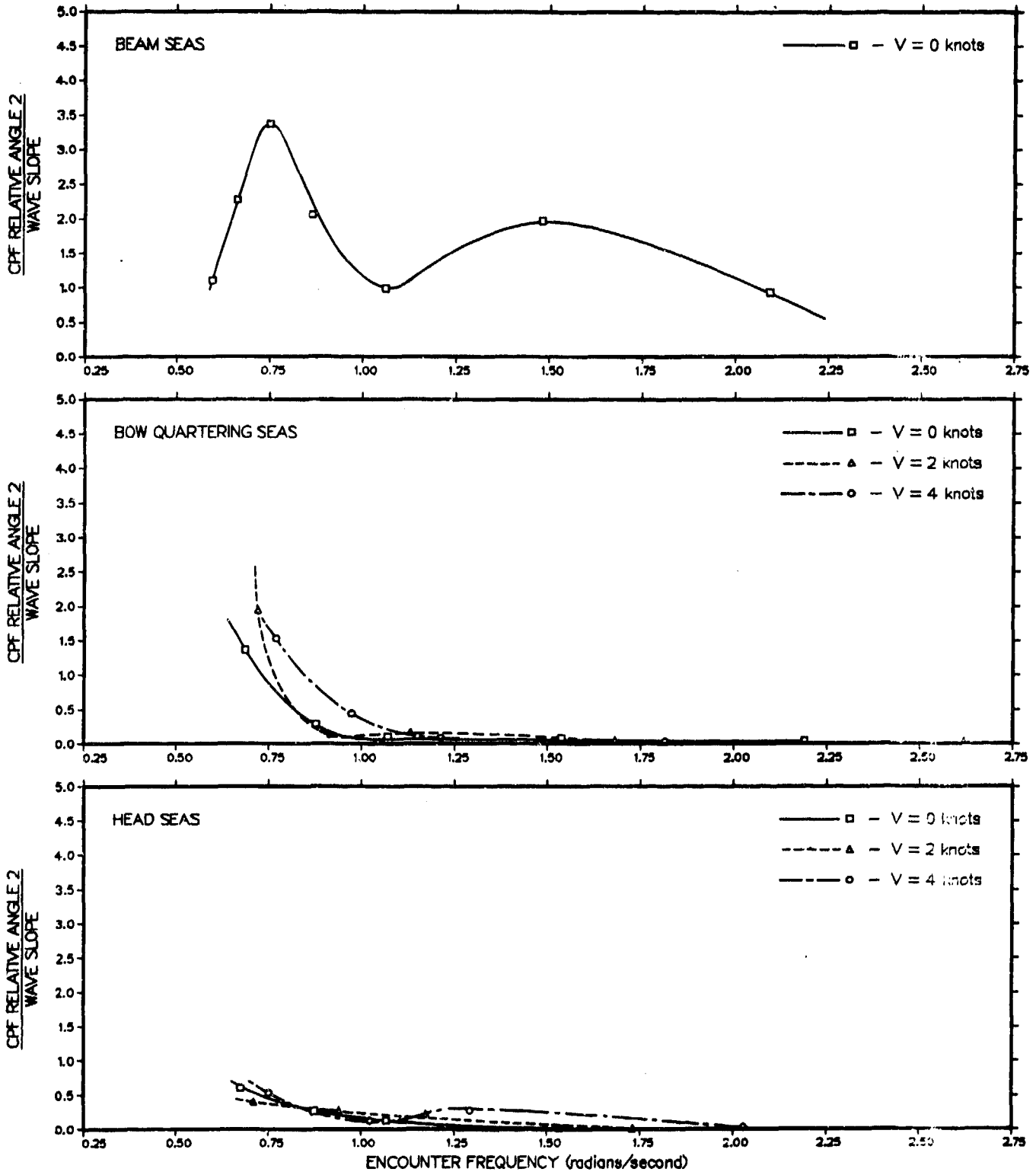

Figure 14B - With Ramp and Causeway Ferry Connected

Figure 15 - Pitch Transfer Function of the RO/RO Ship

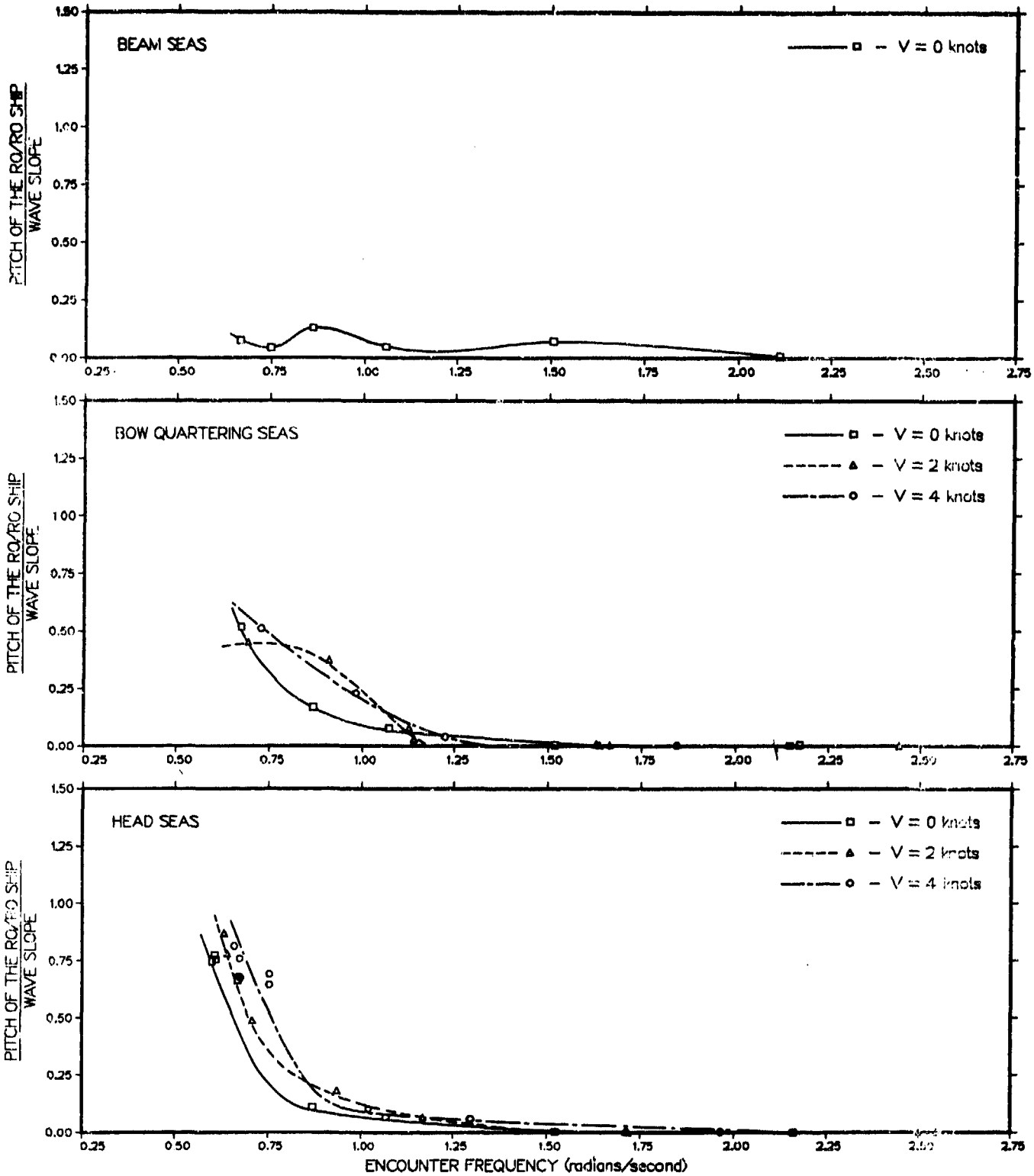

Figure 15A - Without Ramp and Causeway Ferry Connected

Figure 15 (Continued)

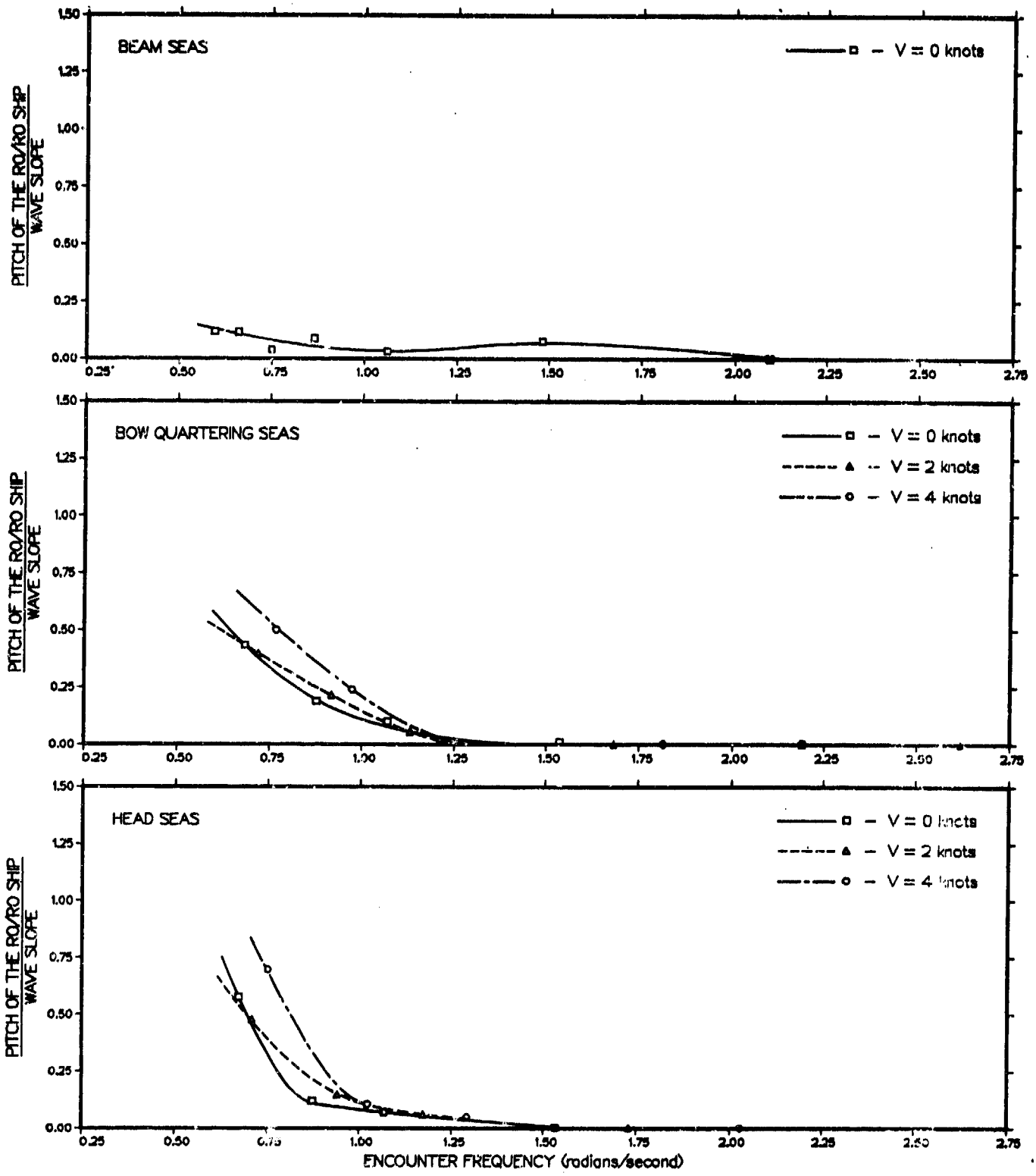

Figure 15B - With Ramp and Causeway Ferry Connected

Figure 16 - Pitch Transfer Function of the Causeway Platform Facility

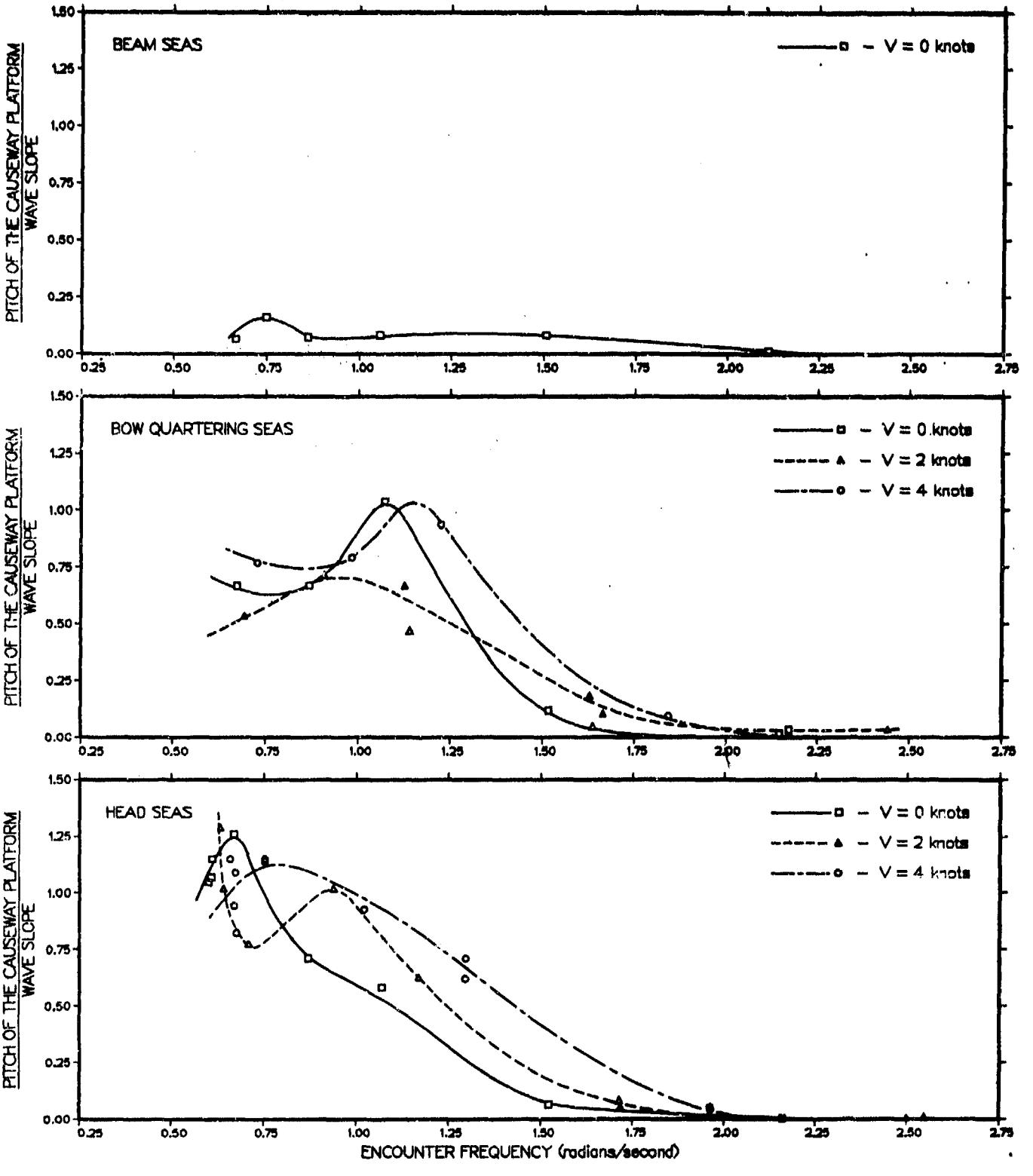

Figure 16A - Without Ramp and Causeway Ferry Connected

Figure 16 (Continued)

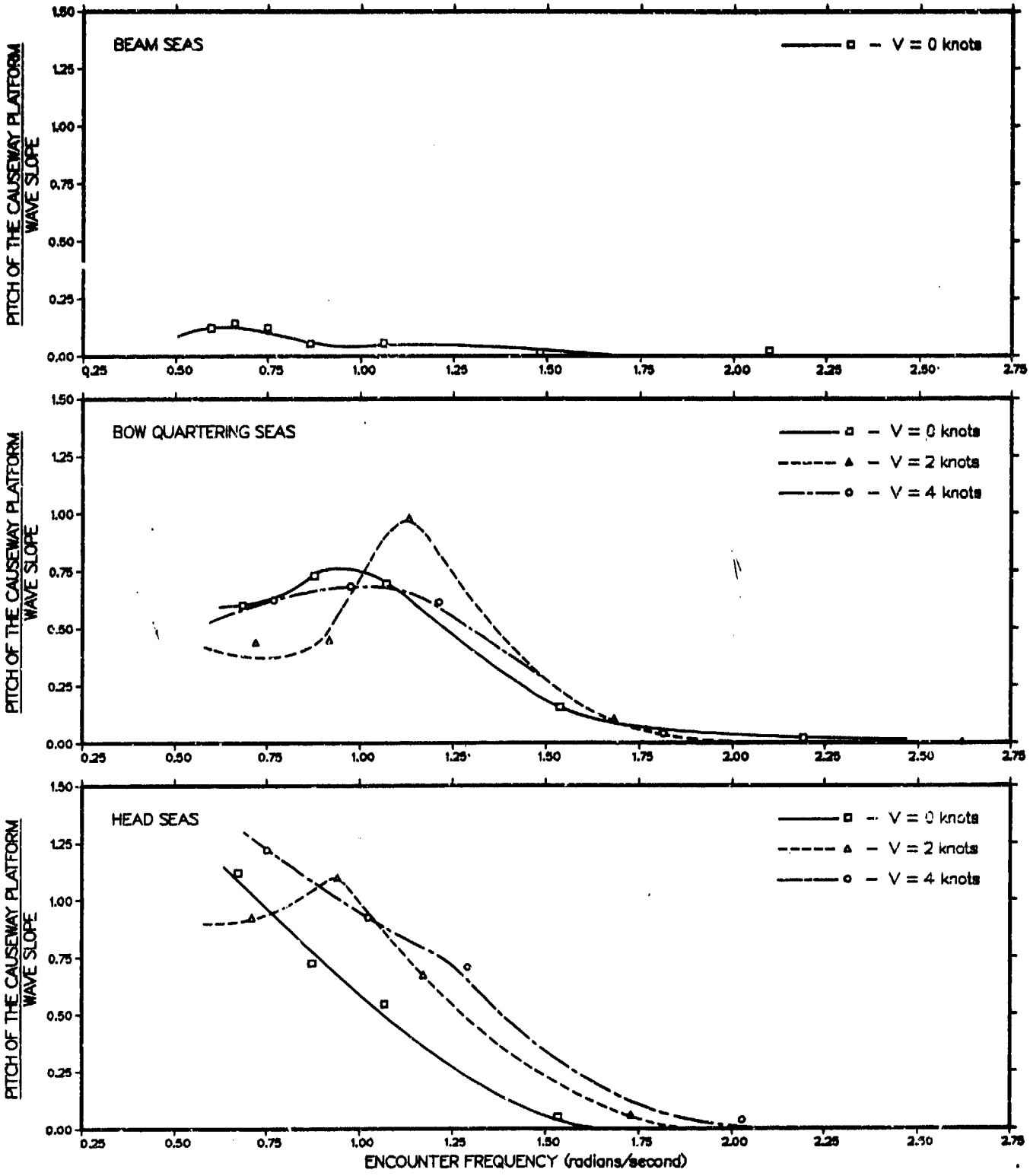

Figure 16B - With Ramp and Causeway Ferry Connected

Figure 17 - Transfer Function of the Relative Angular Displacement at the Transverse Junction of the Causeway Platform Facility

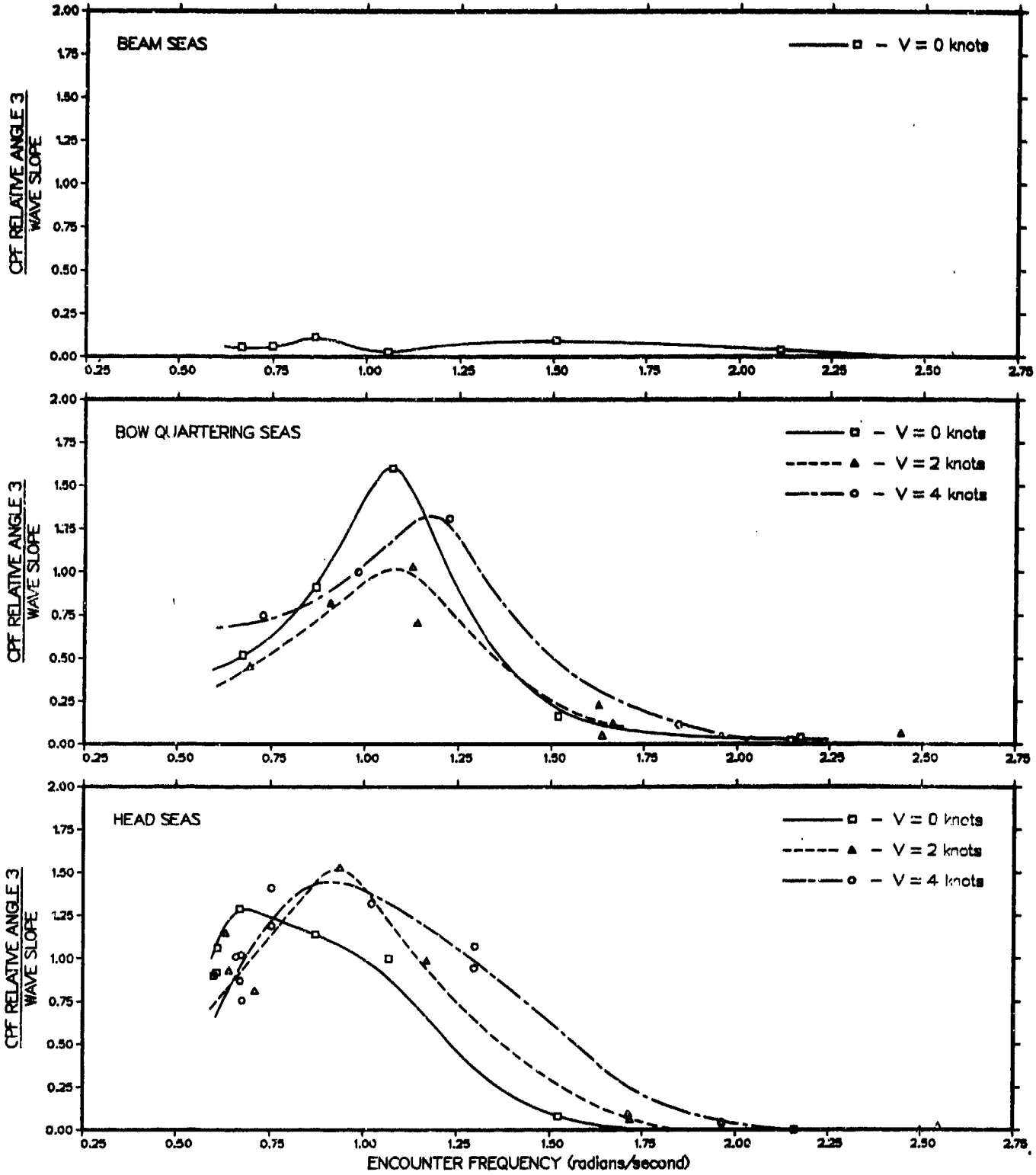

Figure 17A - Without Ramp and Causeway Ferry Connected

Figure 17 (Continued)

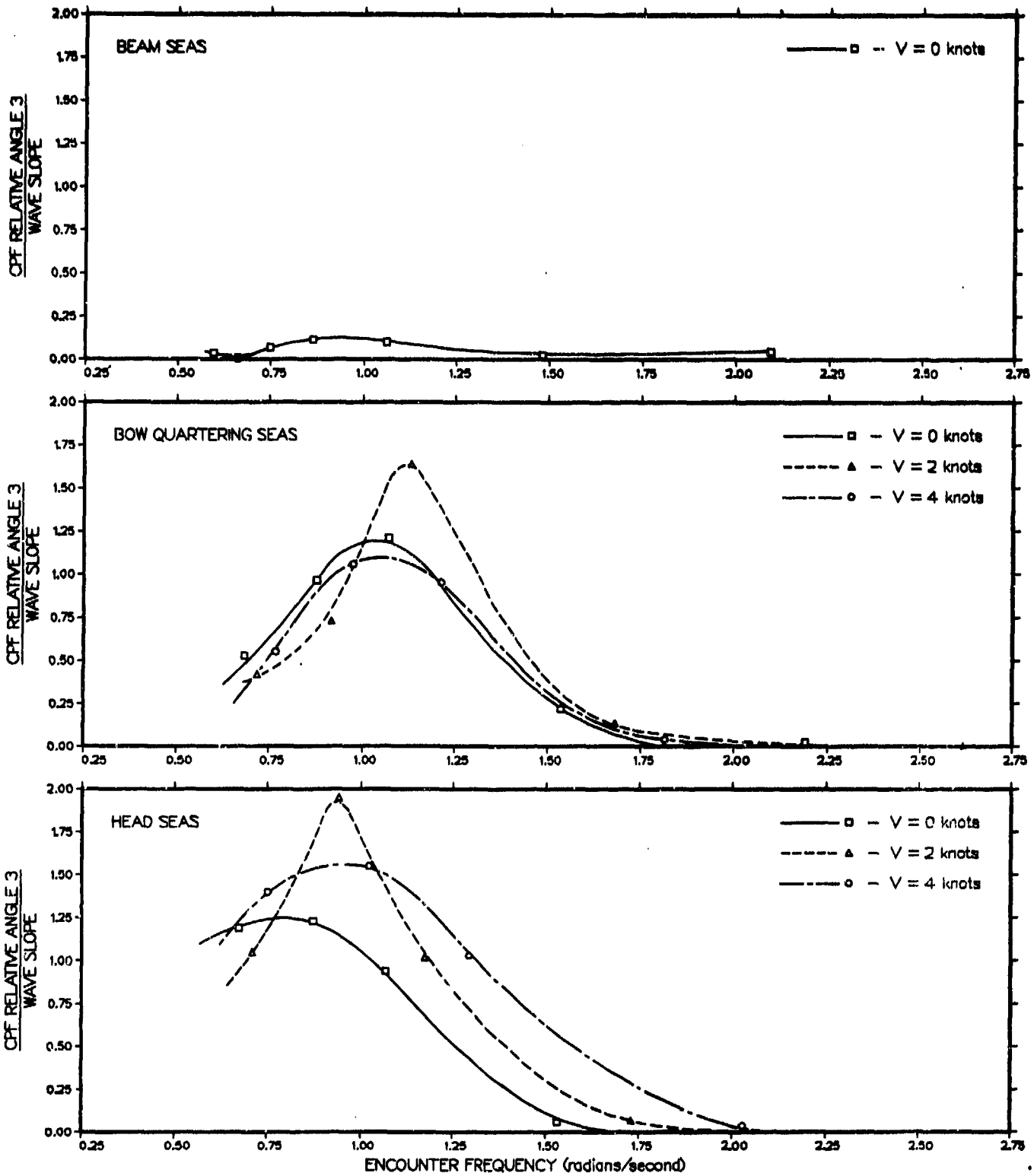

Figure 17B - With Ramp and Causeway Ferry Connected

Figure 18 - Transfer Function of the Relative Vertical Displacement Between the Stern of the RO/RO Ship and the Causeway Platform Facility

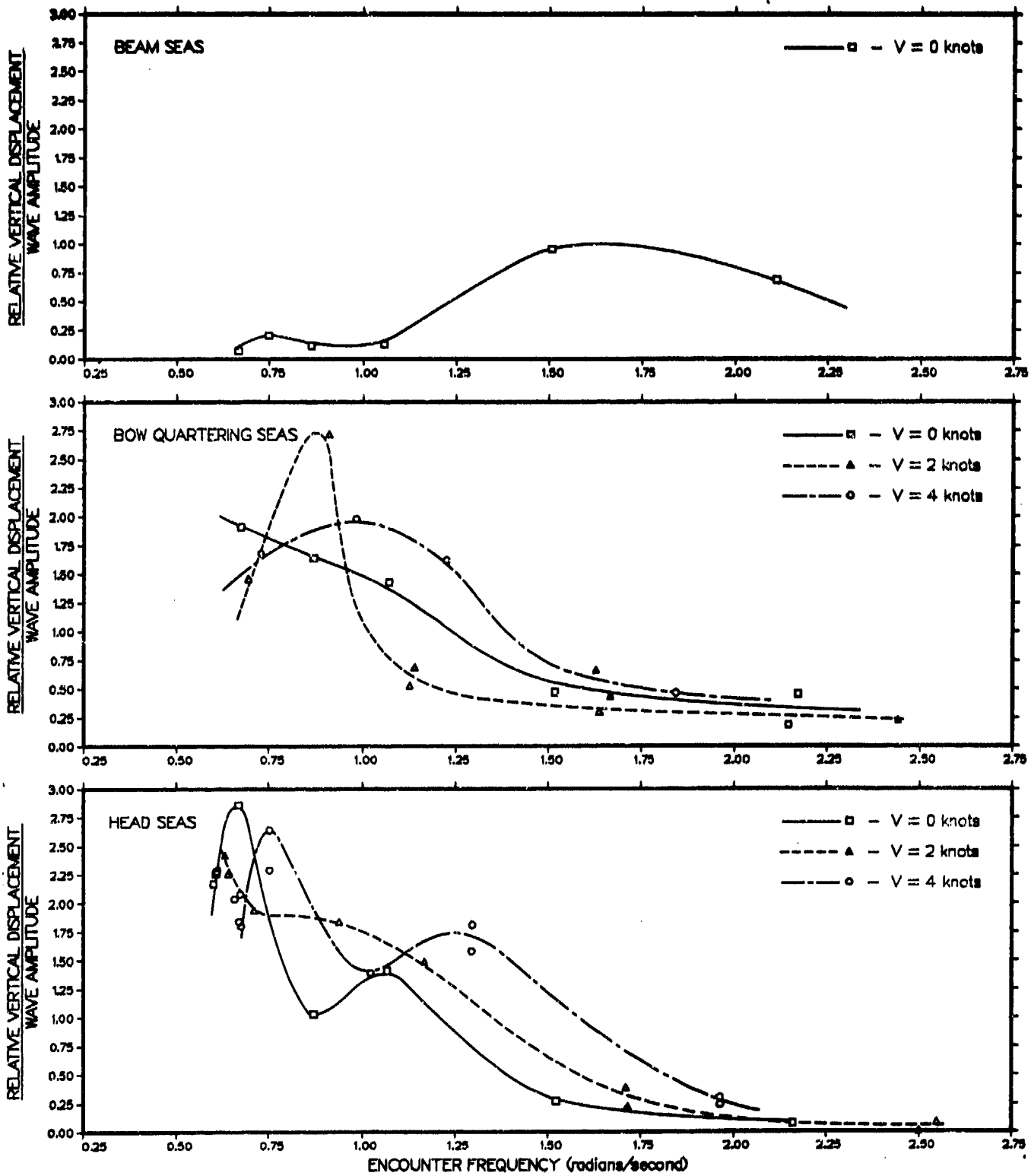

Figure 18A - Without Ramp and Causeway Ferry Connected

Figure 18 (Continued)

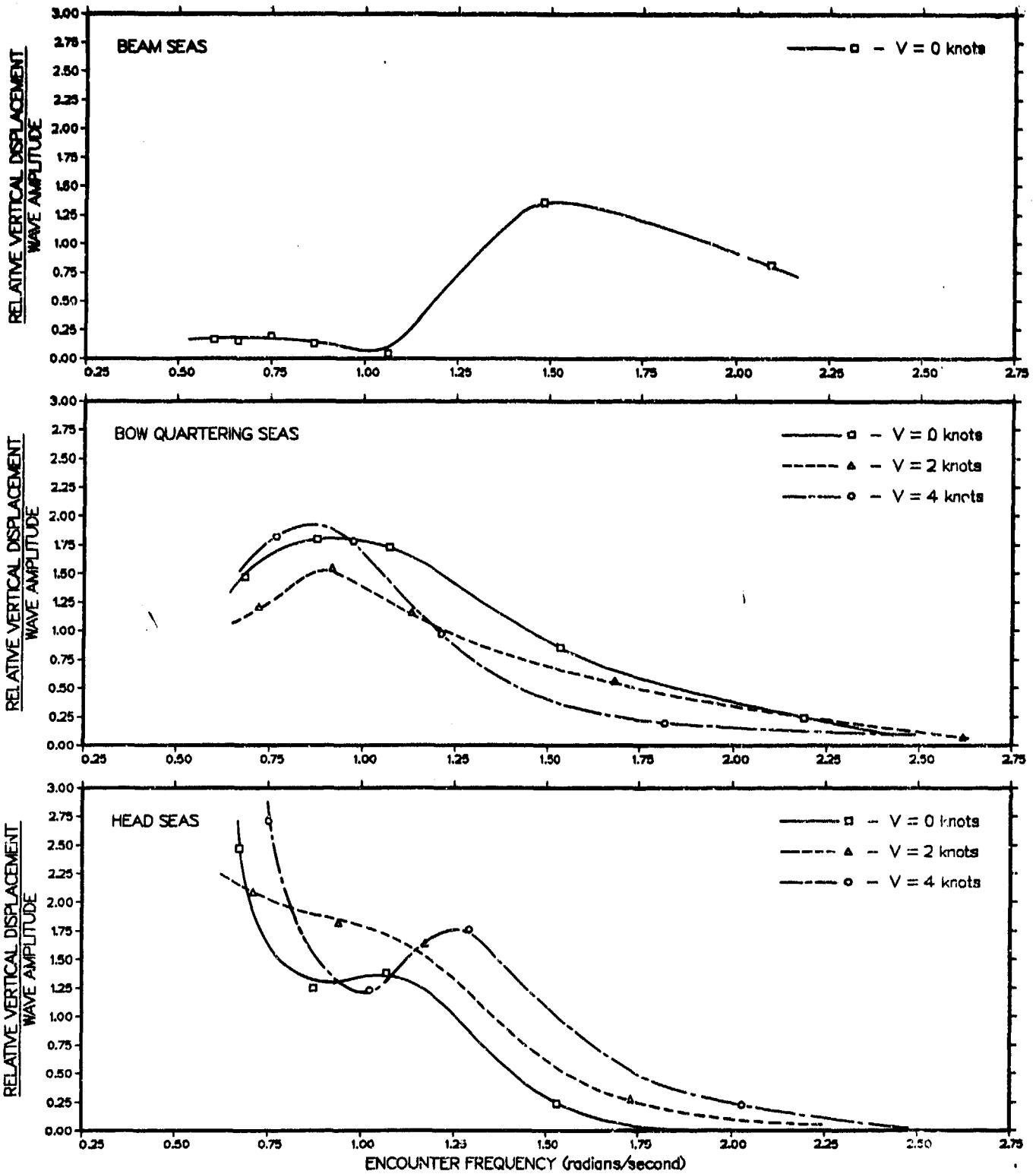

Figure 18B – With Ramp and Causeway Ferry Connected

Figure 19 - Heave Transfer Function of the RO/RC Ship

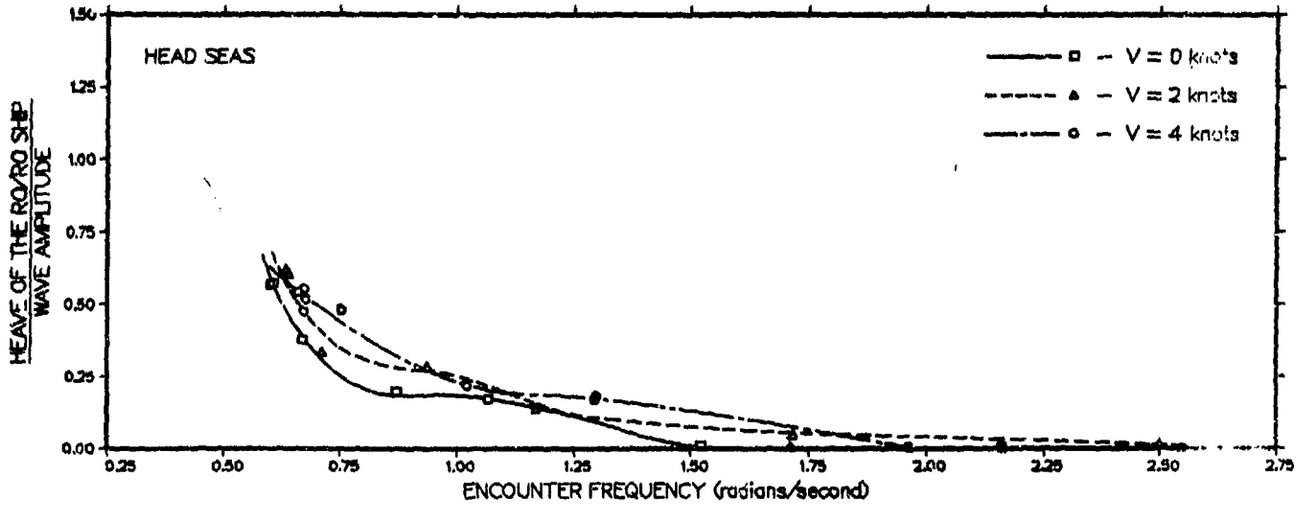

Figure 19A - Without Ramp and Causeway Ferry Connected

Figure 19 (Continued)

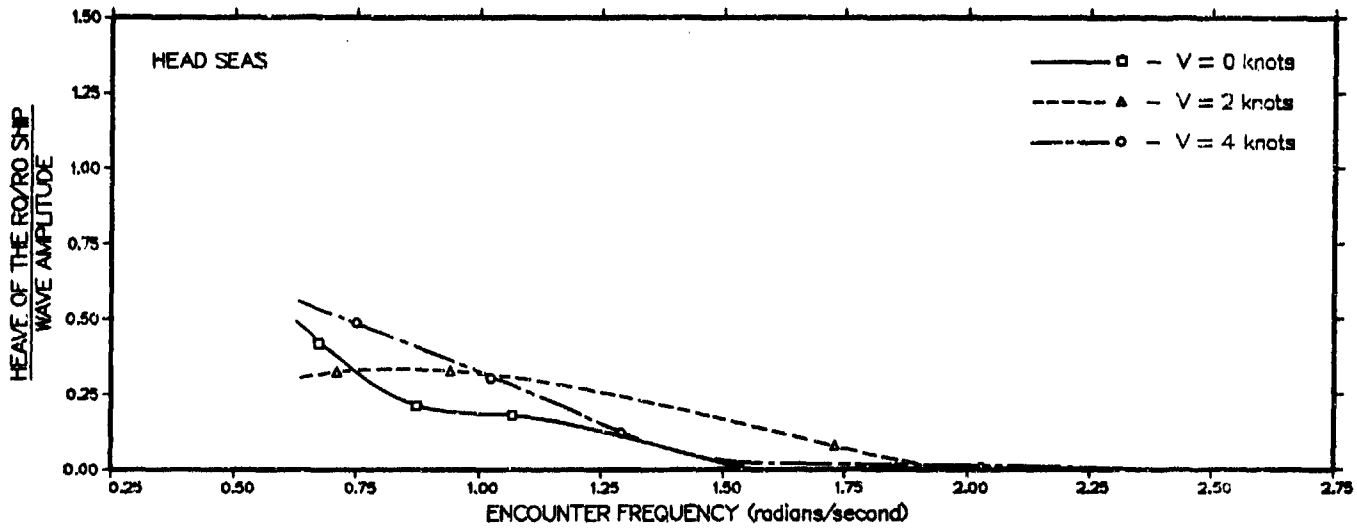

Figure 19B - With Ramp and Causeway Ferry Connected

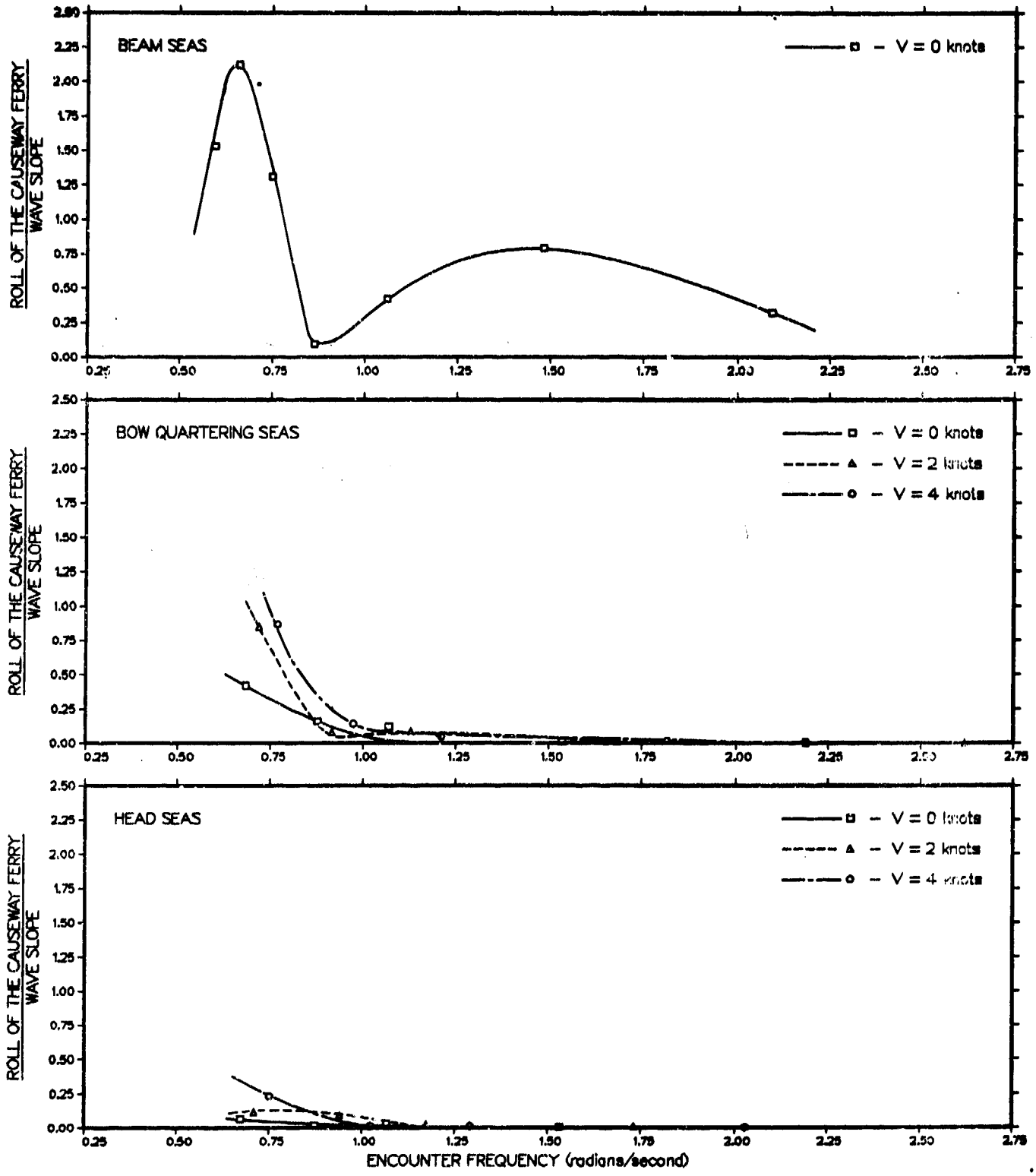

Figure 20 – Roll Transfer Function of the Causeway Ferry

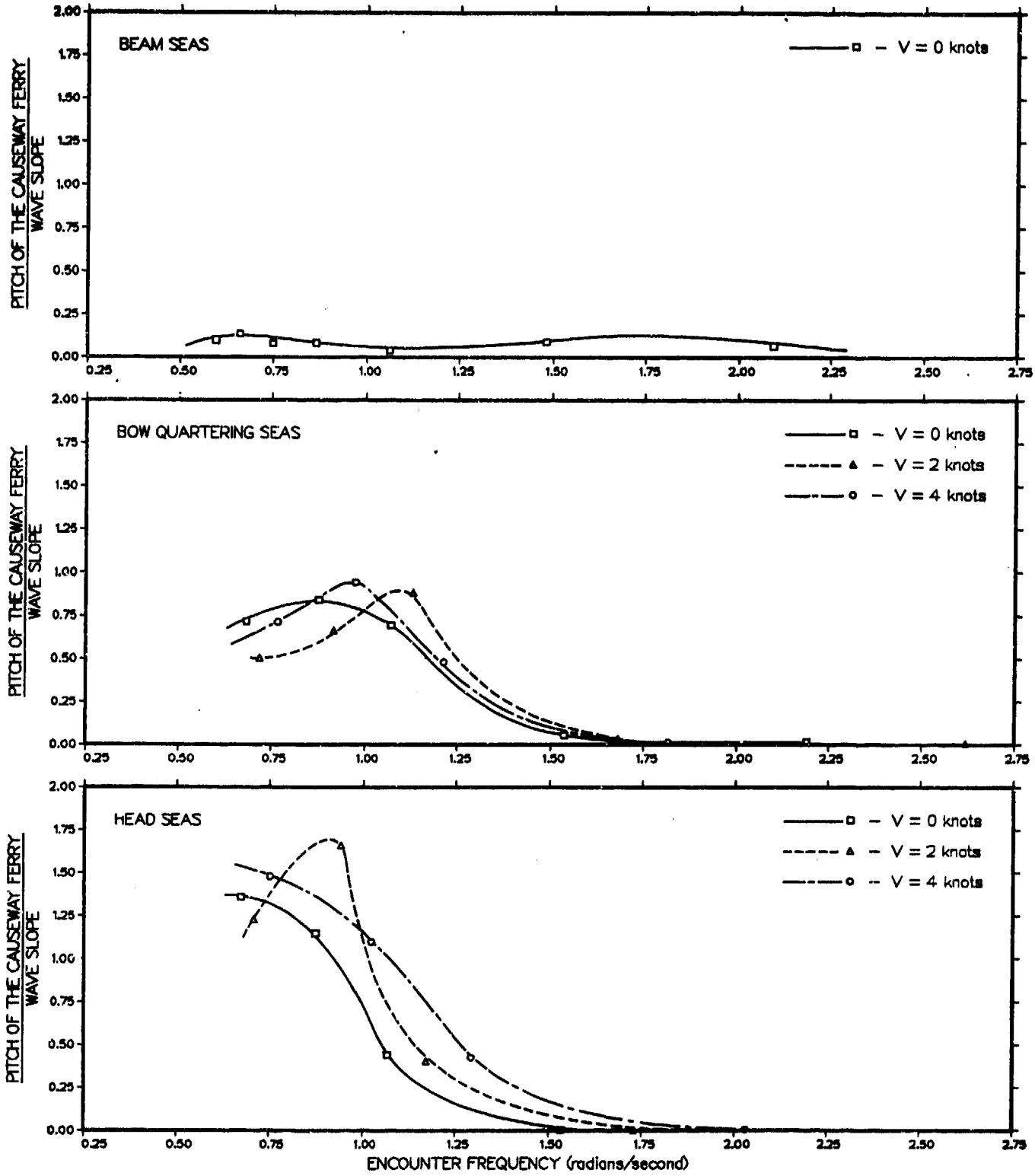

Figure 21 - Pitch Transfer Function of the Causeway Ferry

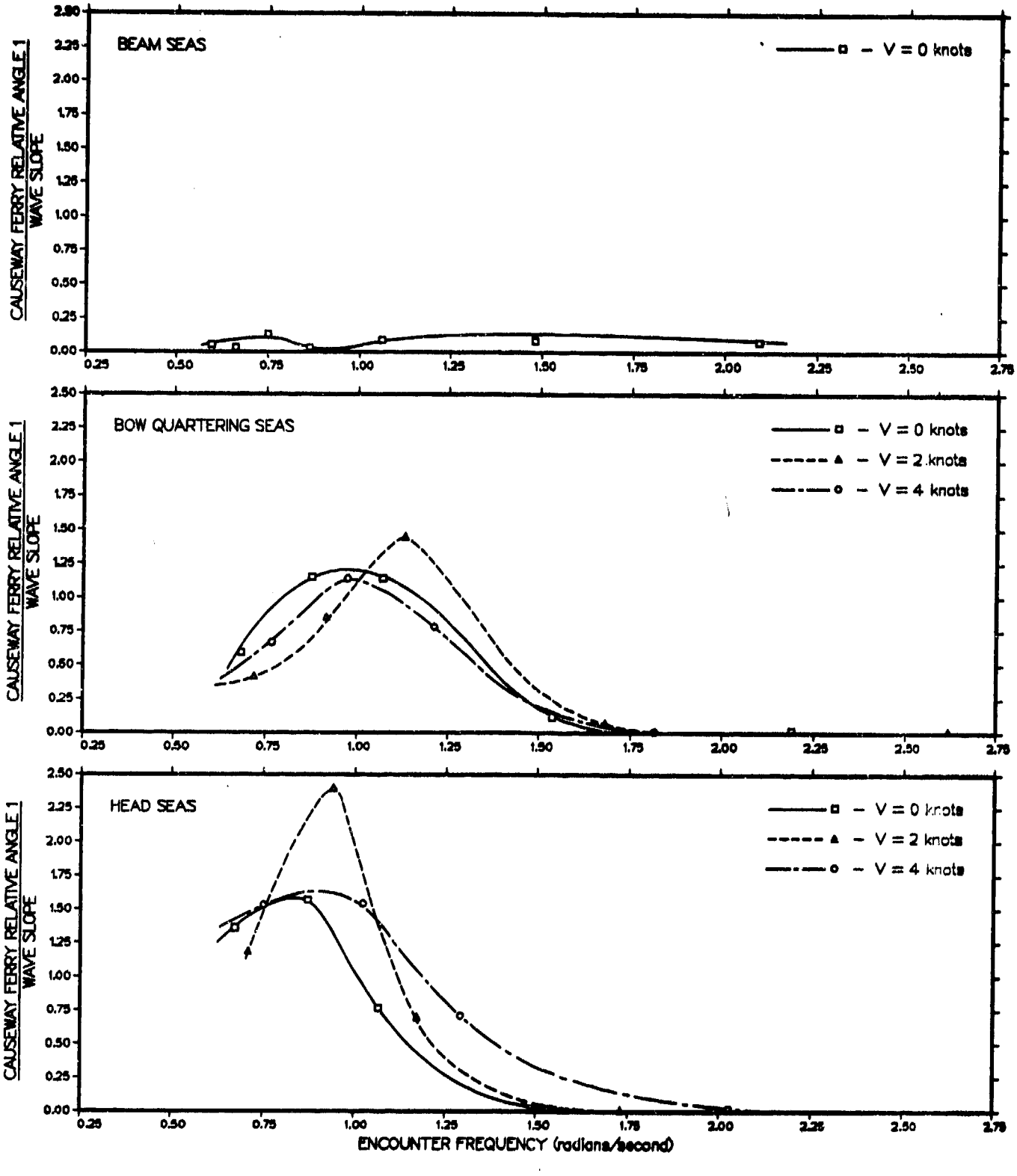

Figure 22 - Transfer Function of the Relative Angular Displacement at the Junction Between the Causeway Platform Facility and the Causeway Ferry

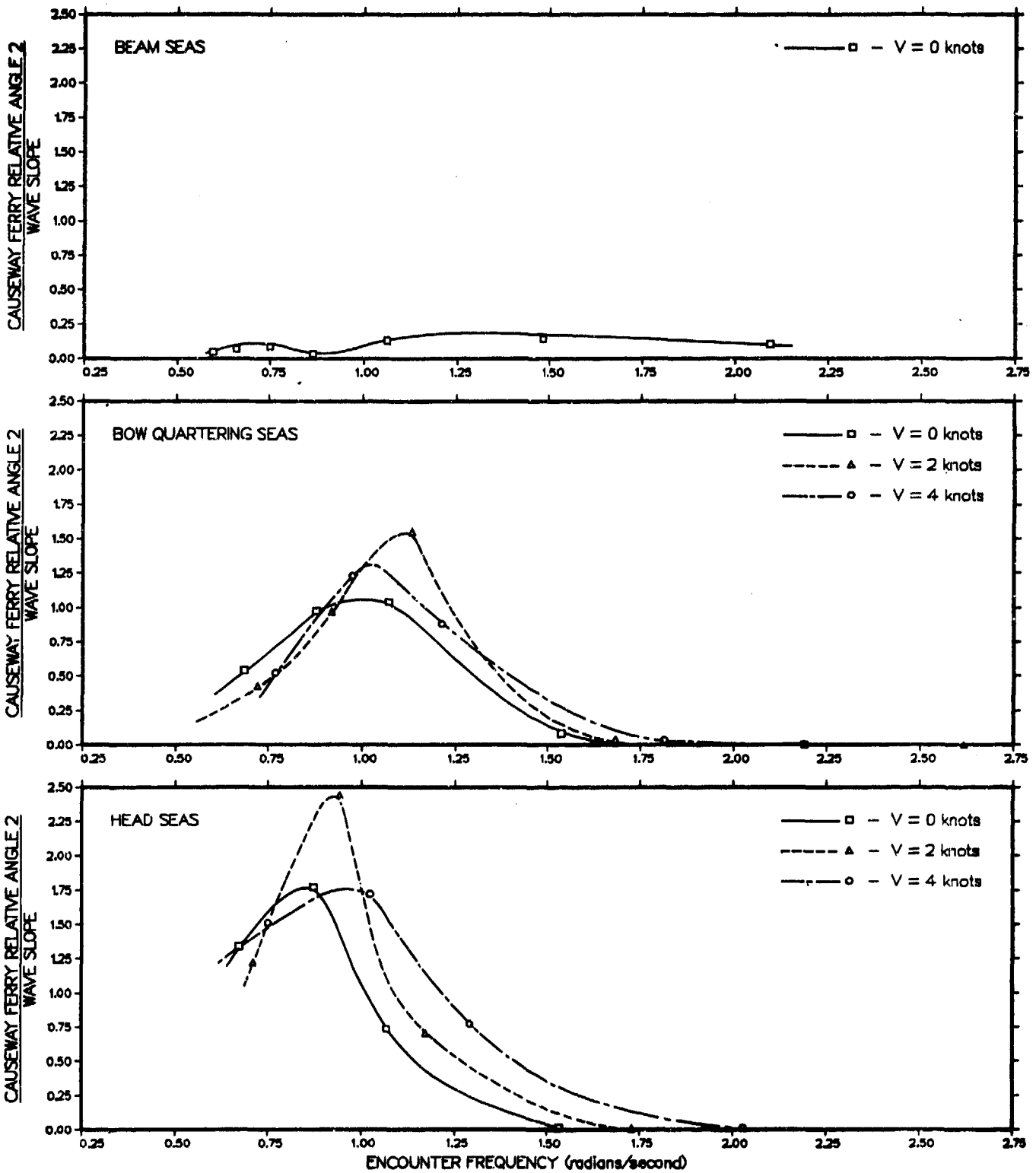

Figure 23 - Transfer Function of the Relative Angular Displacement at the Junction Between the First and Second Sections of the Causeway Ferry

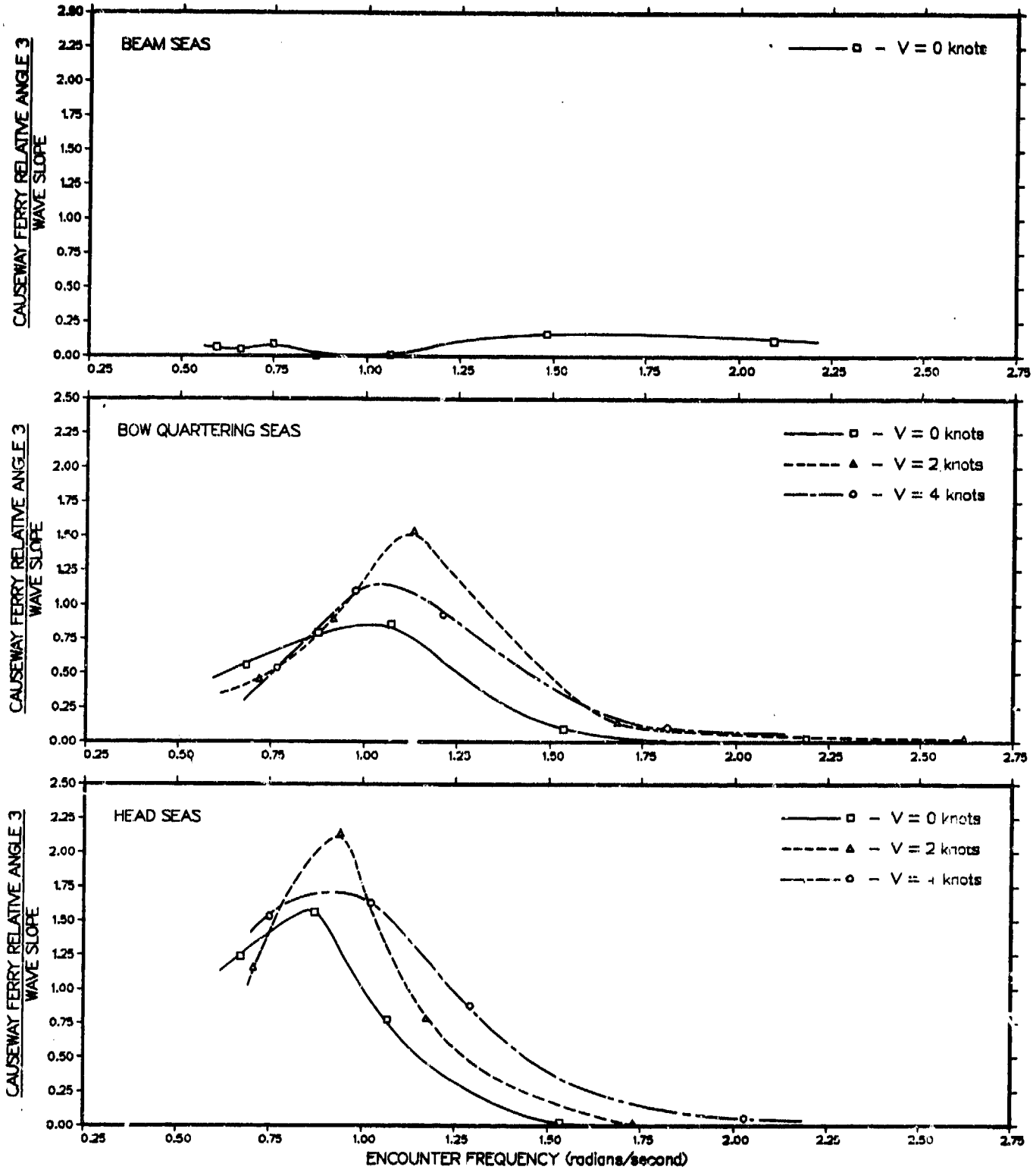

Figure 24 - Transfer Function of the Relative Angular Displacement at the Junction Between the Second and Third Sections of the Causeway Ferry

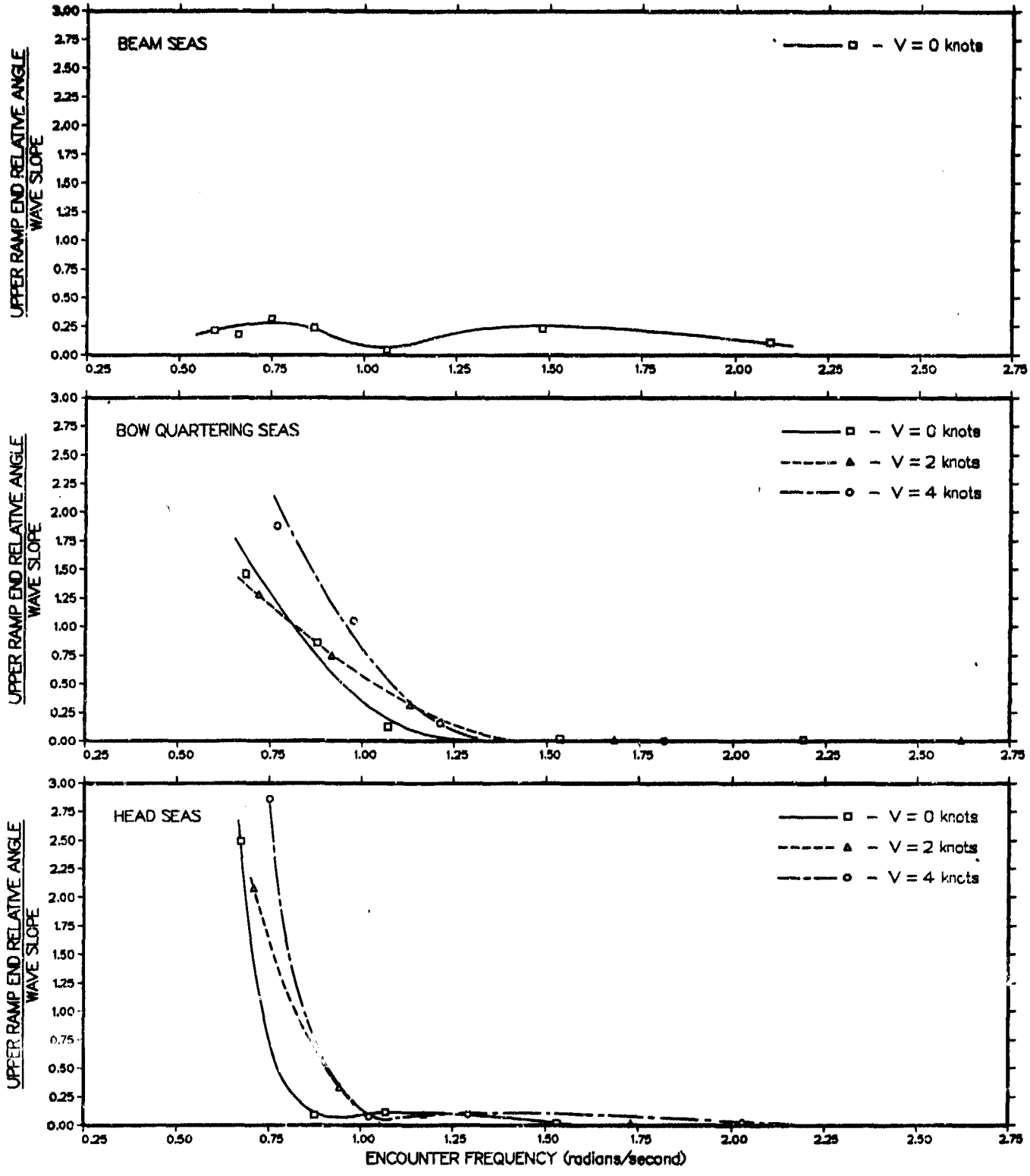

Figure 25 - Transfer Function of the Relative Angular Displacement at the Upper End of the Off-loading Ramp

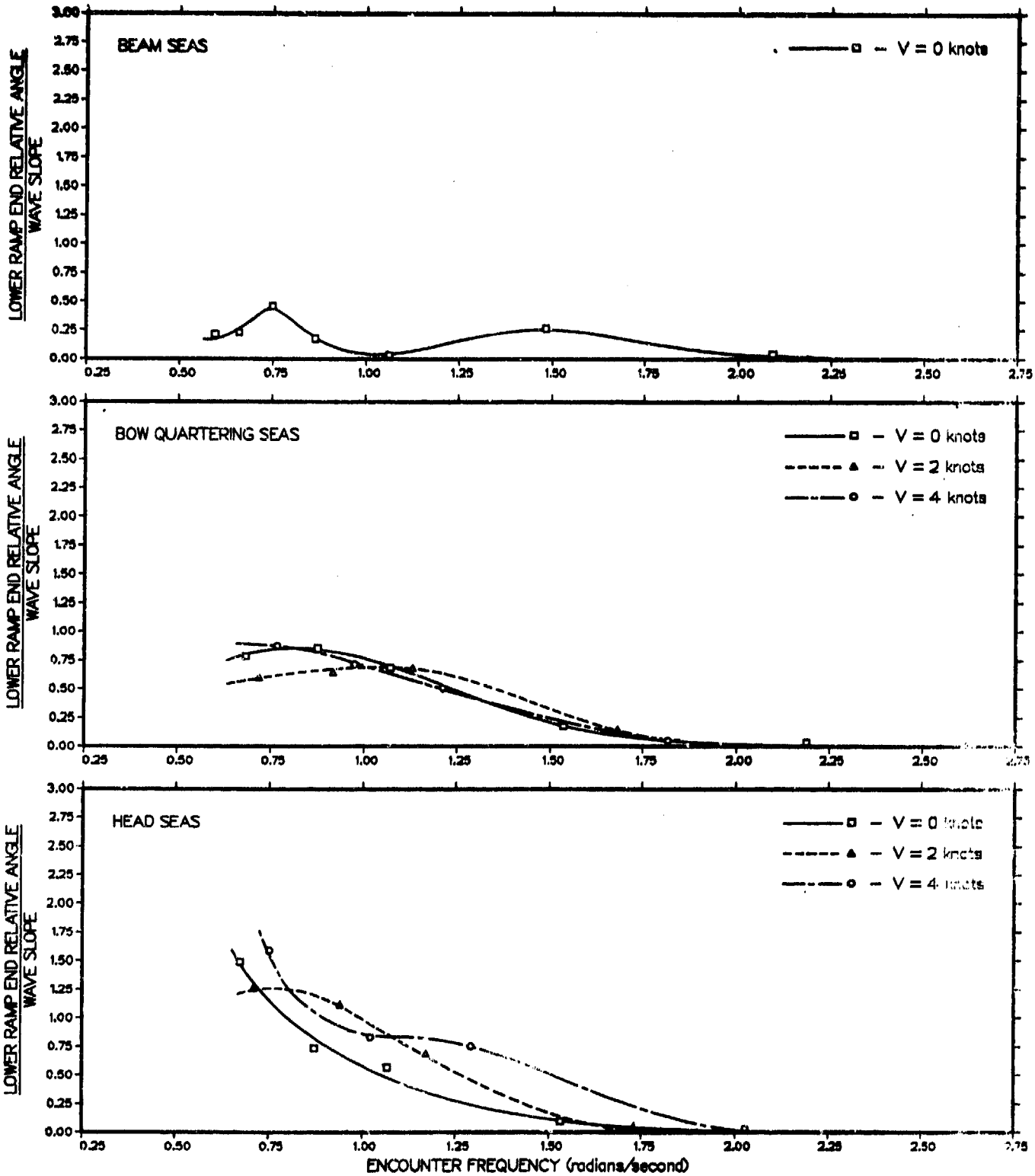

Figure 26 - Transfer Function of the Relative Angular Displacement at the Lower End of the Off-loading Ramp

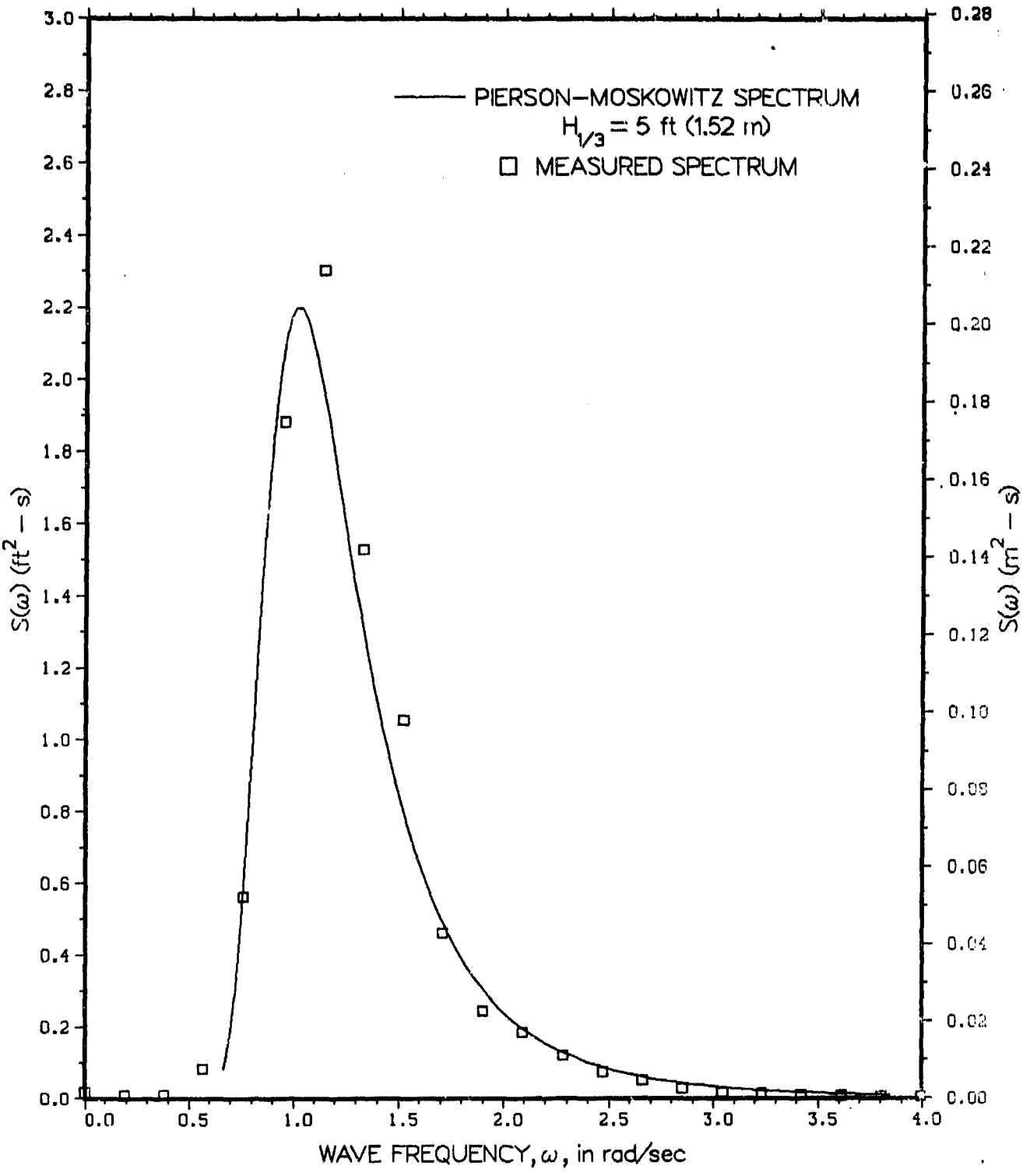

Figure 27 - Irregular Wave Spectrum — Sea State 3

Figure 28 - Significant Double Amplitude of Roll of the RO/RO Ship in Sea State 3

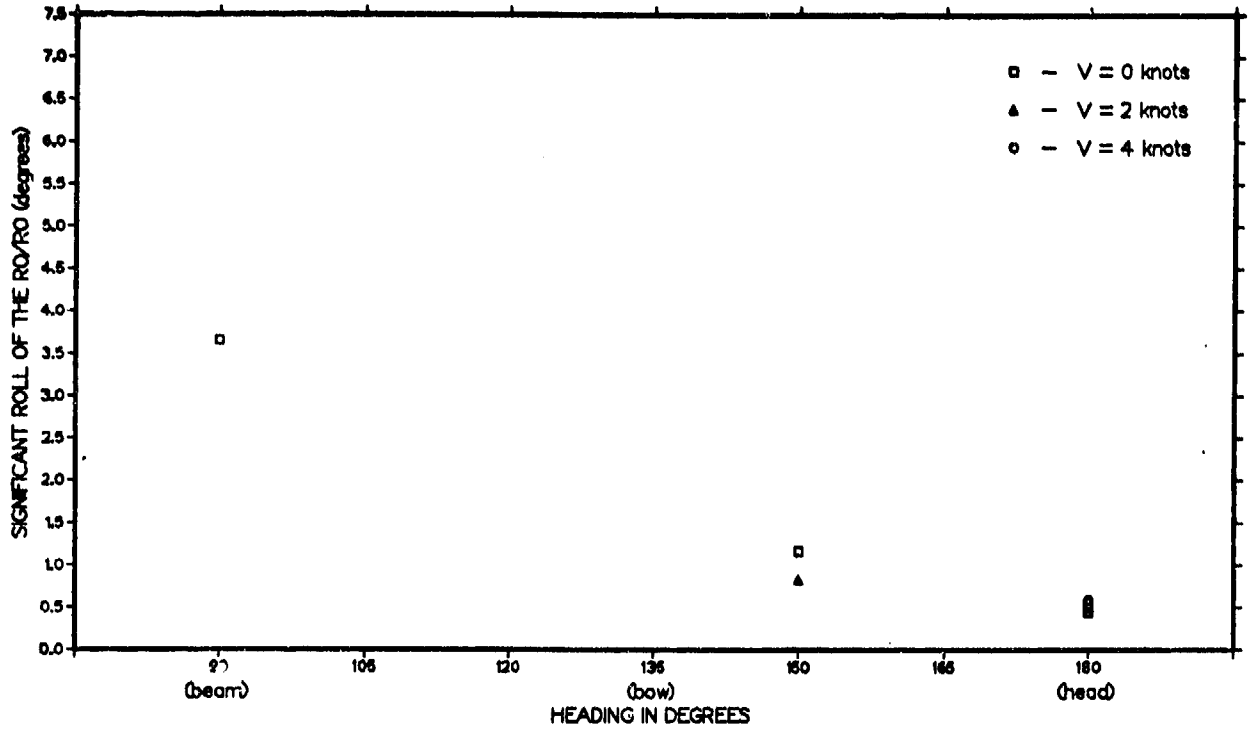

Figure 28A - Without Ramp and Causeway Ferry Connected

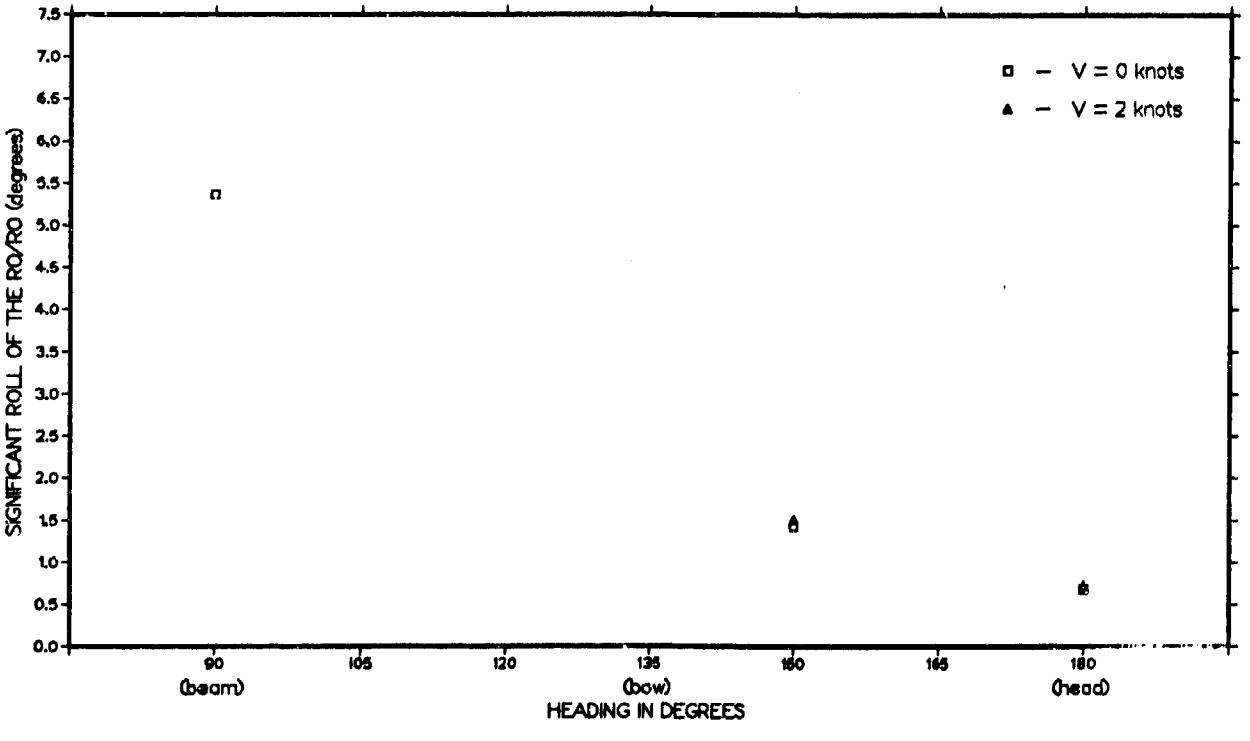

Figure 28B - With Ramp and Causeway Ferry Connected

Figure 29 - Significant Double Amplitude of Roll of the Causeway Platform Facility in Sea State 3

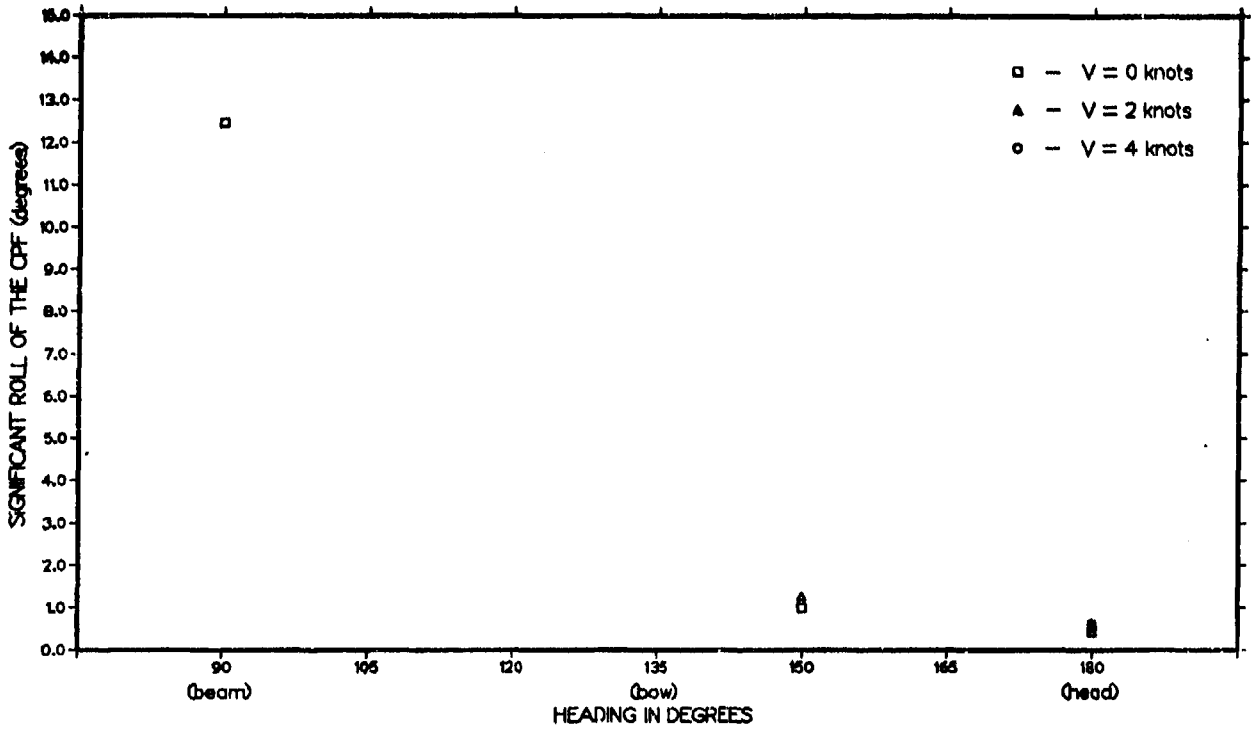

Figure 29A - Without Ramp and Causeway Ferry Connected

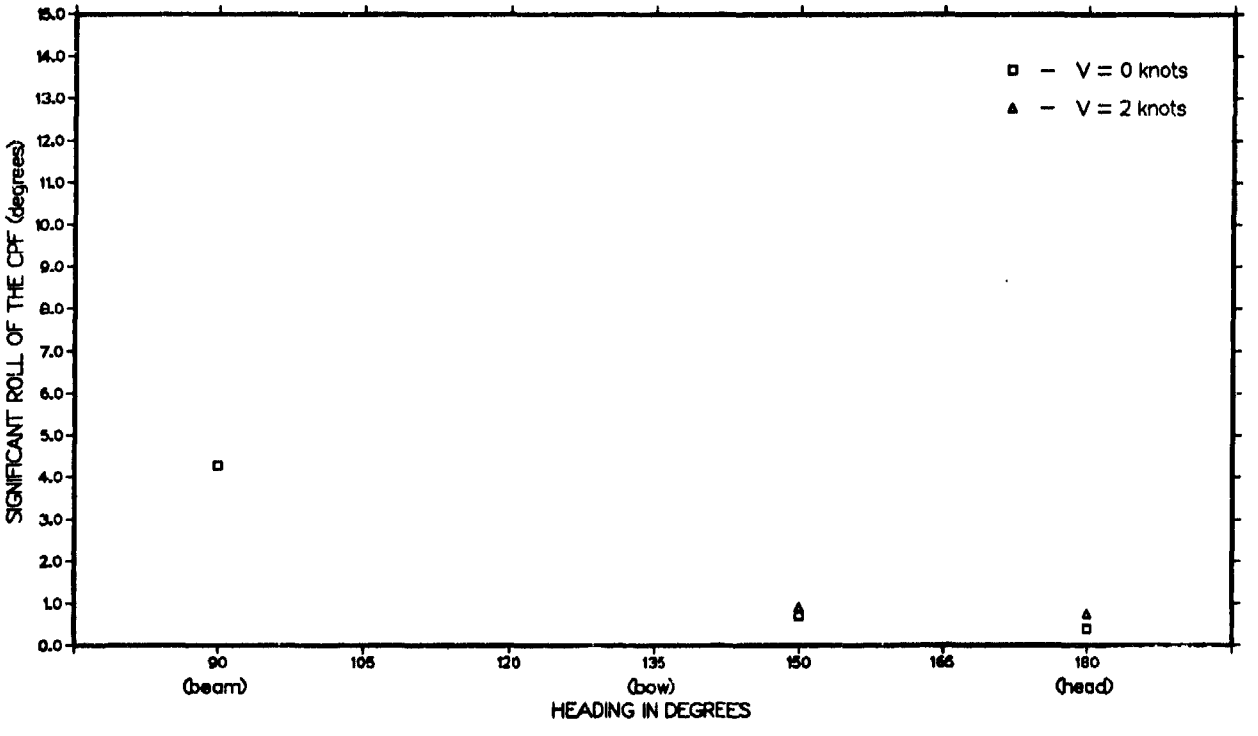

Figure 29B - With Ramp and Causeway Ferry Connected

Figure 30 - Significant Double Amplitude of Relative Angular Displacement at the Port Junction of the Causeway Platform Facility in Sea State 3

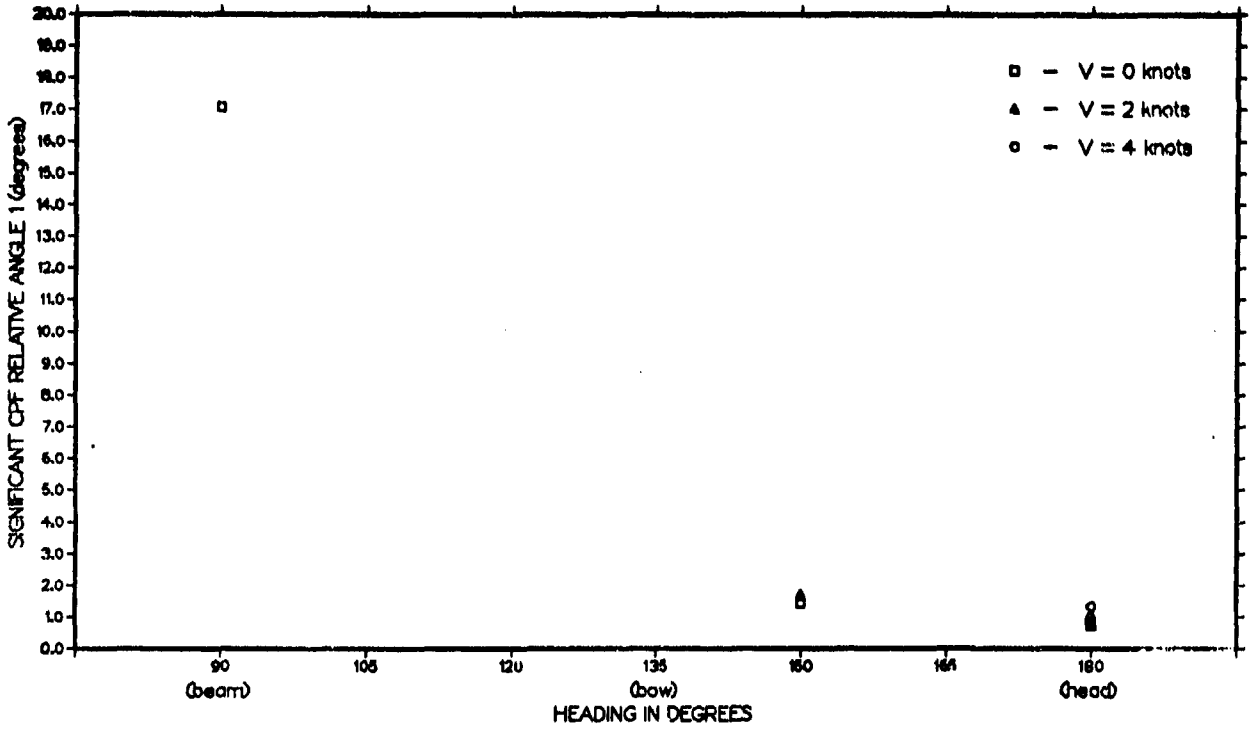

Figure 30A - Without Ramp and Causeway Ferry Connected

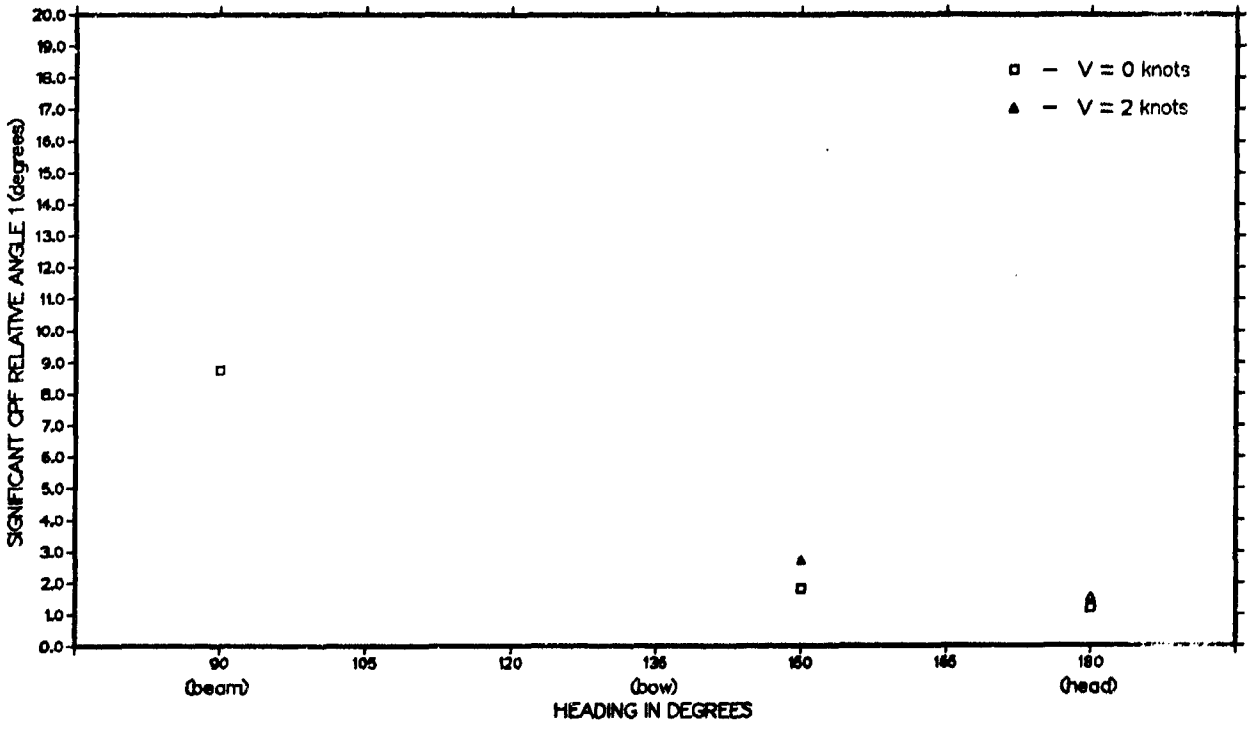

Figure 30B - With Ramp and Causeway Ferry Connected

Figure 31 - Significant Double Amplitude of Relative Angular Displacement at the Starboard Junction of the Causeway Platform Facility in Sea State 3

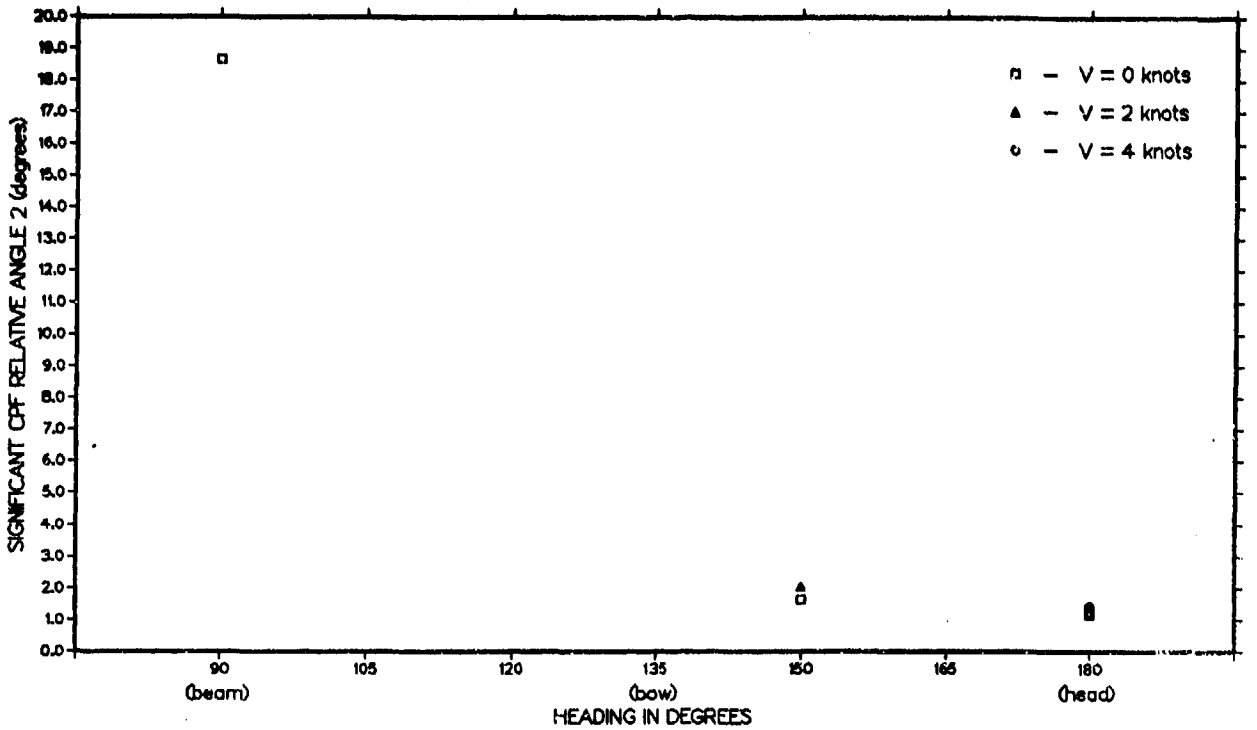

Figure 31A - Without Ramp and Causeway Ferry Connected

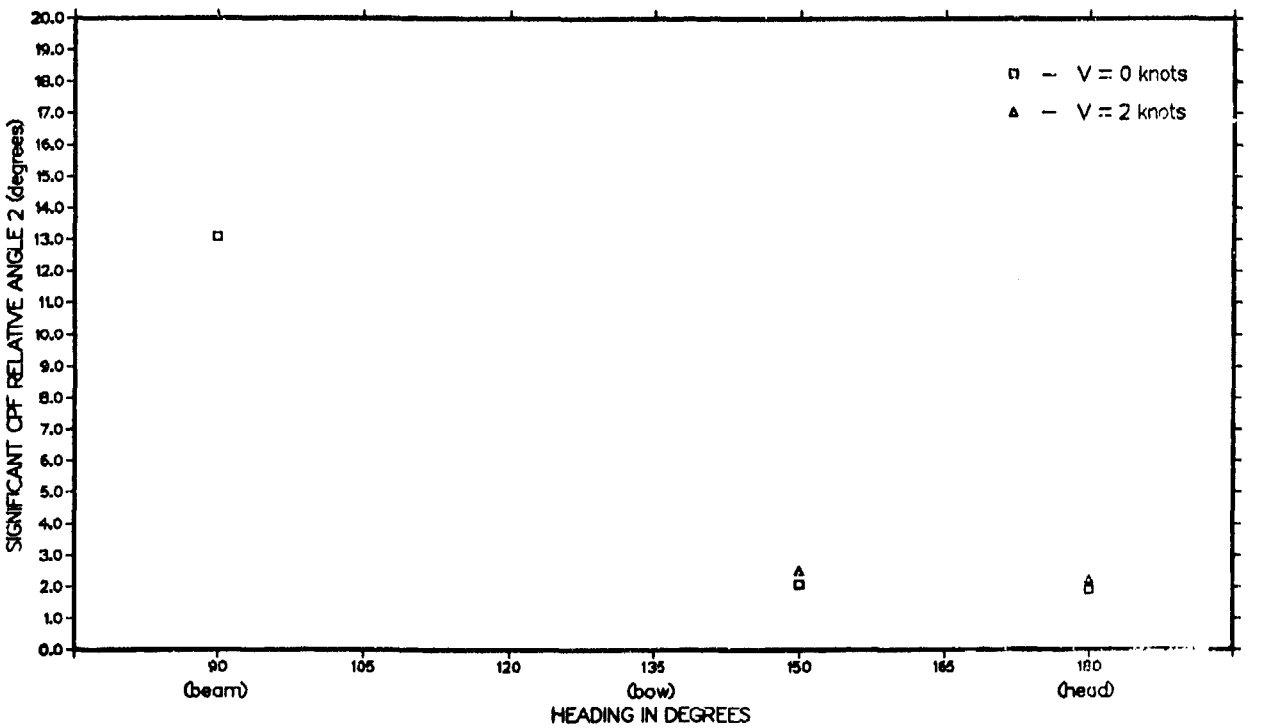

Figure 31B - With Ramp and Causeway Ferry Connected

Figure 32 - Significant Double Amplitude of Pitch of the RO/RO Ship in Sea State 3

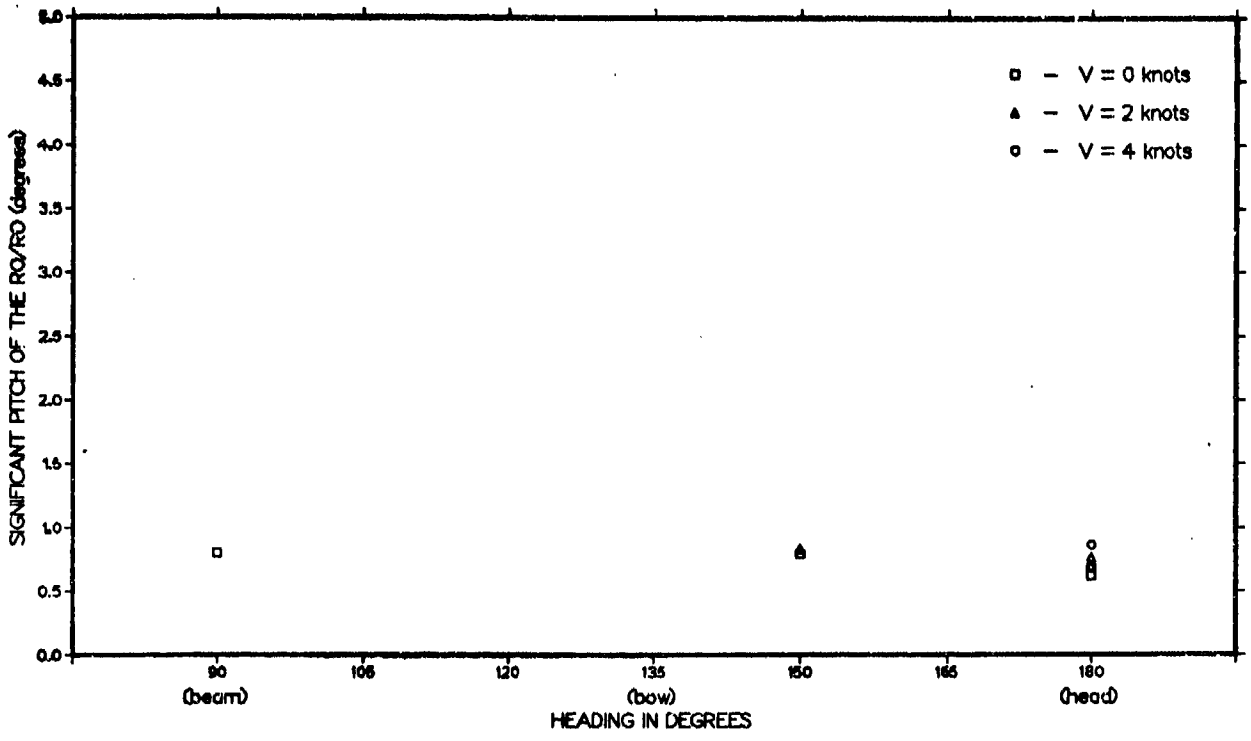

Figure 32A - Without Ramp and Causeway Ferry Connected

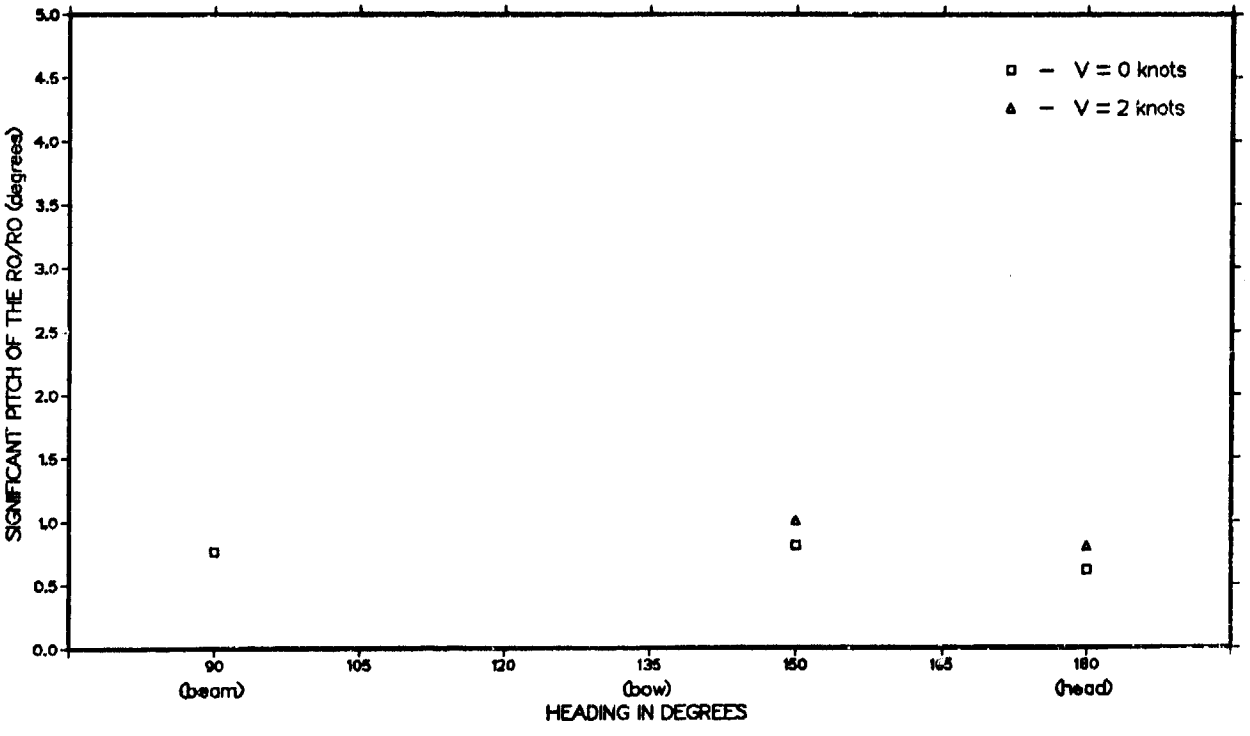

Figure 32B - With Ramp and Causeway Ferry Connected

Figure 33 - Significant Double Amplitude of Pitch of the Causeway Platform Facility in Sea State 3

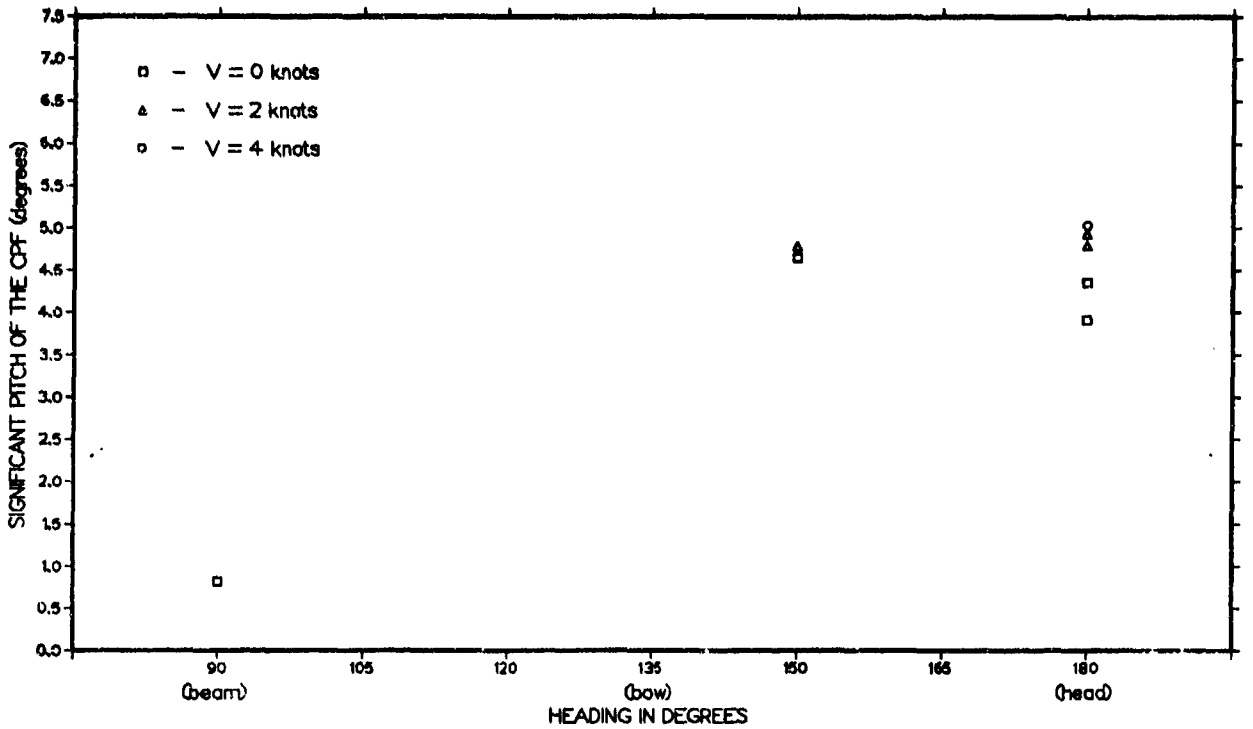

Figure 33A - Without Ramp and Causeway Ferry Connected

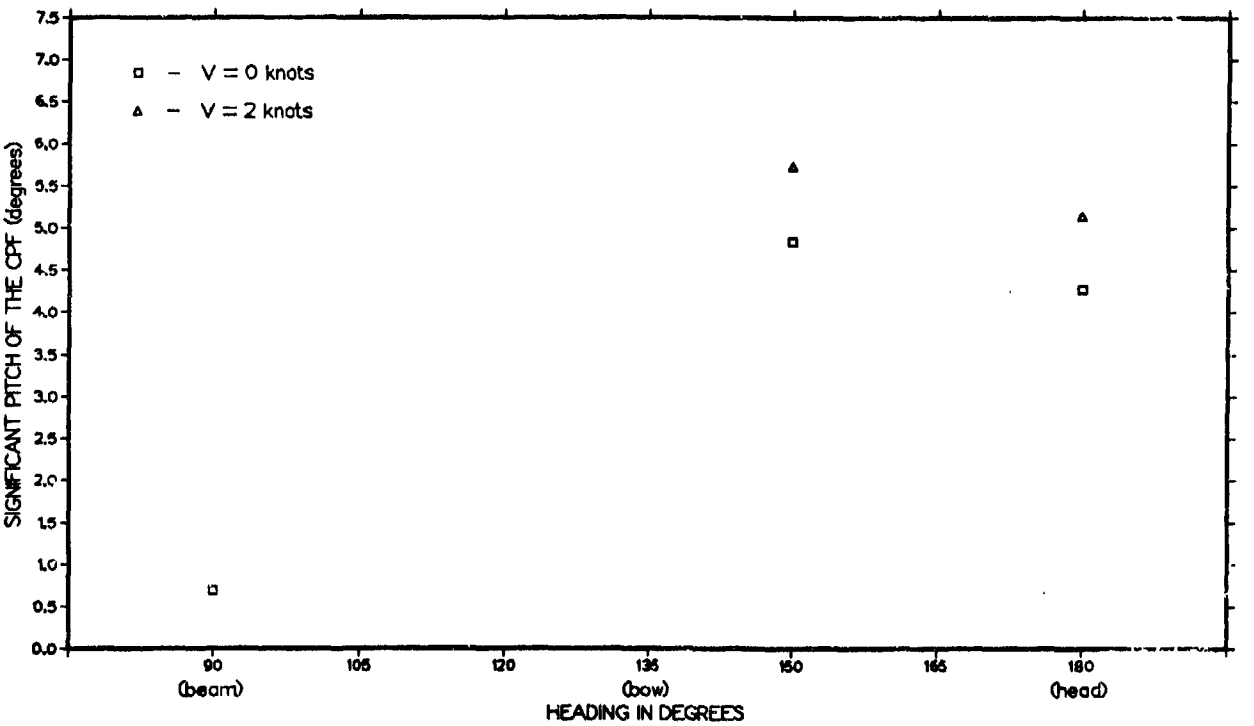

Figure 33B - With Ramp and Causeway Ferry Connected

Figure 34 - Significant Double Amplitude of Relative Angular Displacement at the Transverse Junction of the Causeway Platform Facility in Sea State 3

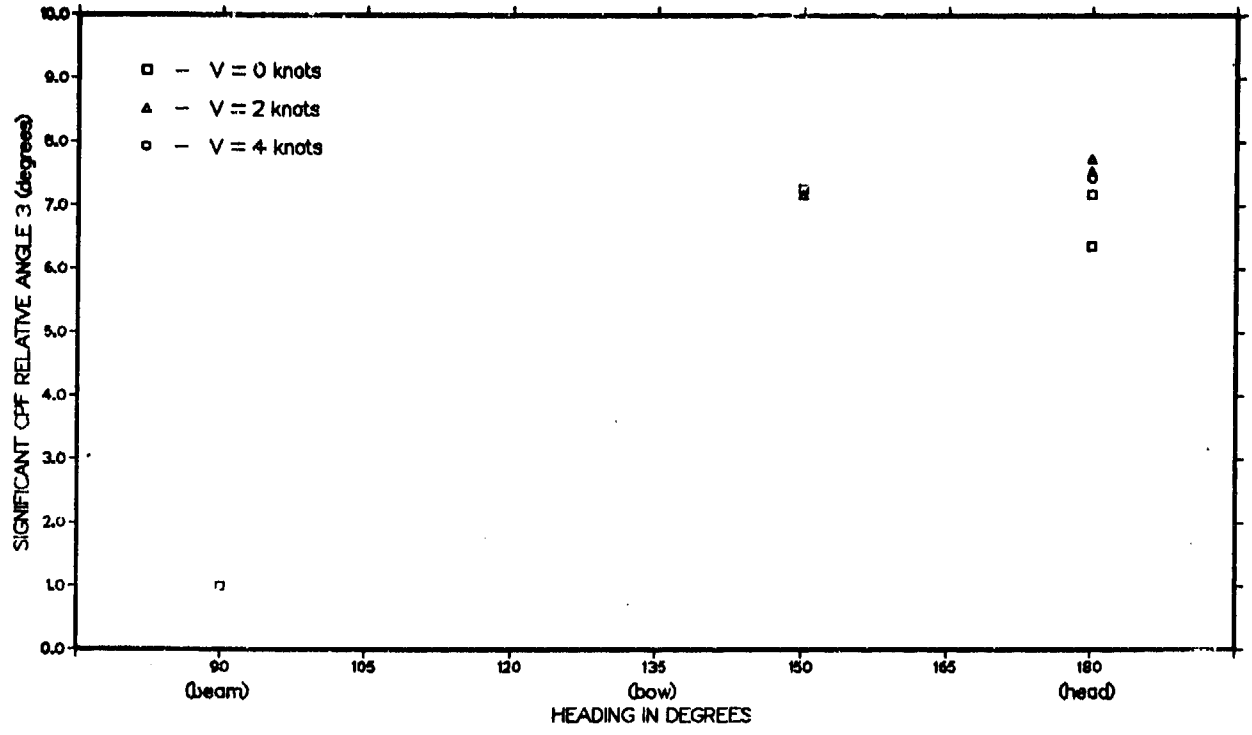

Figure 34A - Without Ramp and Causeway Ferry Connected

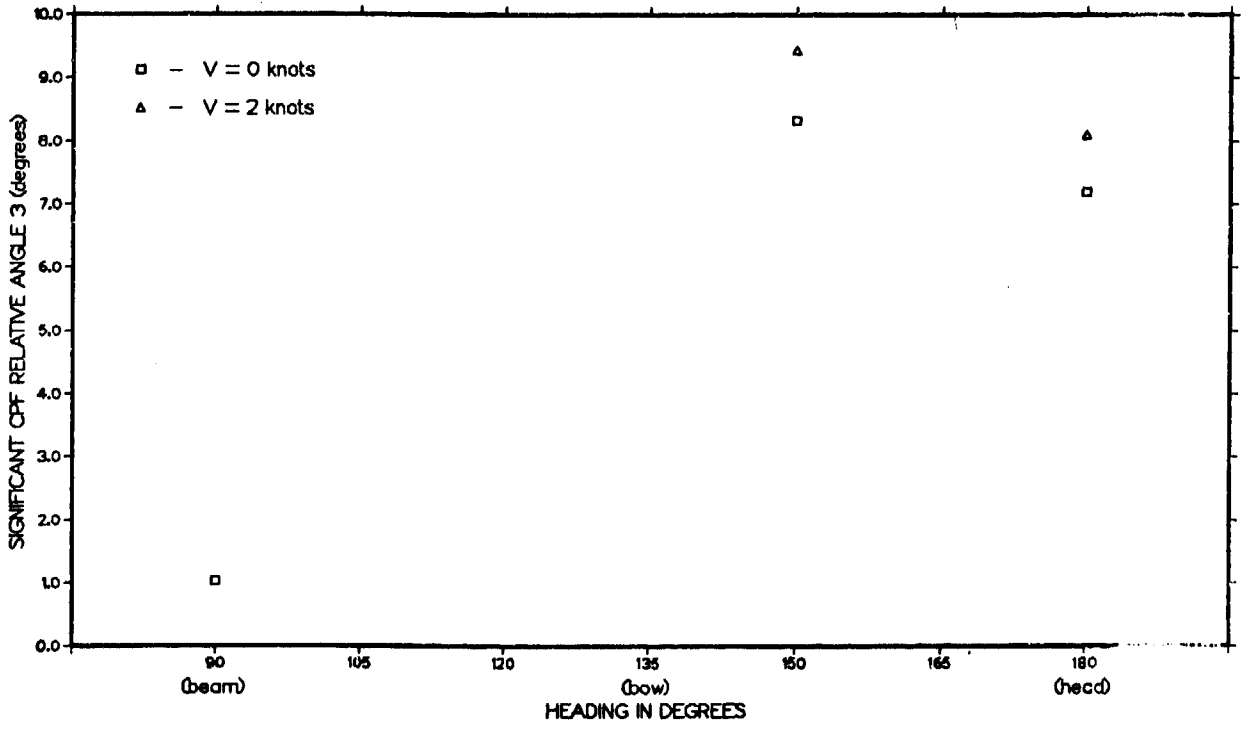

Figure 34B - With Ramp and Causeway Ferry Connected

Figure 35 - Significant Double Amplitude of Relative Vertical Displacement Between the RO/RO Ship and the Causeway Platform Facility in Sea State 3

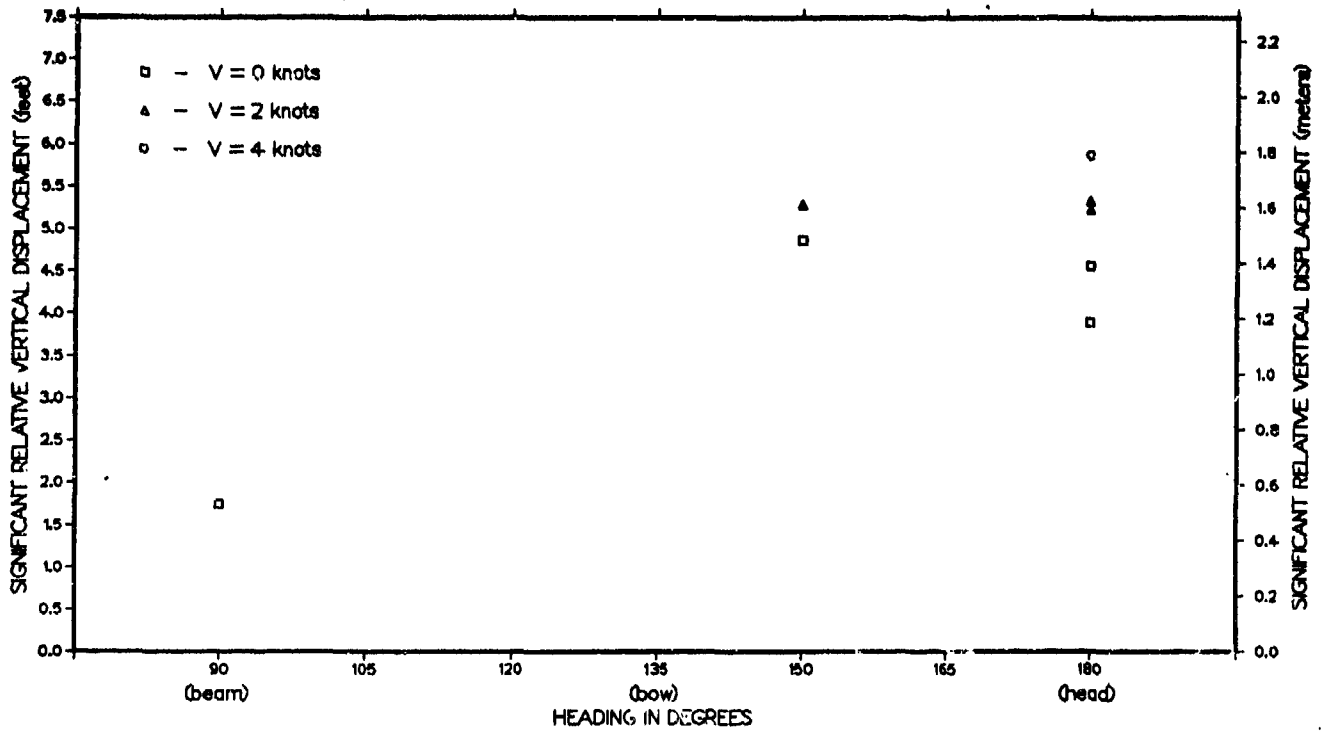

Figure 35A - Without Ramp and Causeway Ferry Connected

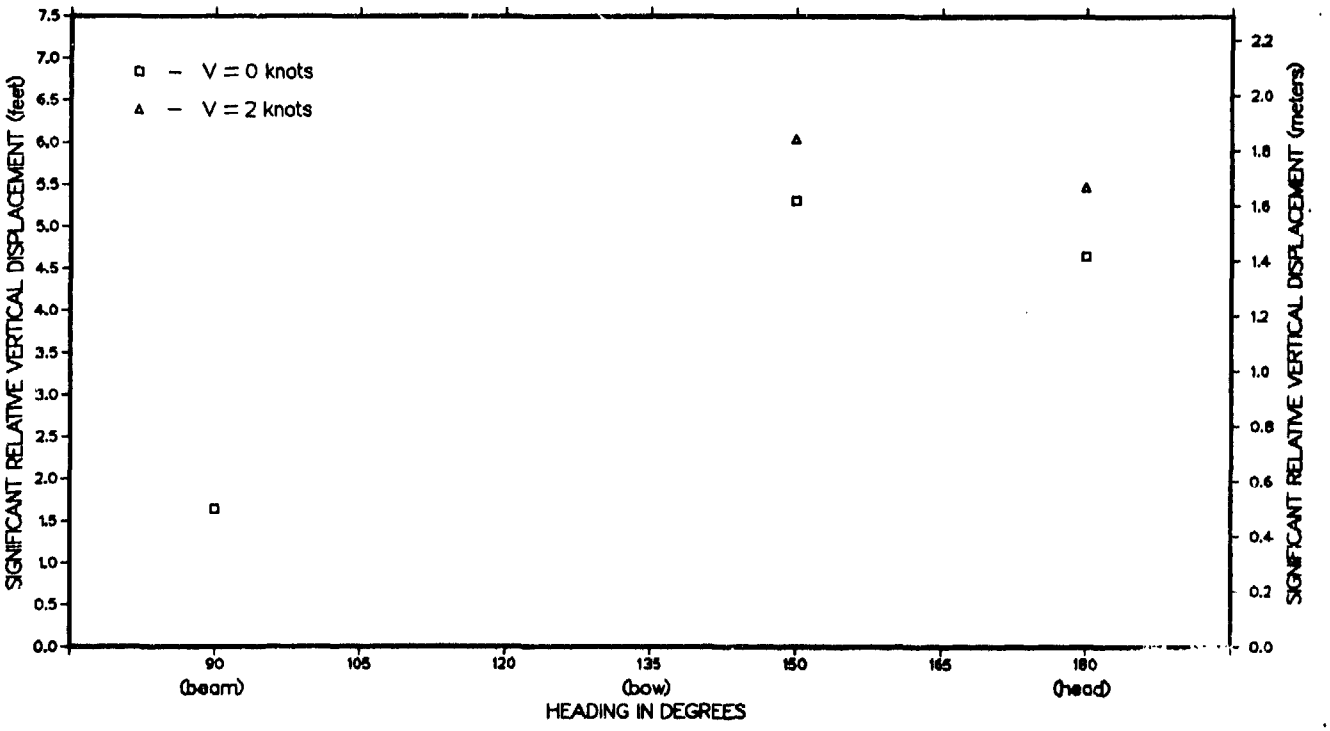

Figure 35B - With Ramp and Causeway Ferry Connected

Figure 36 - Significant Double Amplitude of Heave of the RO/RO Ship in Sea State 3

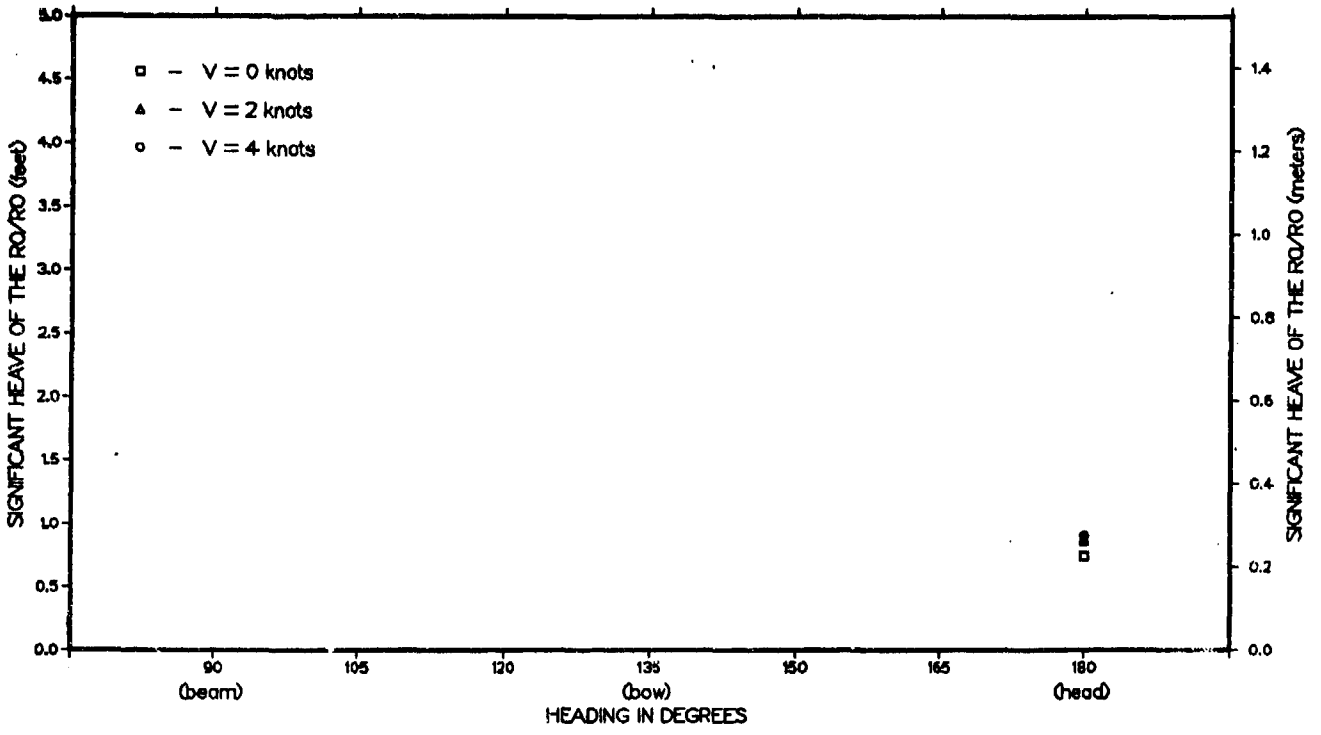

Figure 36A - Without Ramp and Causeway Ferry Connected

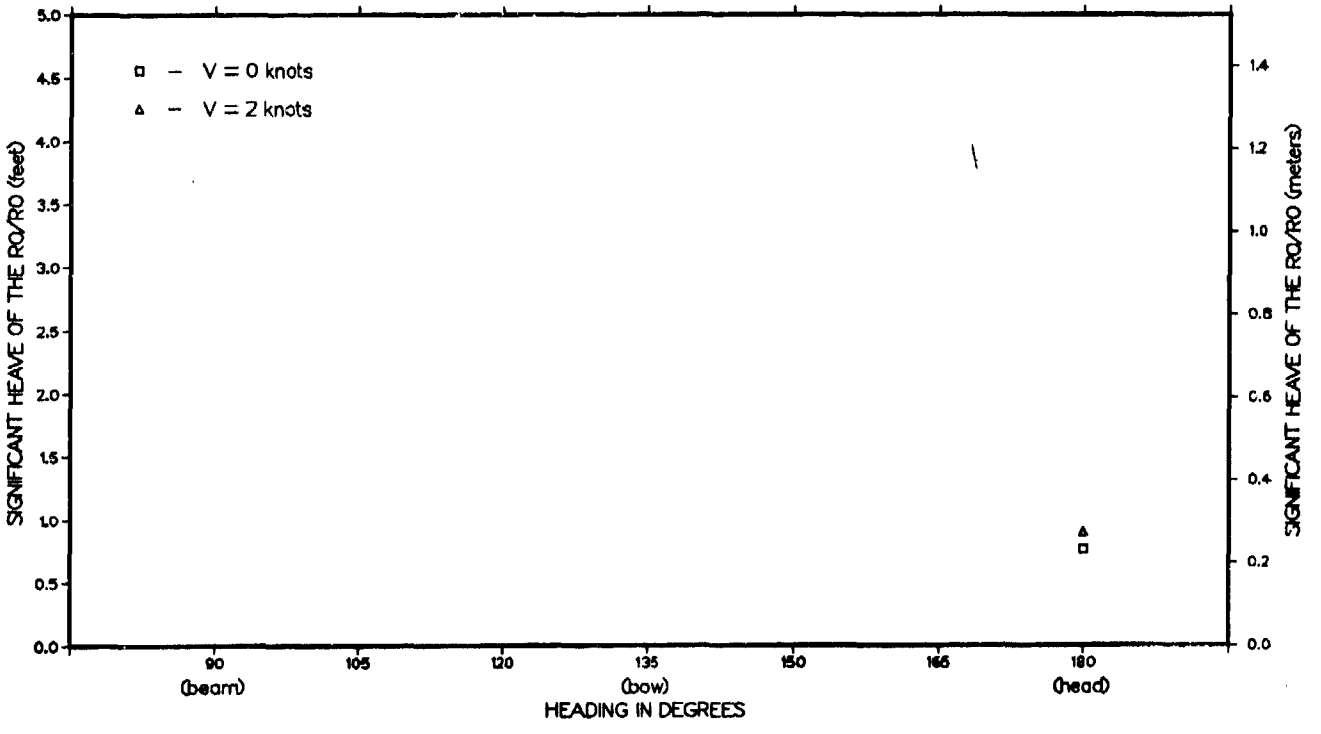

Figure 36B - With Ramp and Causeway Ferry Connected

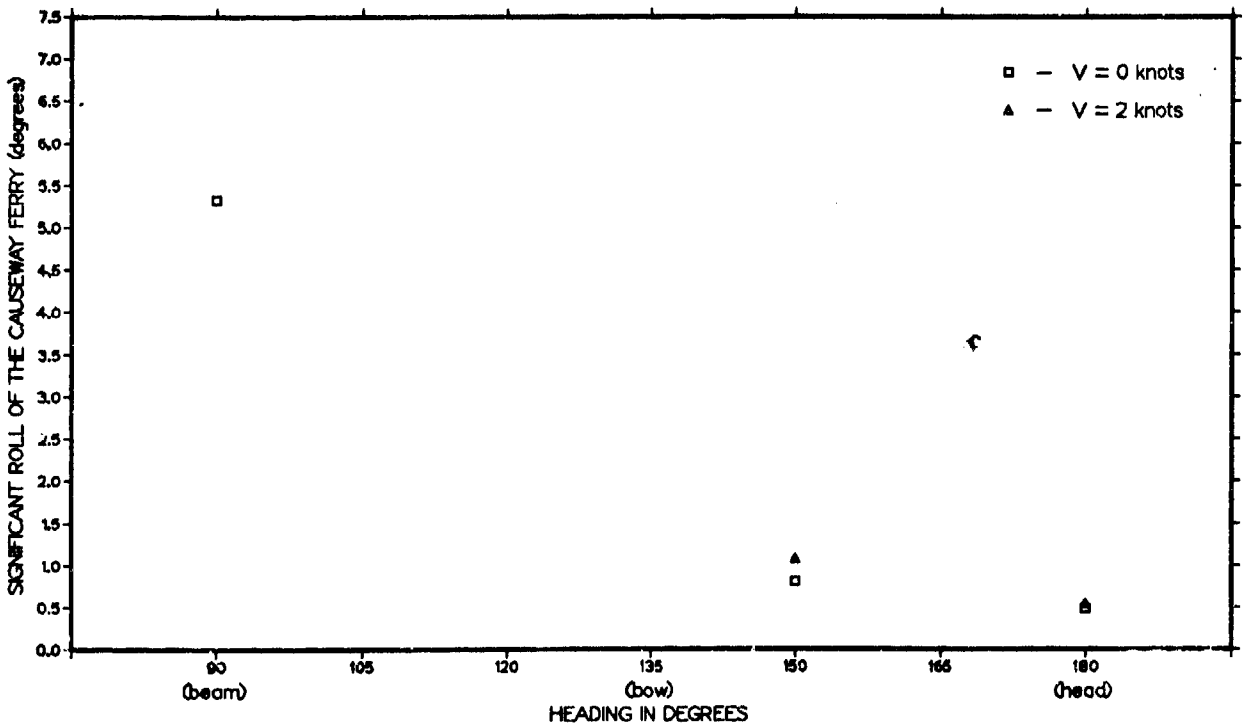

Figure 37 - Significant Double Amplitude of Roll of the Causeway Ferry in Sea State 3

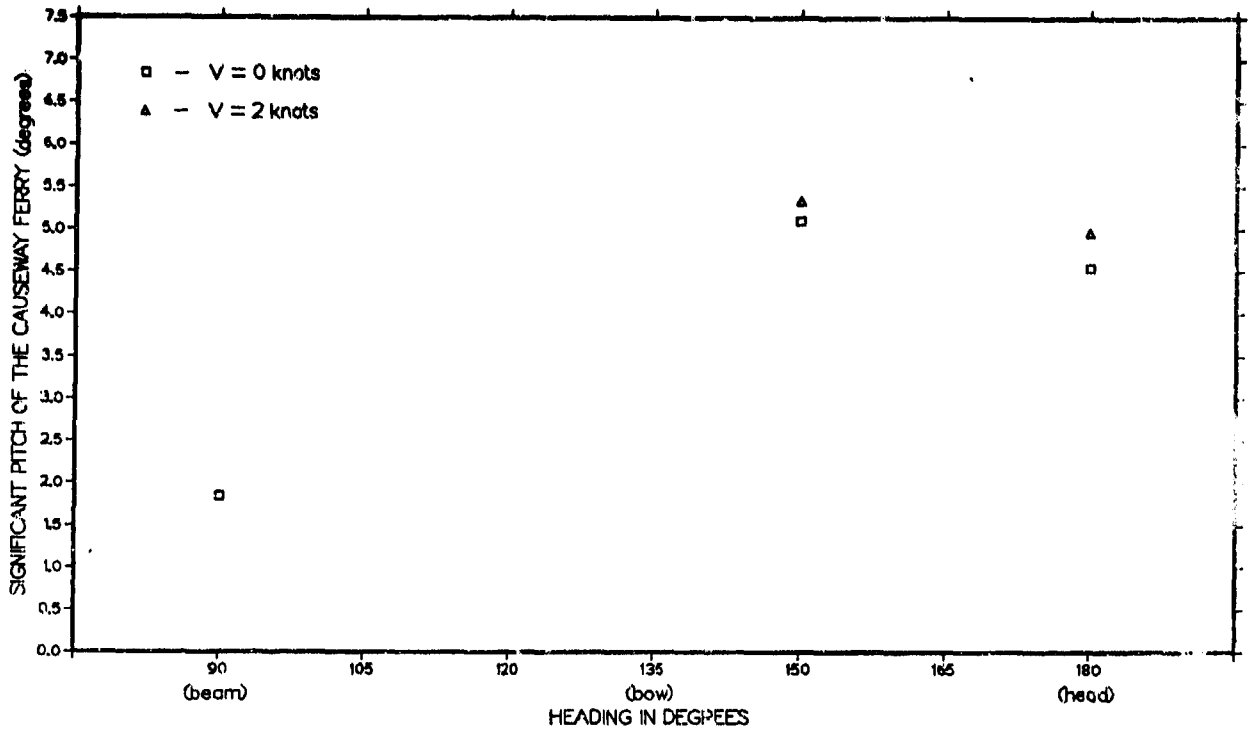

Figure 38 - Significant Double Amplitude of Pitch of the Causeway Ferry in Sea State 3

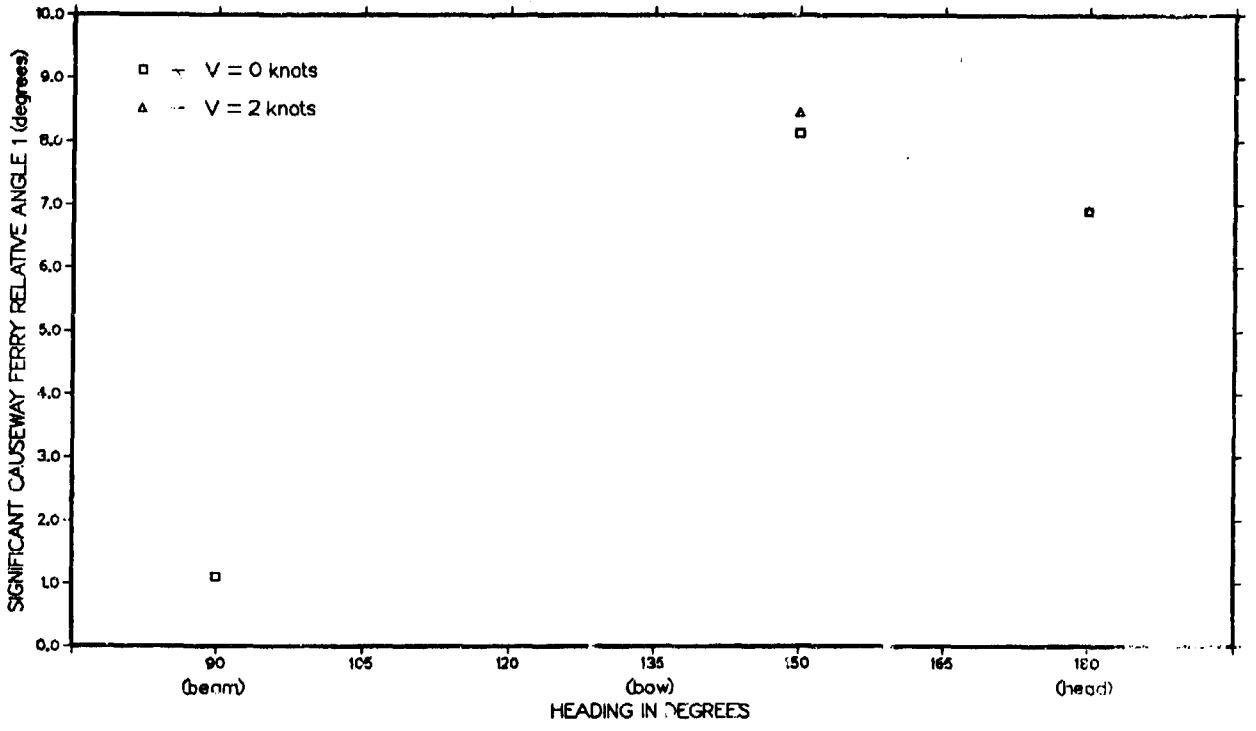

Figure 39 - Significant Double Amplitude of Relative Angular Displacement at the Junction Between the Causeway Platform Facility and the Causeway Ferry in Sea State 3

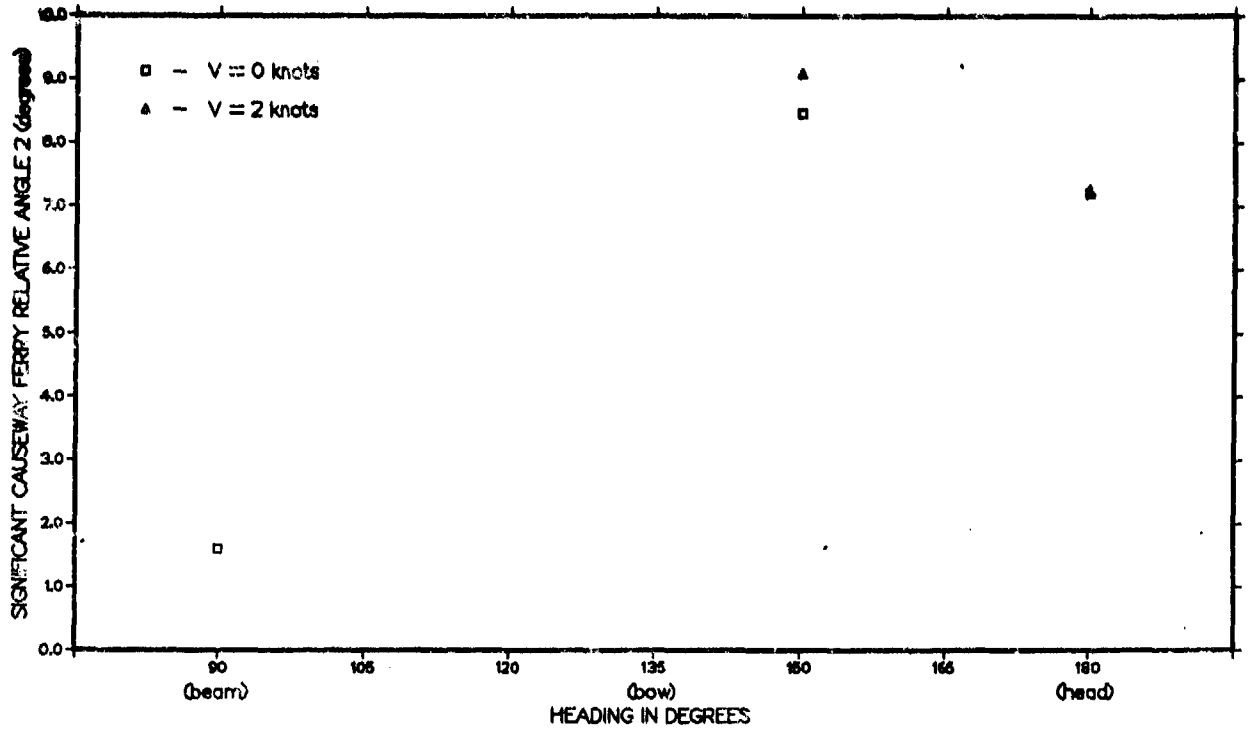

Figure 40 - Significant Double Amplitude of Relative Angular Displacement at the Junction Between the First and Second Sections of the Causeway Ferry in Sea State 3

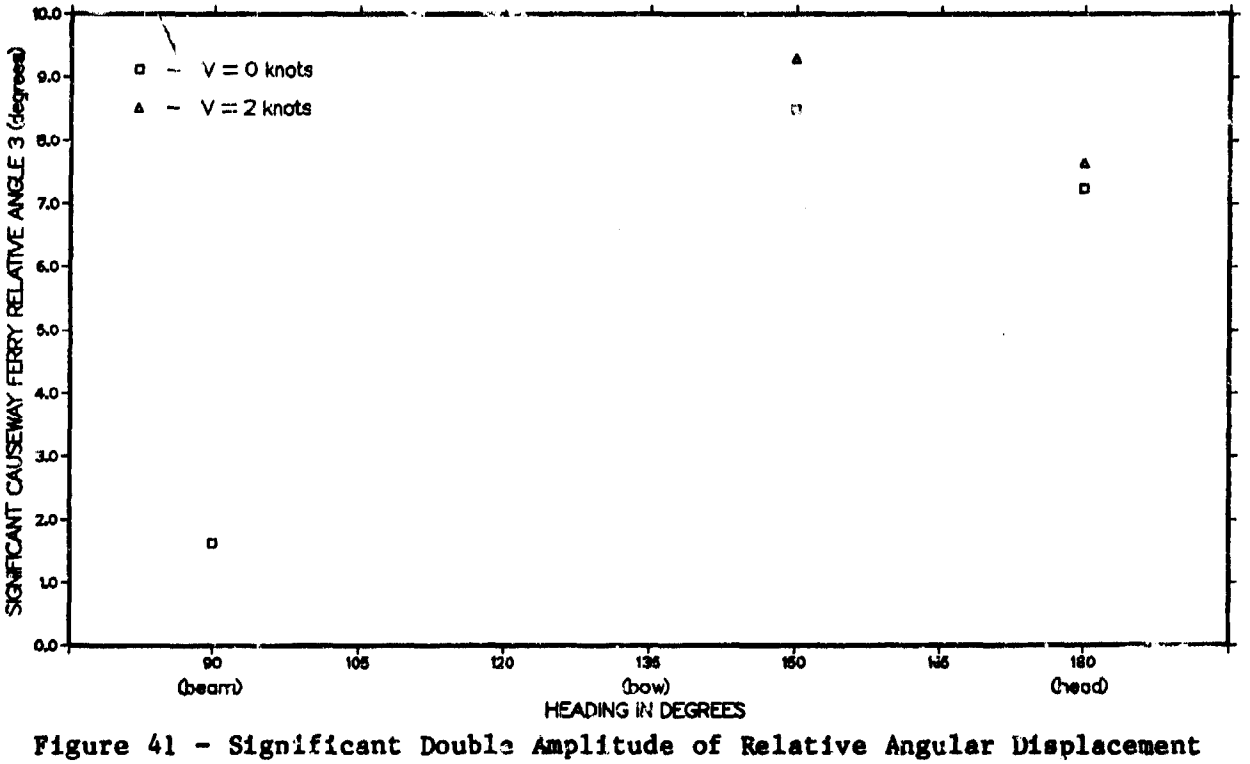

Figure 41 - Significant Double Amplitude of Relative Angular Displacement at the Junction Between the Second and Third Sections of the Causeway Ferry in Sea State 3

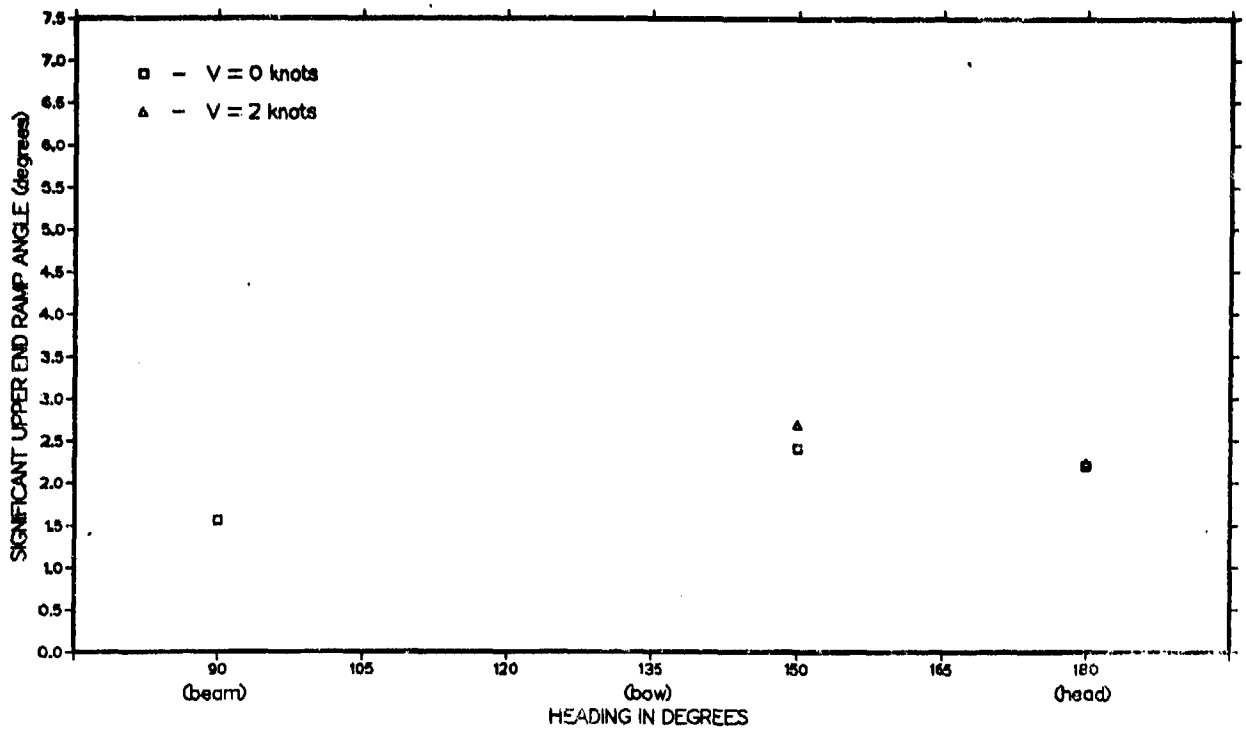

Figure 42 - Significant Double Amplitude of Relative Angular Displacement at the Upper End of the Off-loading Ramp in Sea State 3

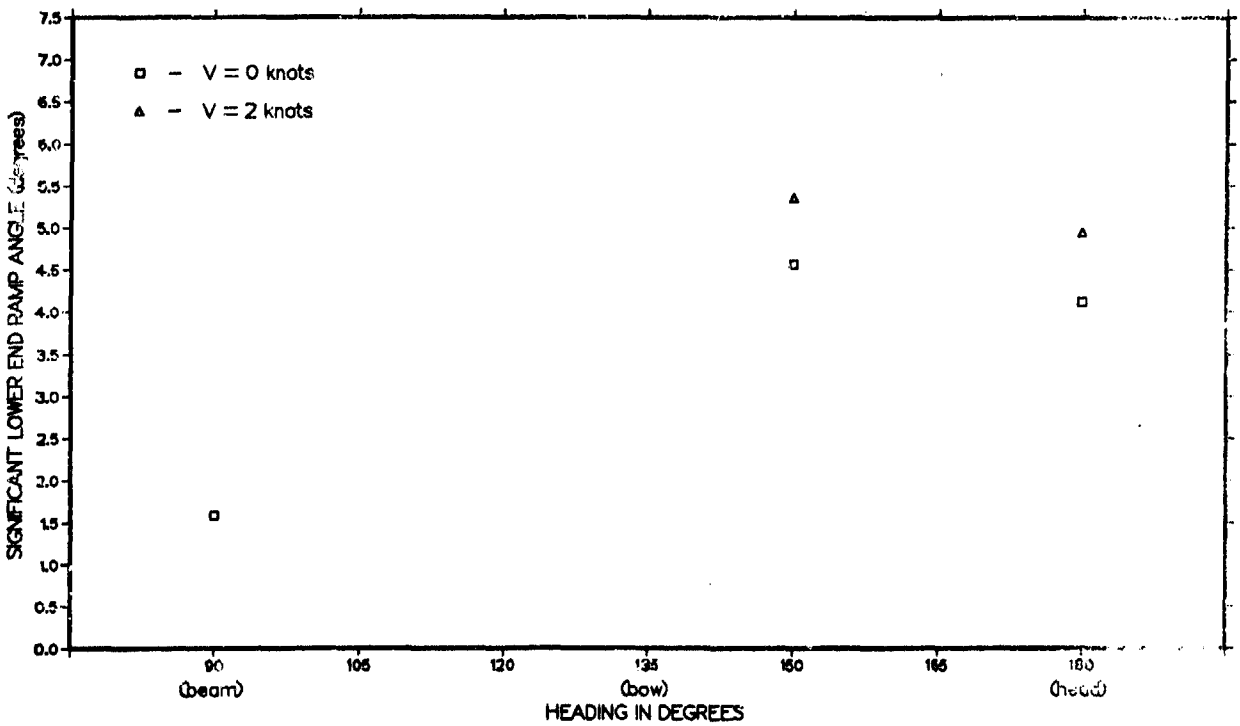

Figure 43 - Significant Double Amplitude of Relative Angular Displacement at the Lower End of the Off-loading Ramp in Sea State 3

TABLE A.1 - CONFIGURATION/SWELL FREQUENCY COMBINATIONS TESTED		
90 deg	CONFIGURATION 1	$\omega_s^* = 1.498$ rps
135 deg	↓	$\omega_s = 0.865$ rps
180 deg	↓	$\omega_s = 0.865$ rps
90 deg	CONFIGURATION 2	$\omega_s = 1.498$ rps
135 deg	↓	$\omega_s = 1.060$ rps
180 deg	↓	$\omega_s = 1.060$ rps
$^*\omega_s$ are full scale values of the superimposed swell frequencies		

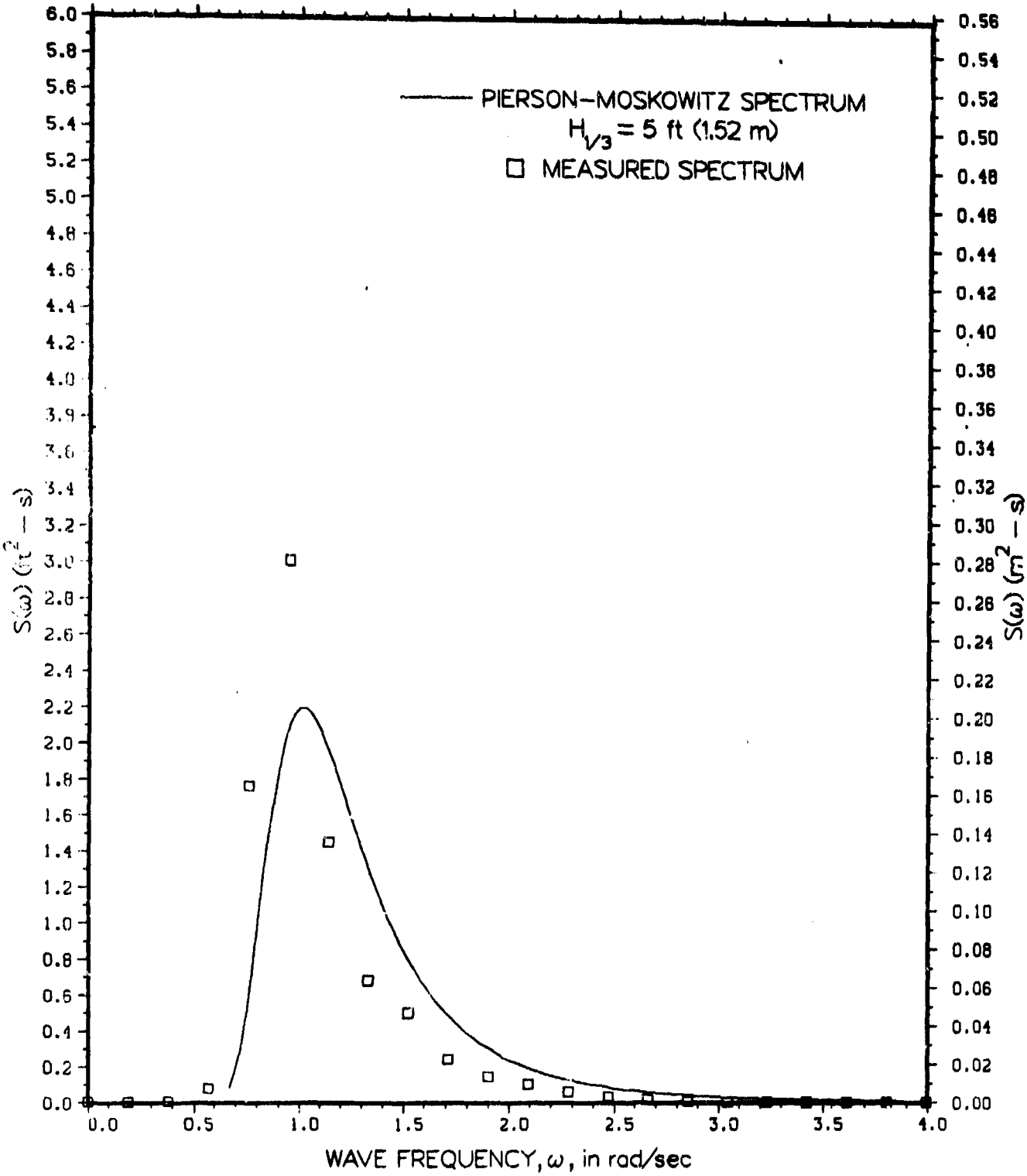

Figure A.1 - Irregular Wave Spectrum with Superimposed Swell Frequency of 0.87 rad/sec — Used for 135 and 180 degree Headings for Configuration 1

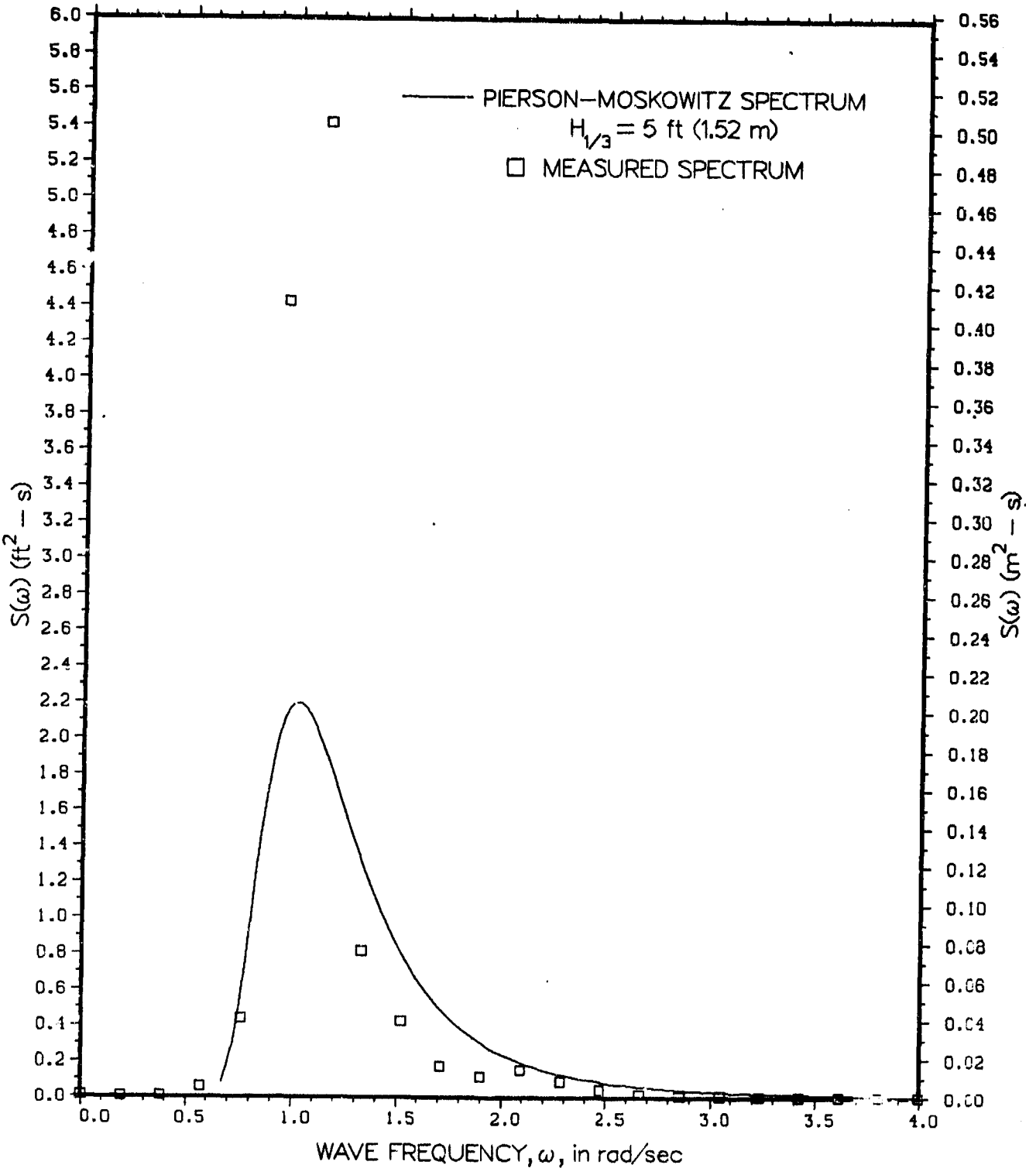

Figure A.2 - Irregular Wave Spectrum with Superimposed Swell Frequency of 1.06 rad/sec — Used for 135 and 180 degree Headings for Configuration 2

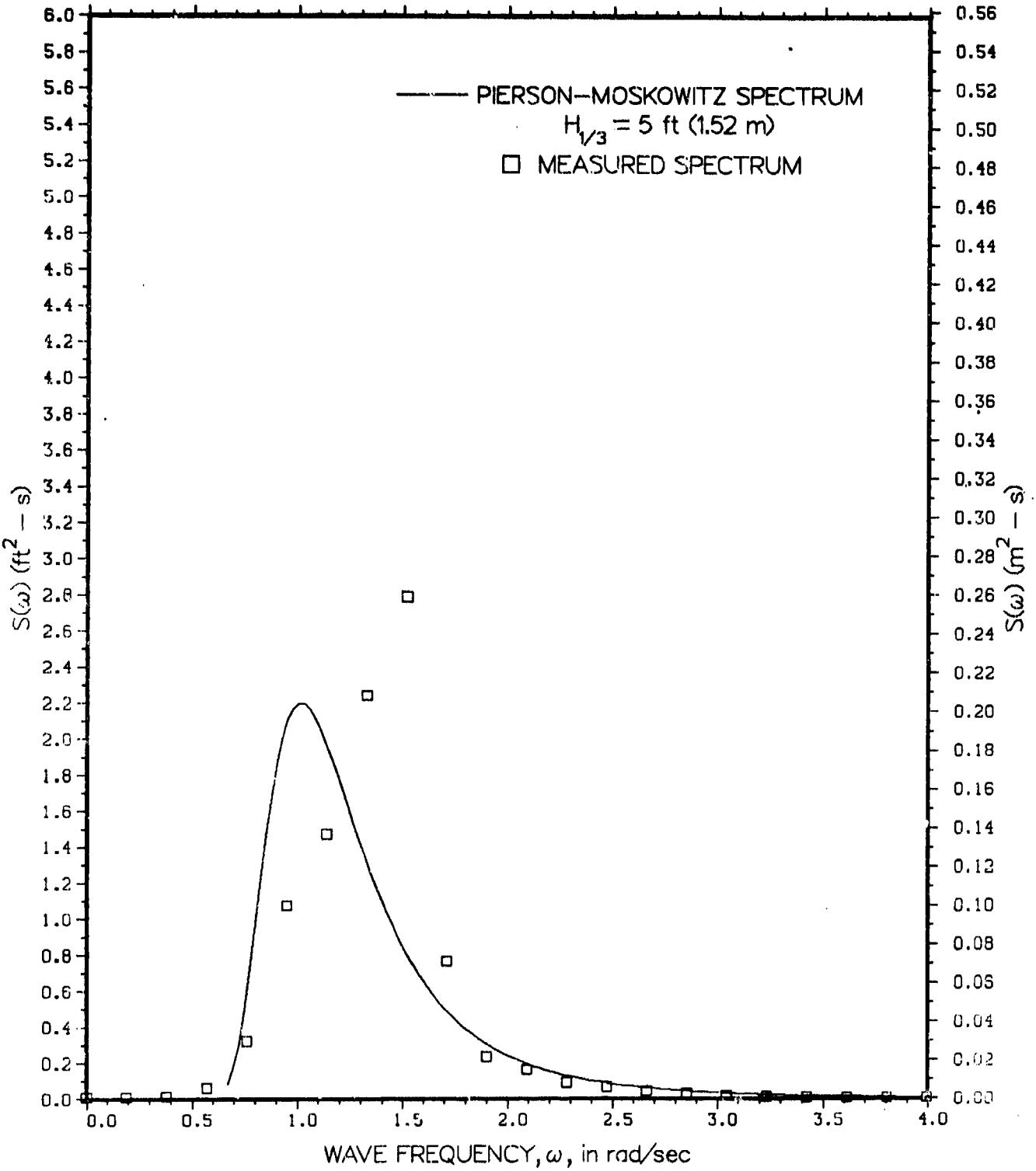

Figure A.3 - Irregular Wave Spectrum with Superimposed Swell Frequency of 1.50 rad/sec — Used for 90 degree Heading for Configurations 1 and 2

Figure A.4 - Significant Double Amplitude of Roll of the RO/RO Ship in Sea State 3 with Swell Superimposed

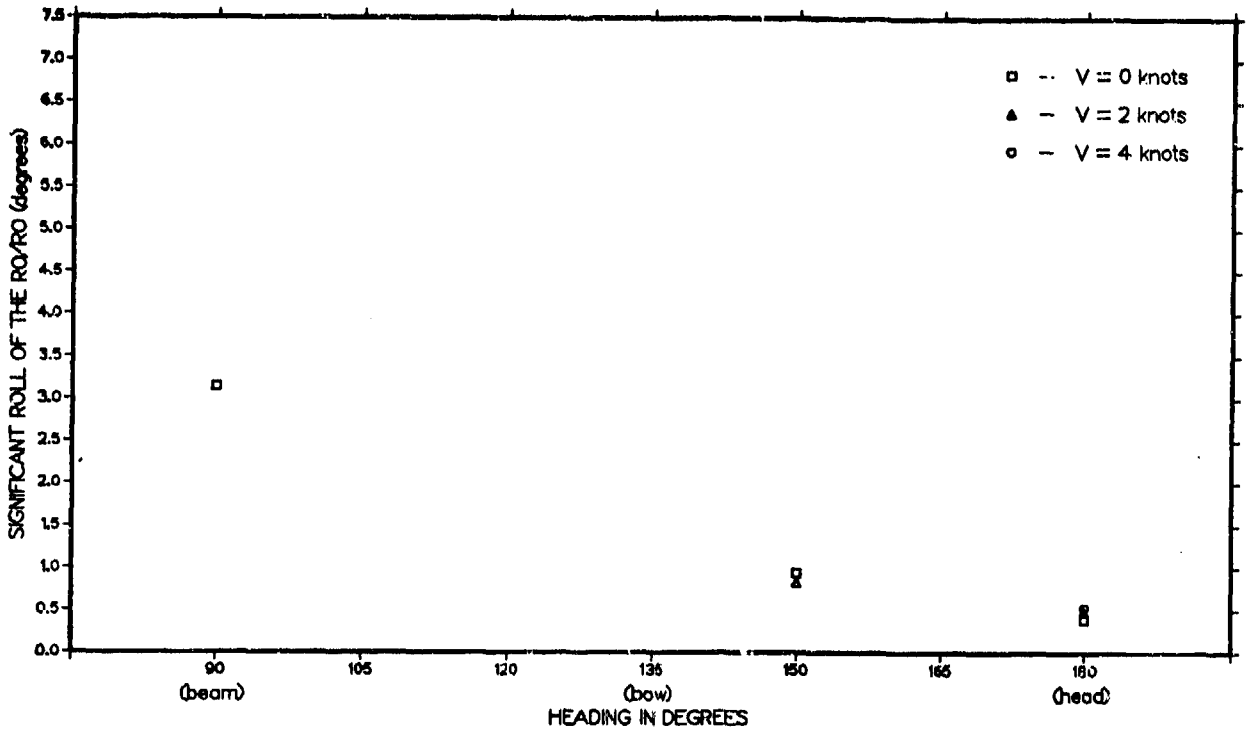

Figure A.4A - Without Ramp and Causeway Ferry Connected

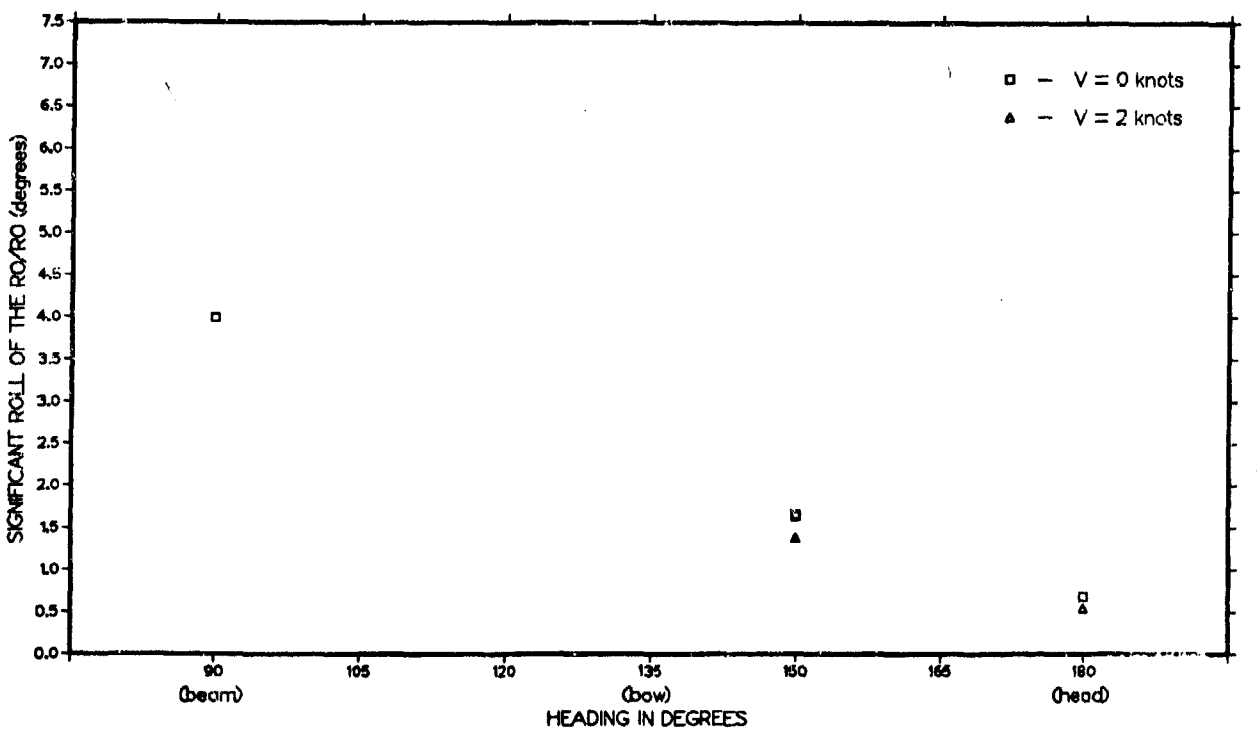

Figure A.4B - With Ramp and Causeway Ferry Connected

Figure A.5 - Significant Double Amplitude of Roll of the Causeway Platform Facility in Sea State 3 with Swell Superimposed

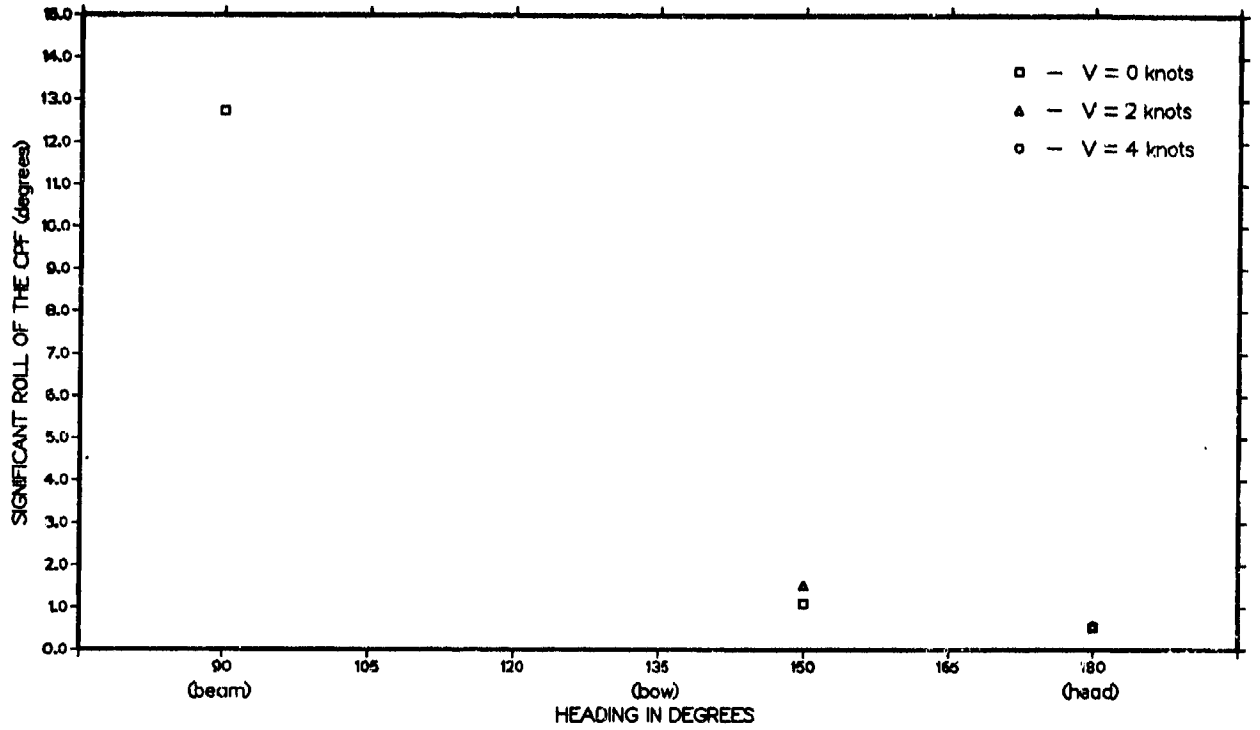

Figure A.5A - Without Ramp and Causeway Ferry Connected

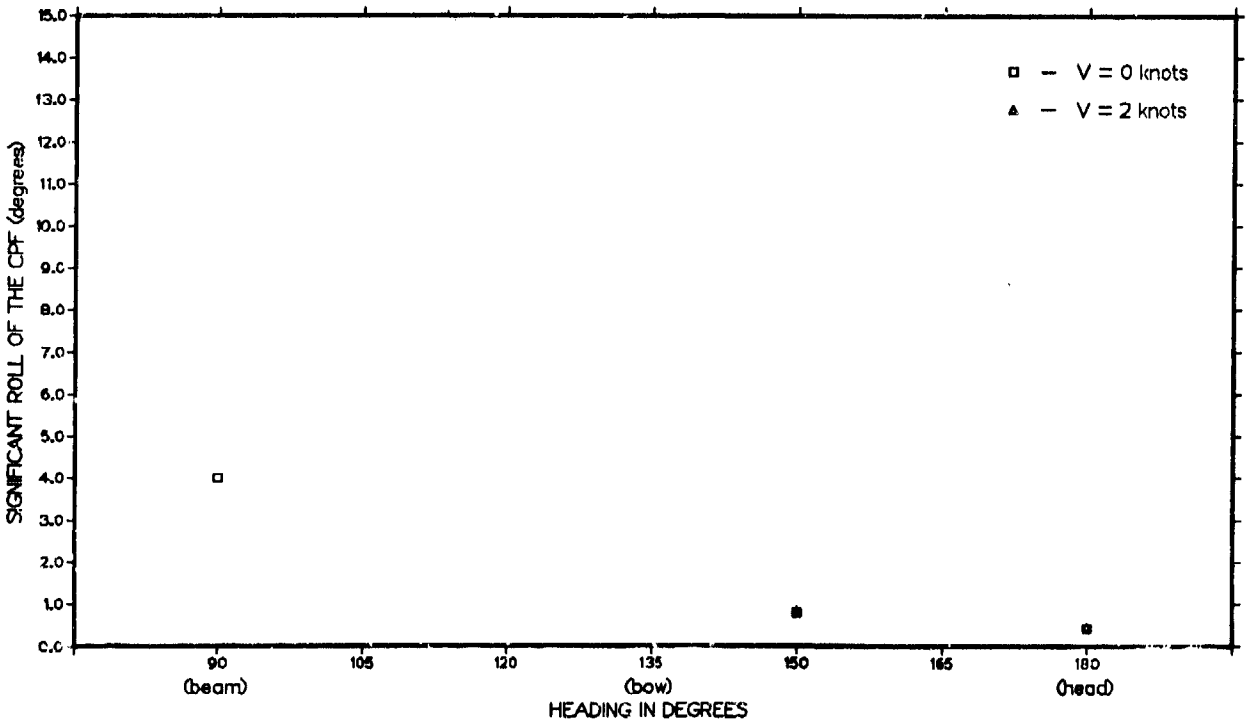

Figure A.5B - With Ramp and Causeway Ferry Connected

Figure A.6 - Significant Double Amplitude of Relative Angular Displacement at the Port Junction of the Causeway Platform Facility in Sea State 3 with Swell Superimposed

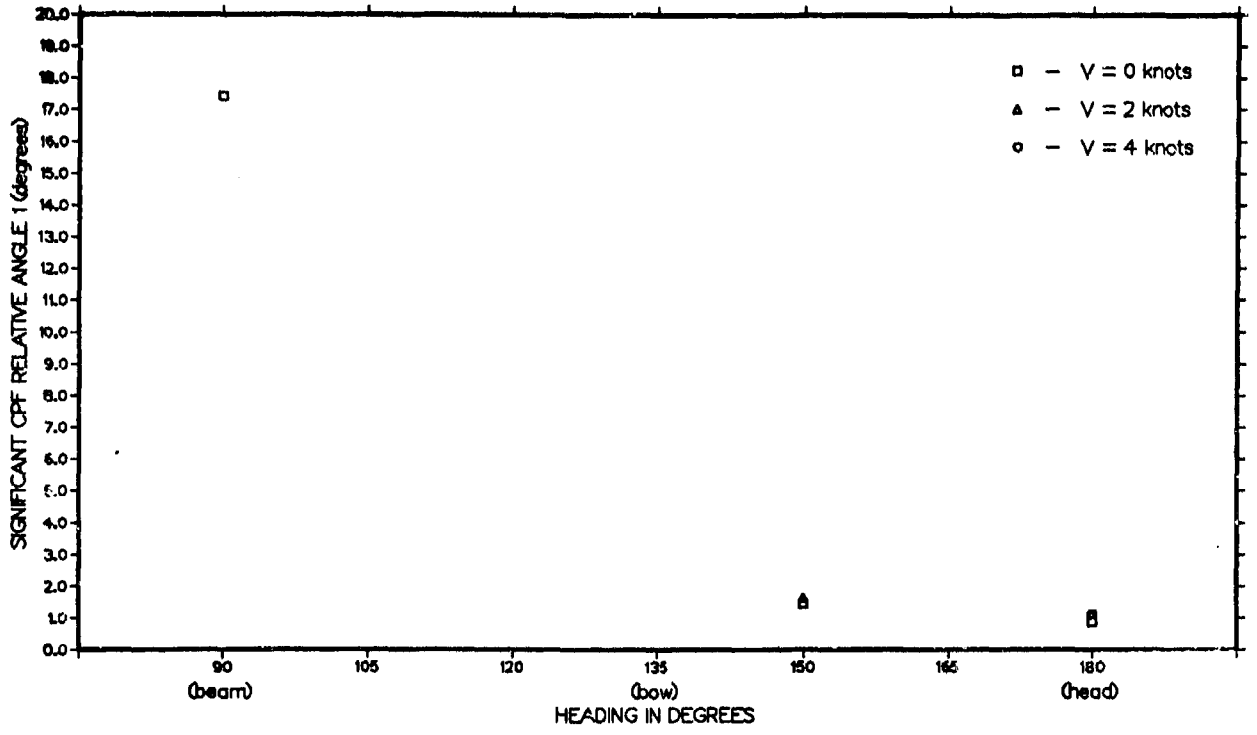

Figure A.6A - Without Ramp and Causeway Ferry Connected

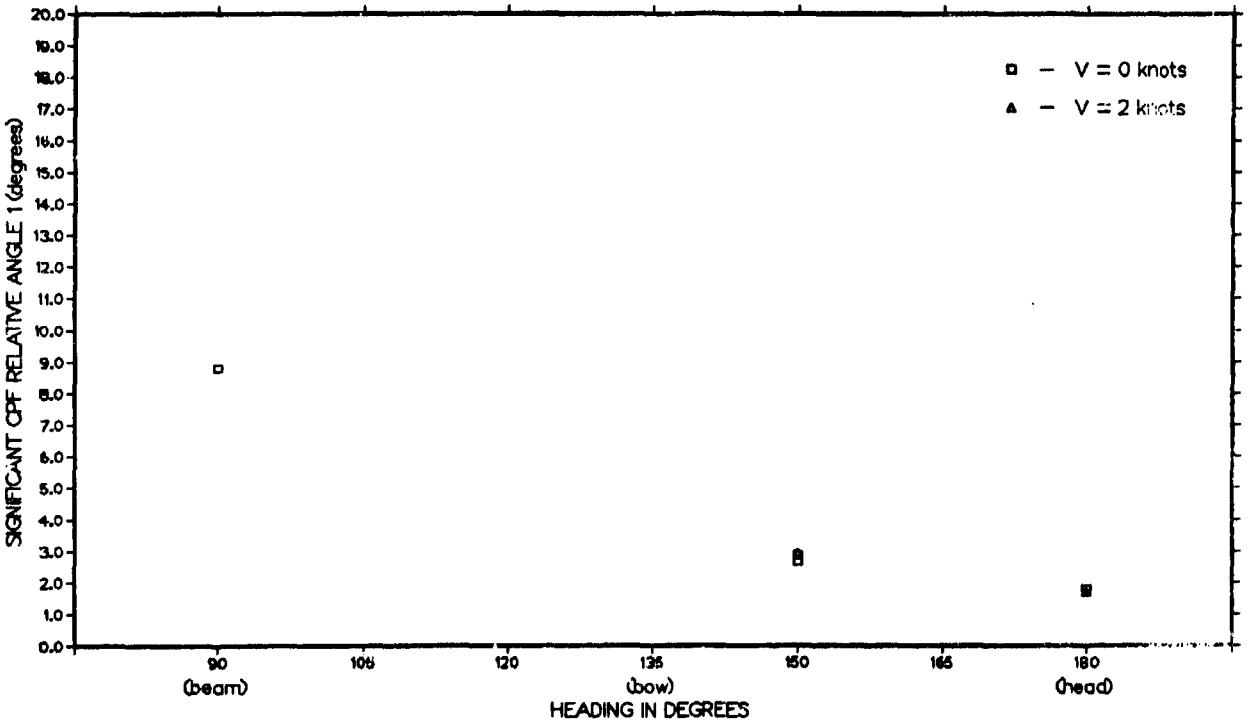

Figure A.6B - With Ramp and Causeway Ferry Connected

Figure A.7 - Significant Double Amplitude of Relative Angular Displacement at the Starboard Junction of the Causeway Platform Facility in Sea State 3 with Swell Superimposed

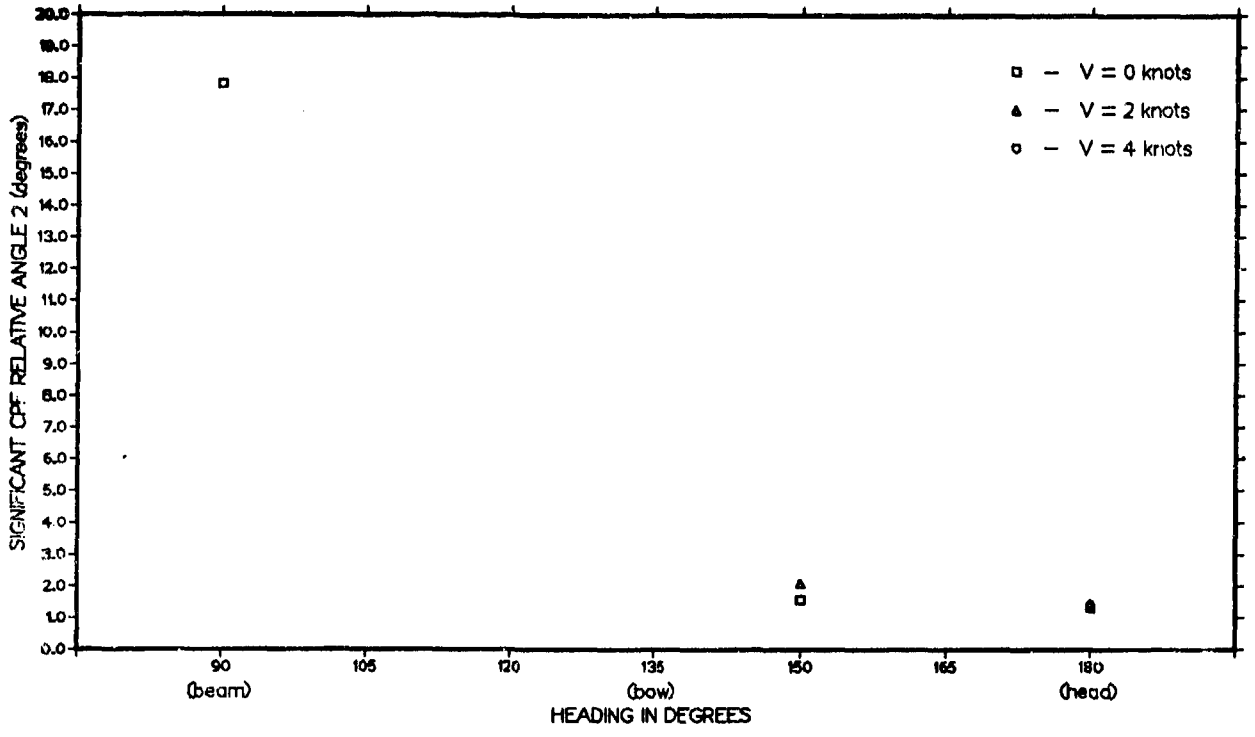

Figure A.7A - Without Ramp and Causeway Ferry Connected

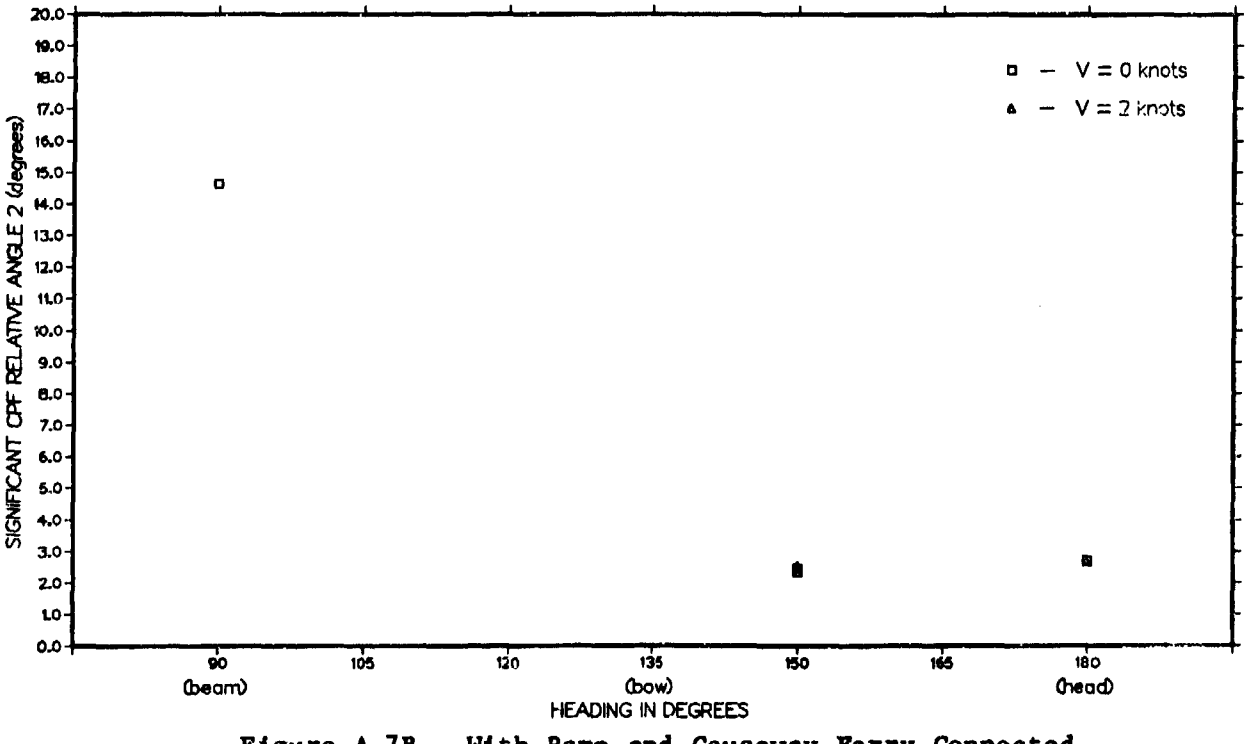

Figure A.7B - With Ramp and Causeway Ferry Connected

Figure A.8 - Significant Double Amplitude of Pitch of the RO/RO Ship in Sea State 3 with Swell Superimposed

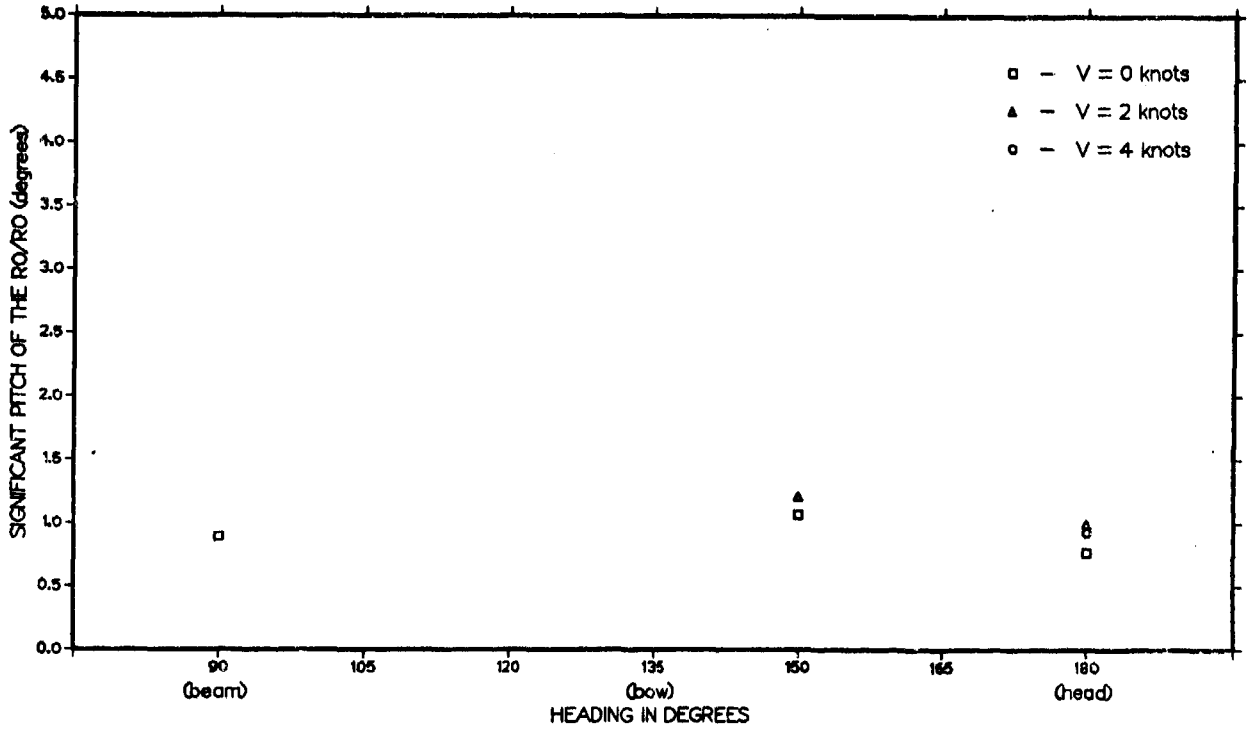

Figure A.8A - Without Ramp and Causeway Ferry Connected

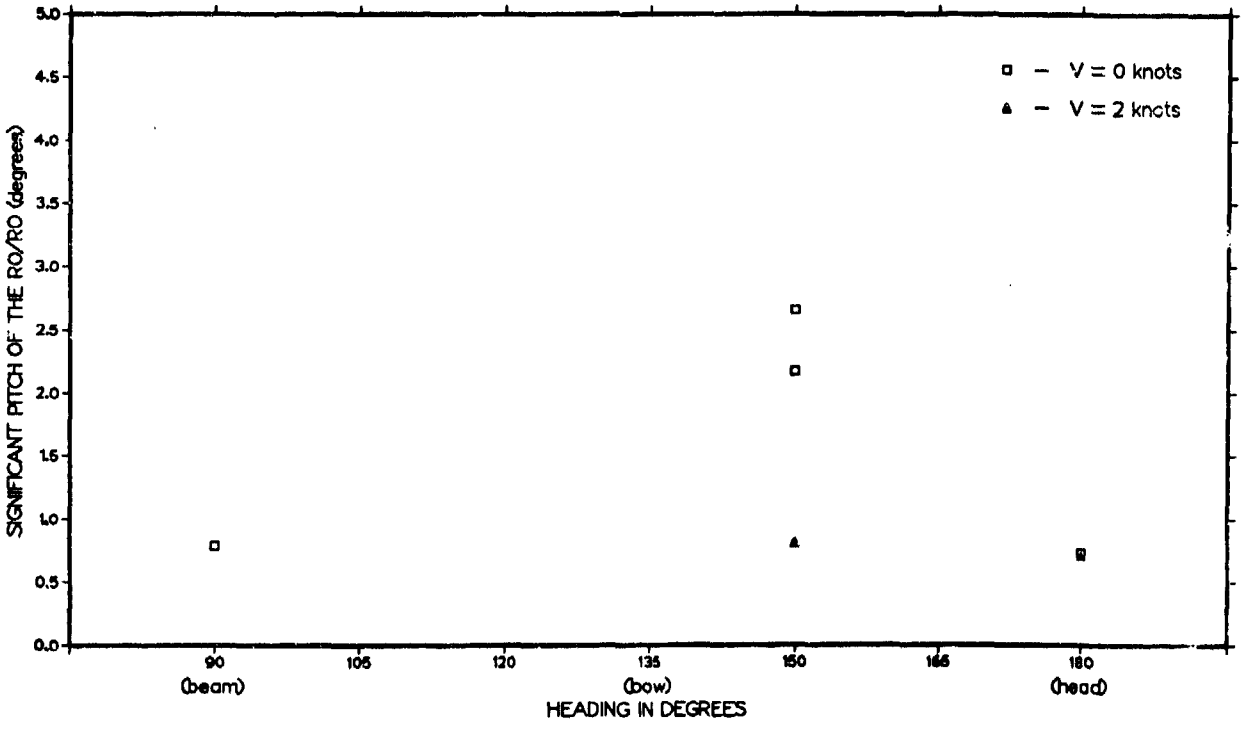

Figure A.8B - With Ramp and Causeway Ferry Connected

Figure A.9 - Significant Double Amplitude of Pitch of the Causeway Platform Facility in Sea State 3 with Swell Superimposed

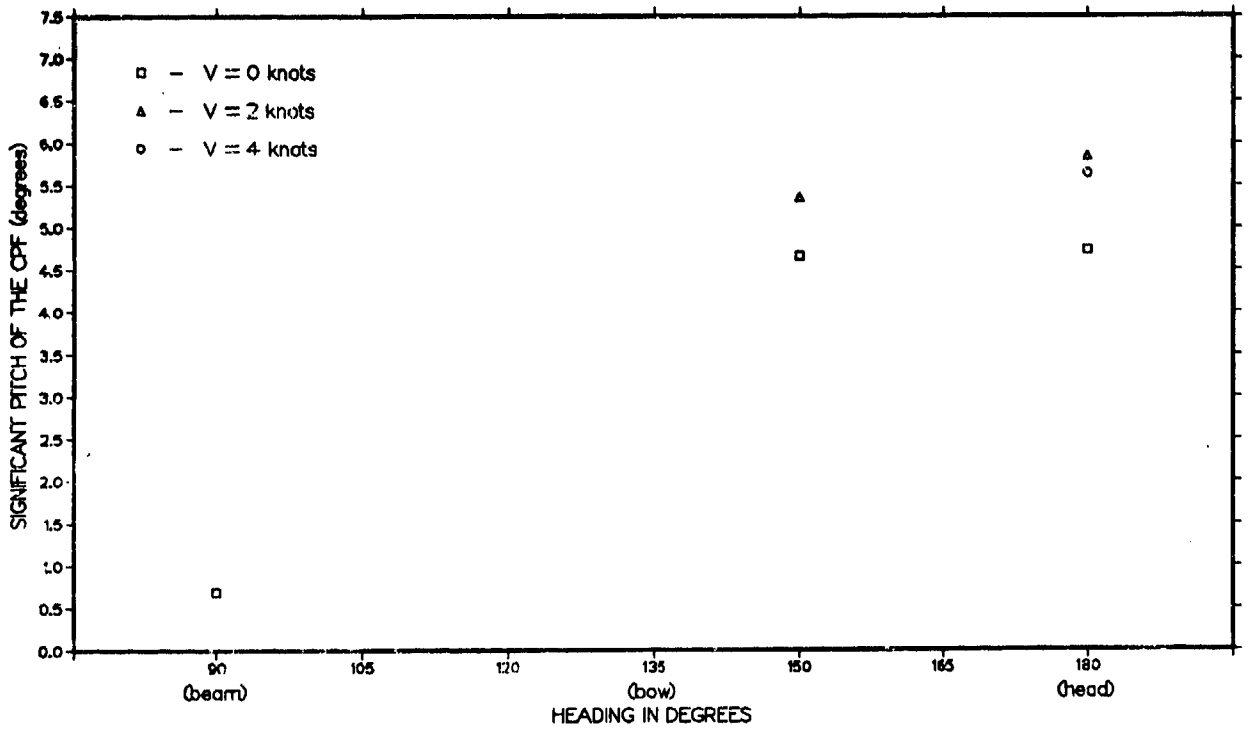

Figure A.9A - Without Ramp and Causeway Ferry Connected

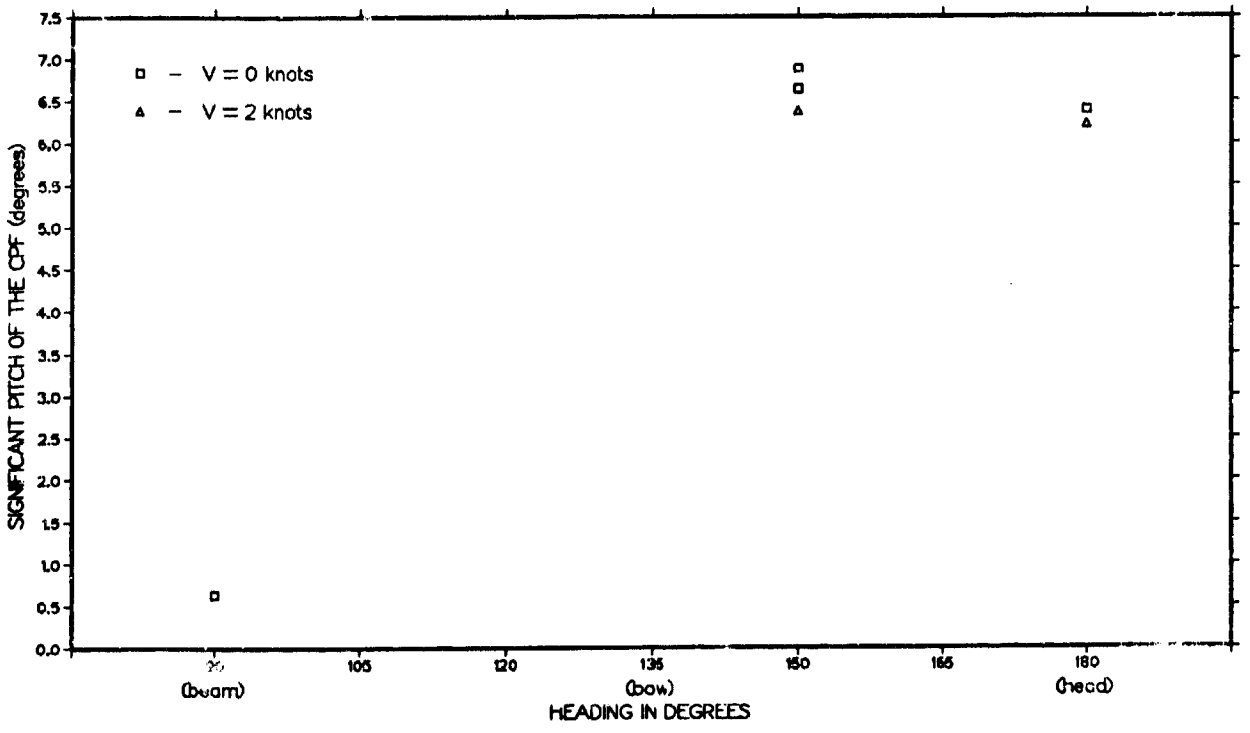

Figure A.9B - With Ramp and Causeway Ferry Connected

Figure A.10 - Significant Double Amplitude of Relative Angular Displacement at the Transverse Junction of the Causeway Platform Facility in Sea State 3 with Swell Superimposed

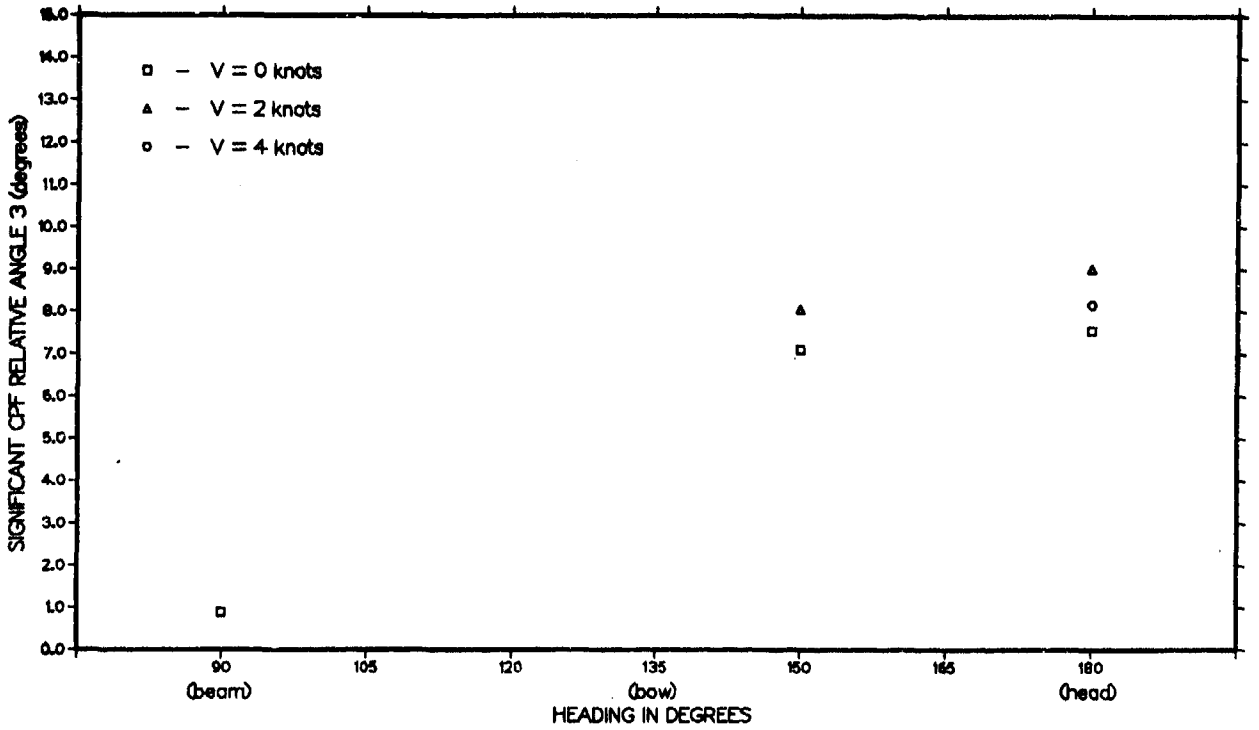

Figure A.10A - Without Ramp and Causeway Ferry Connected

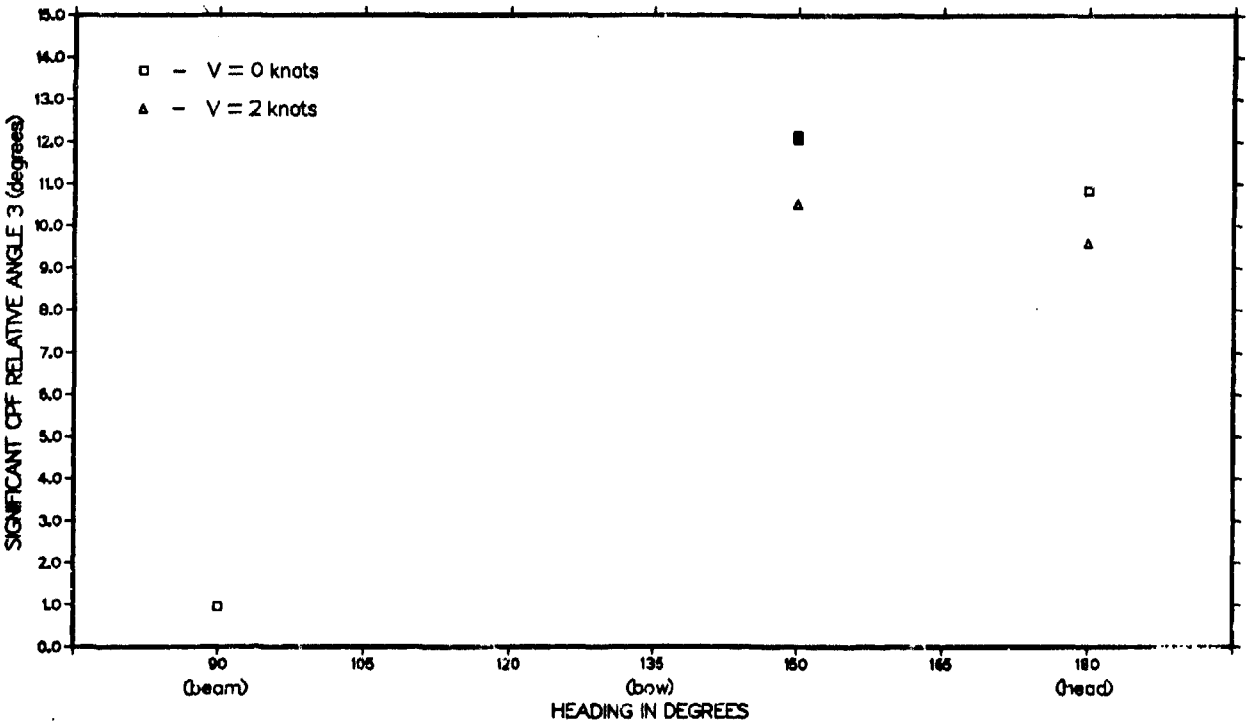

Figure A.10B - With Ramp and Causeway Ferry Connected

Figure A.11 - Significant Double Amplitude of Relative Vertical Displacement Between the RO/RO Ship and the Causeway Platform Facility in Sea State 3 with Swell Superimposed

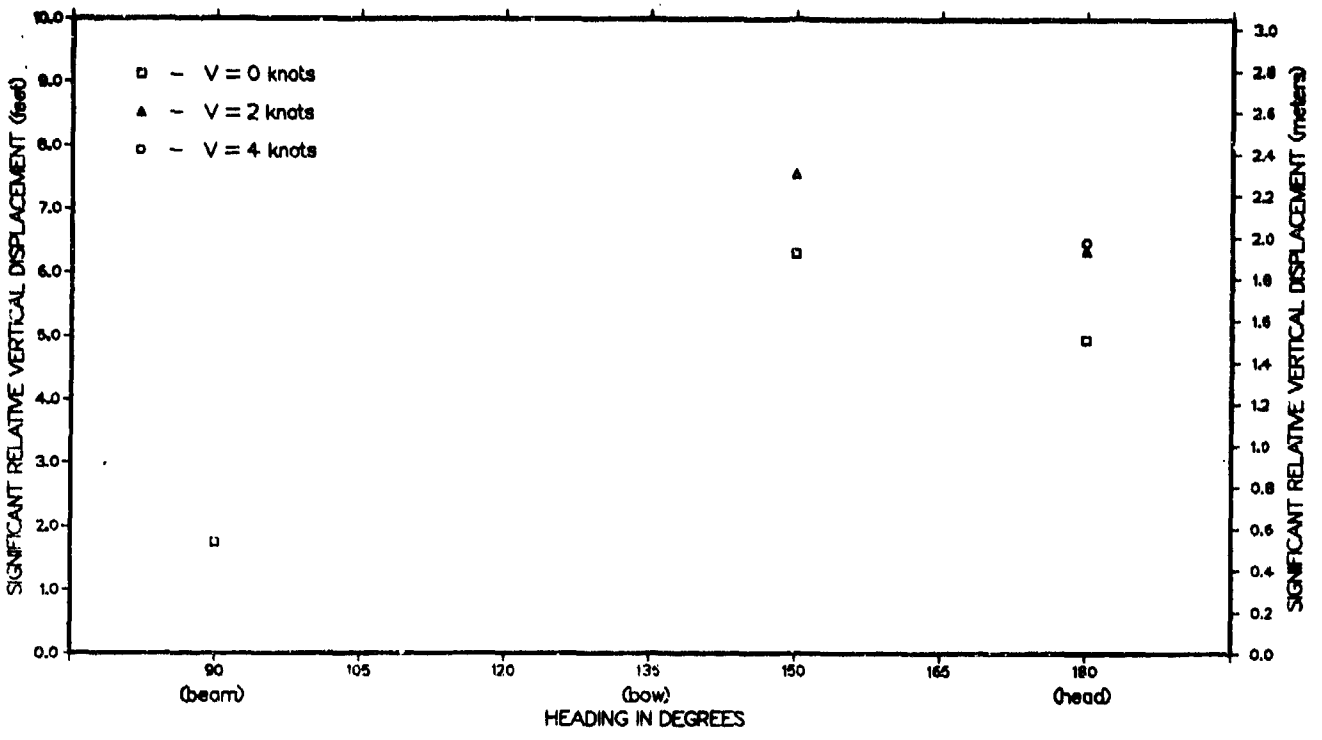

Figure A.11A - Without Ramp and Causeway Ferry Connected

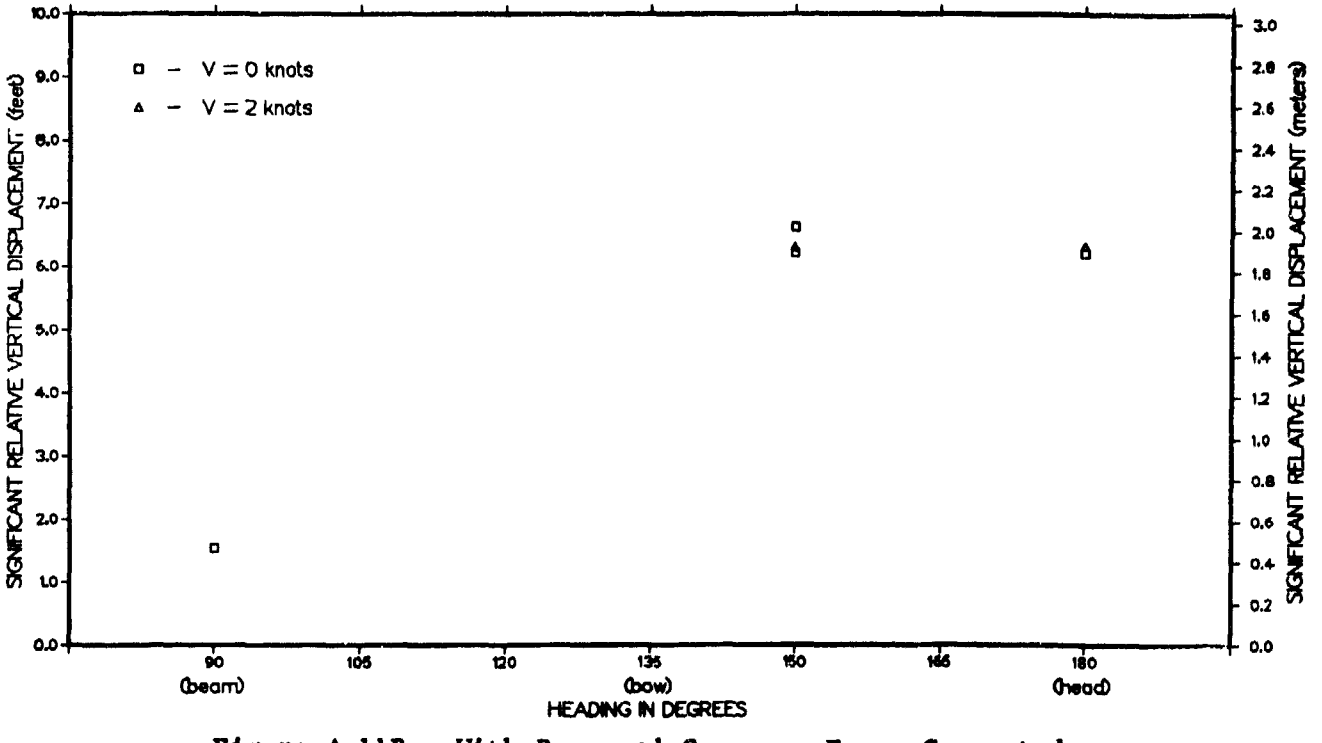

Figure A.11B - With Ramp and Causeway Ferry Connected

Figure A.12 - Significant Double Amplitude of Heave of the RO/RO Ship in Sea State 3 with Swell Superimposed

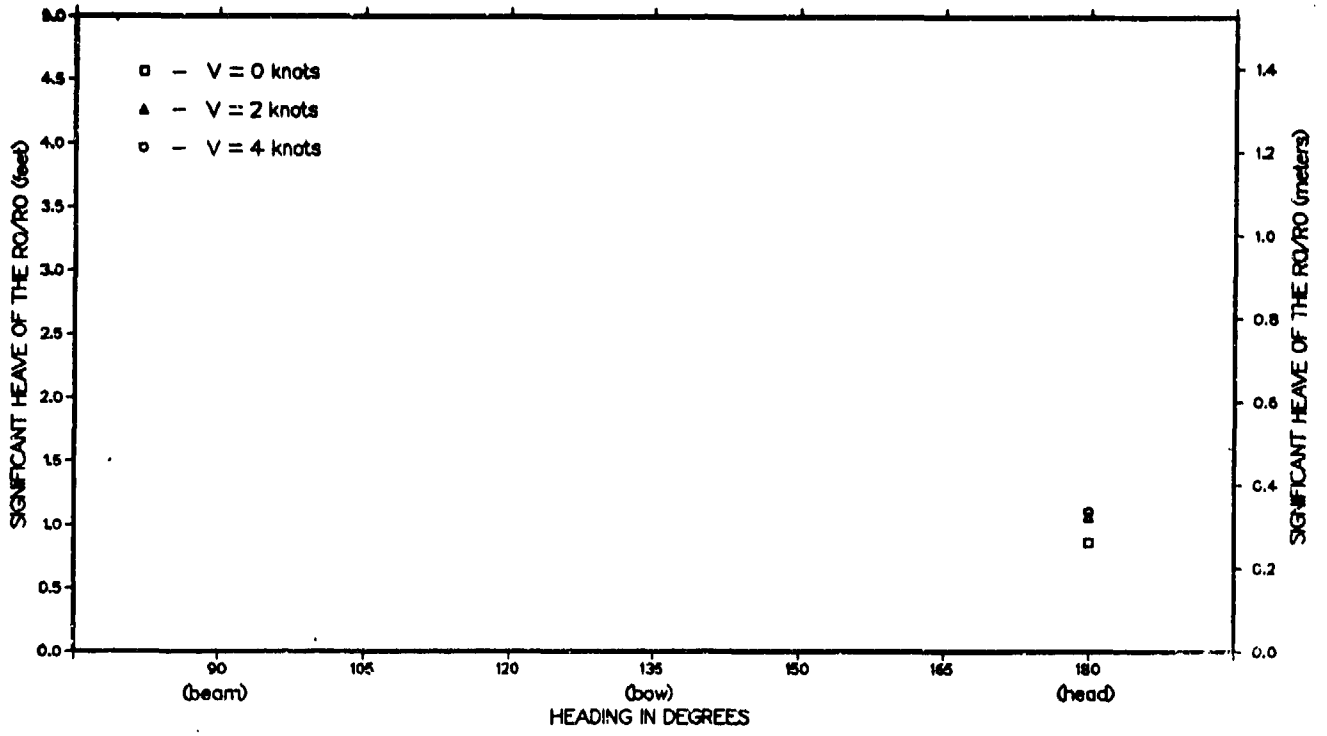

Figure A.12A - Without Ramp and Causeway Ferry Connected

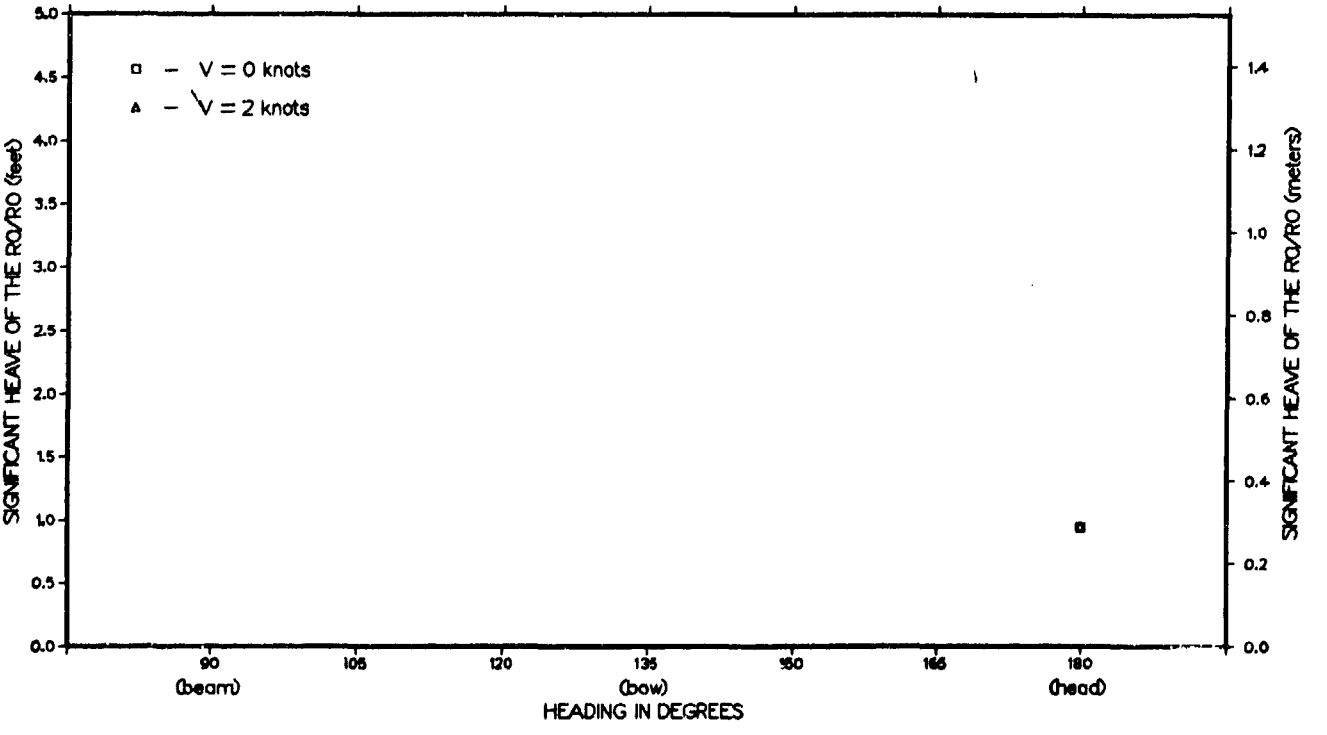

Figure A.12B - With Ramp and Causeway Ferry Connected

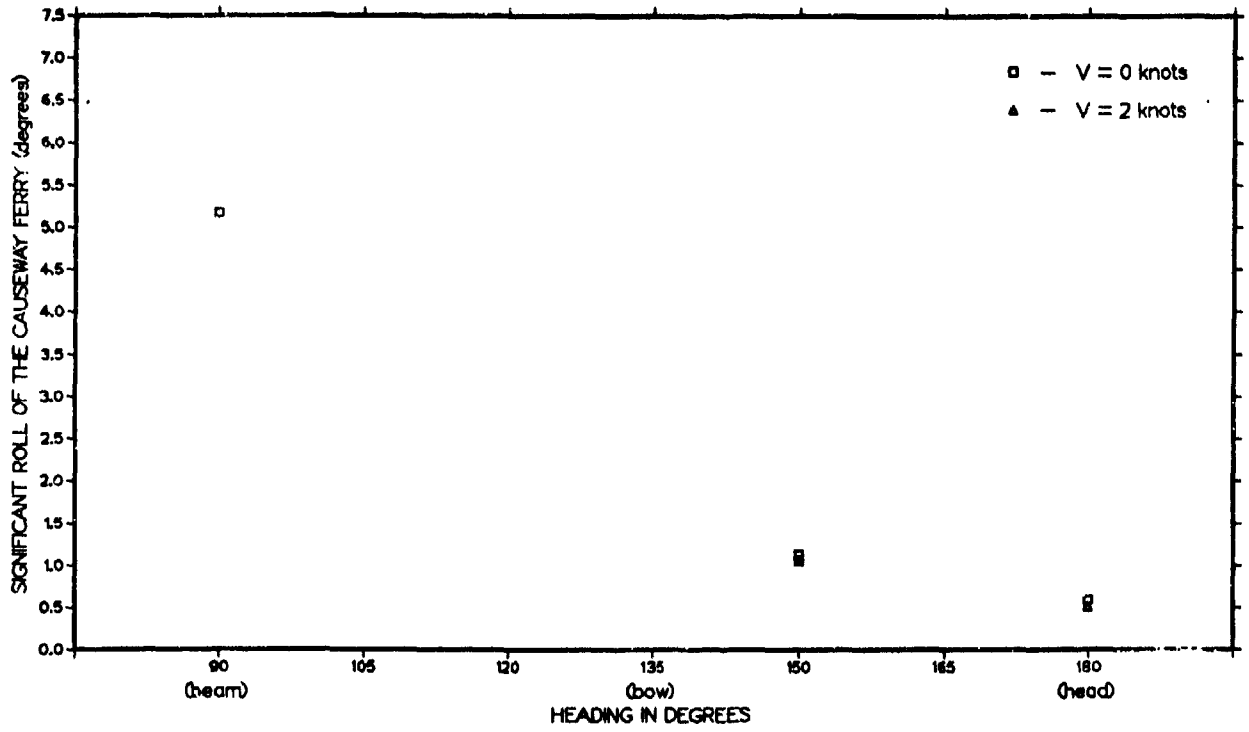

Figure A.13 - Significant Double Amplitude of Roll of the Causeway Ferry in Sea State 3 with Swell Superimposed

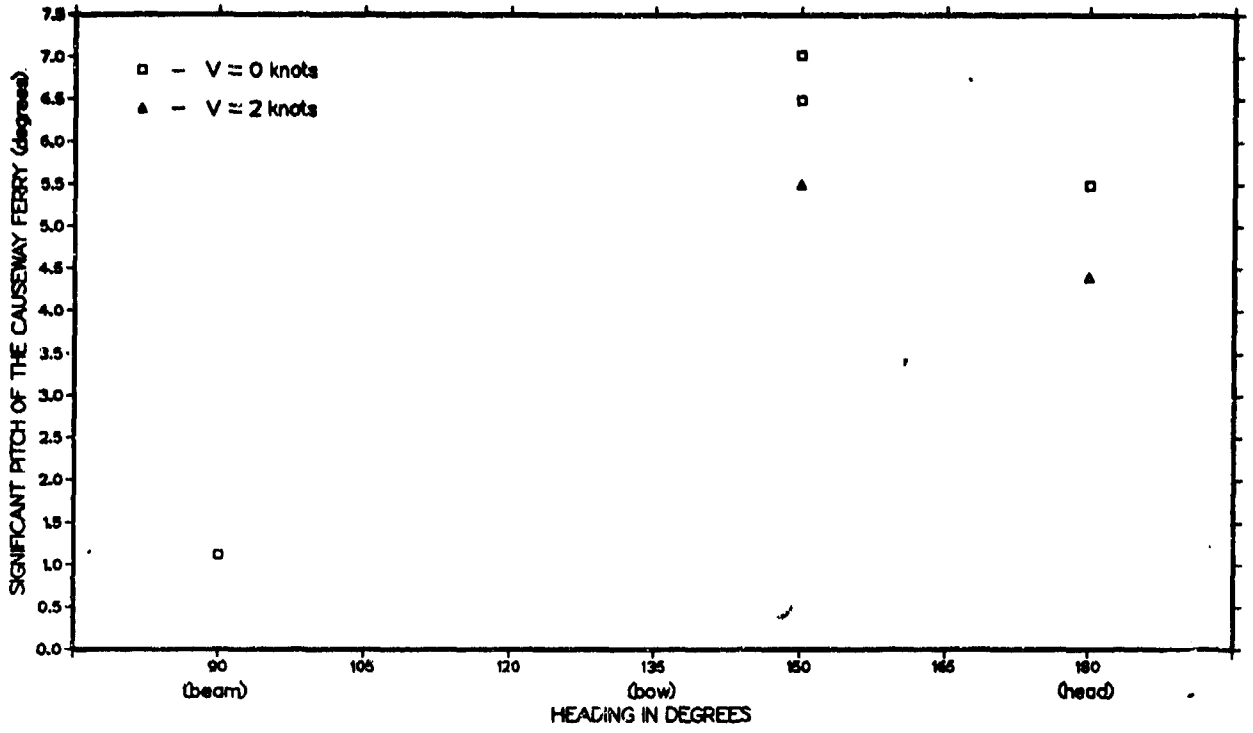

Figure A.14 - Significant Double Amplitude of Pitch of the Causeway Ferry in Sea State 3 with Swell Superimposed

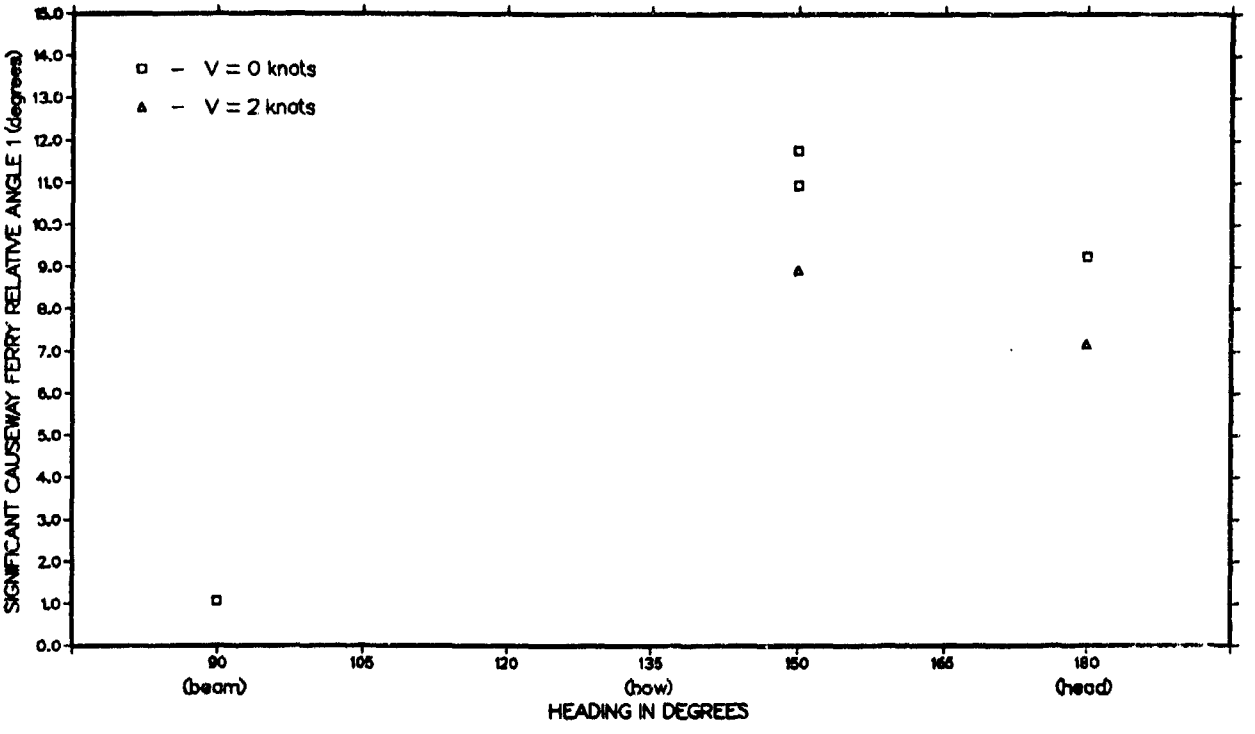

Figure A.15 - Significant Double Amplitude of Relative Angular Displacement at the Junction Between the Causeway Platform Facility and Causeway Ferry in Sea State 3 with Swell Superimposed

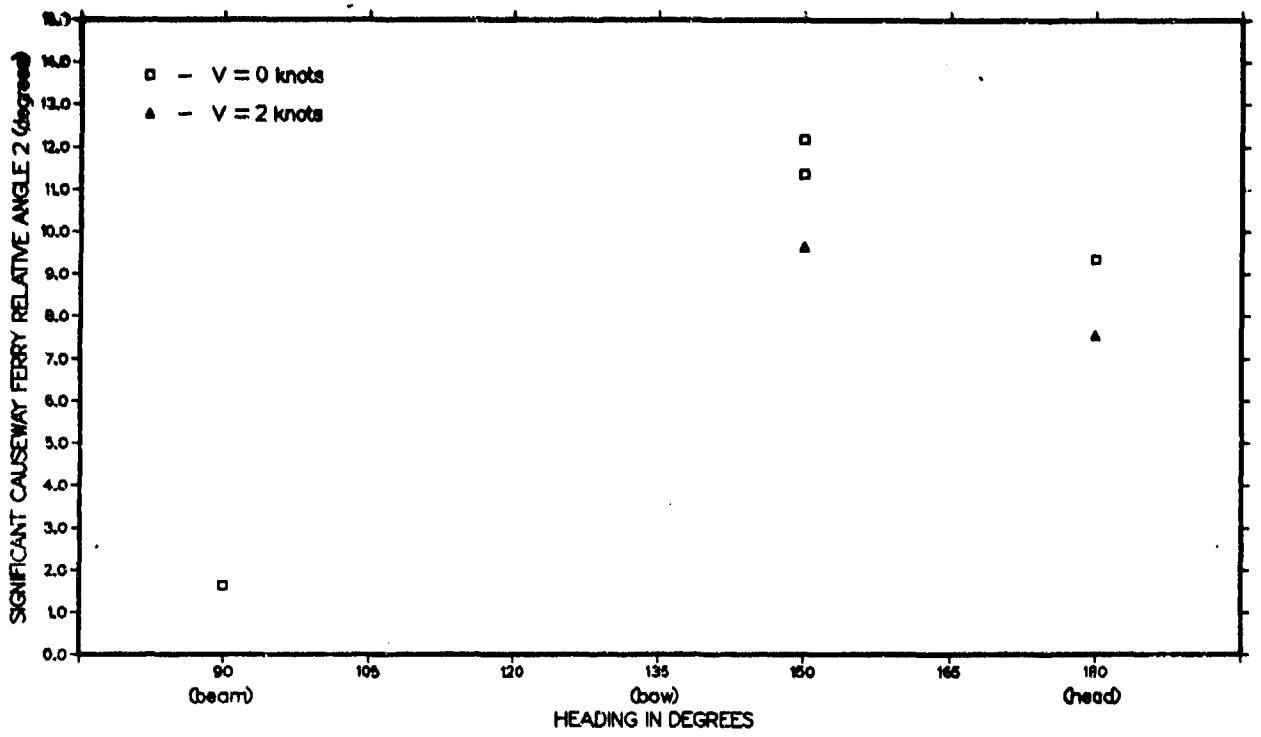

Figure A.16 - Significant Double Amplitude of Relative Angular Displacement at the Junction Between the First and Second Sections of the Causeway Ferry in Sea State 3 with Swell Superimposed

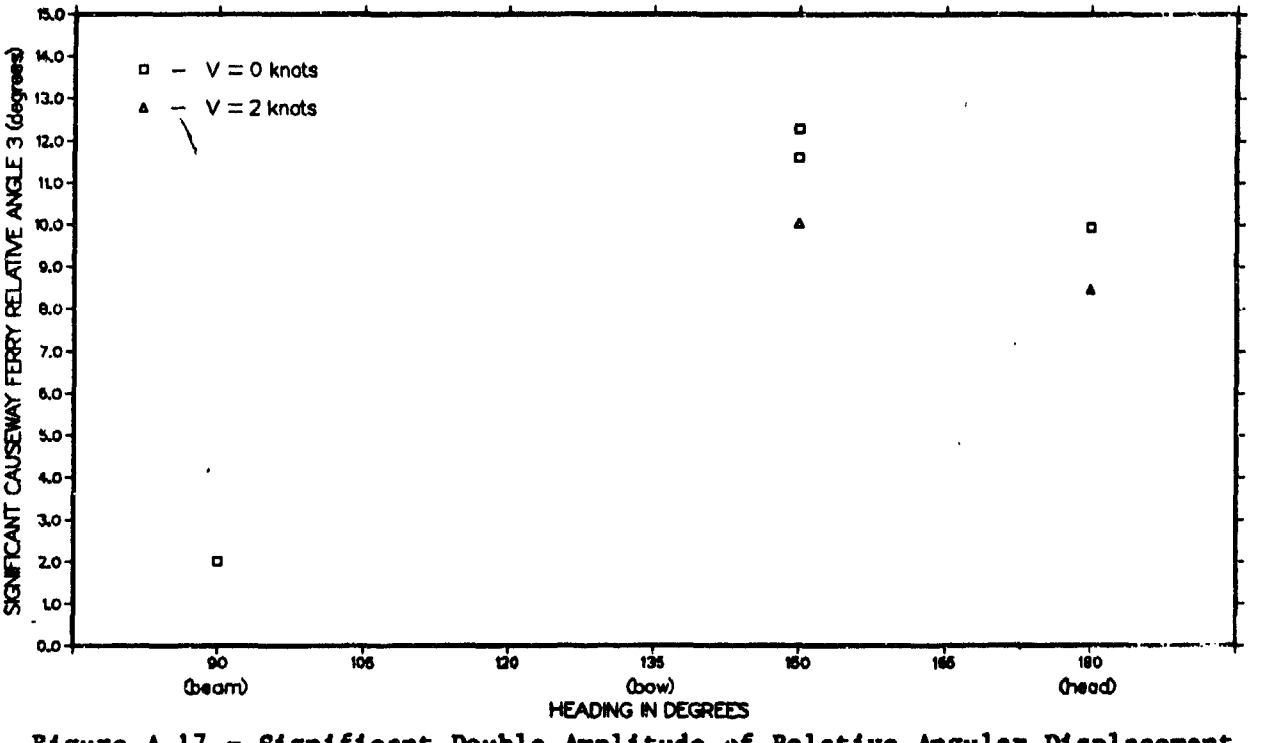

Figure A.17 - Significant Double Amplitude of Relative Angular Displacement at the Junction Between the Second and Third Sections of the Causeway Ferry in Sea State 3 with Swell Superimposed

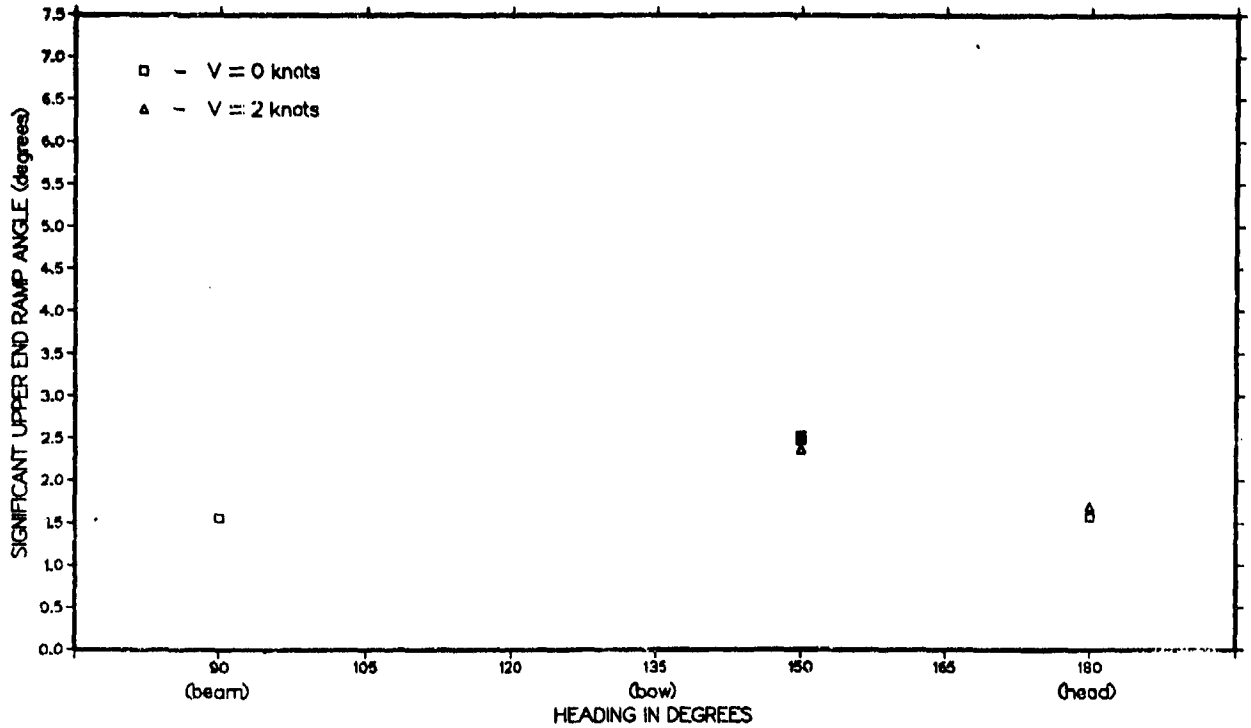

Figure A.18 - Significant Double Amplitude of Relative Angular Displacement at the Upper End of the Off-loading Ramp in Sea State 3 with Swell Superimposed

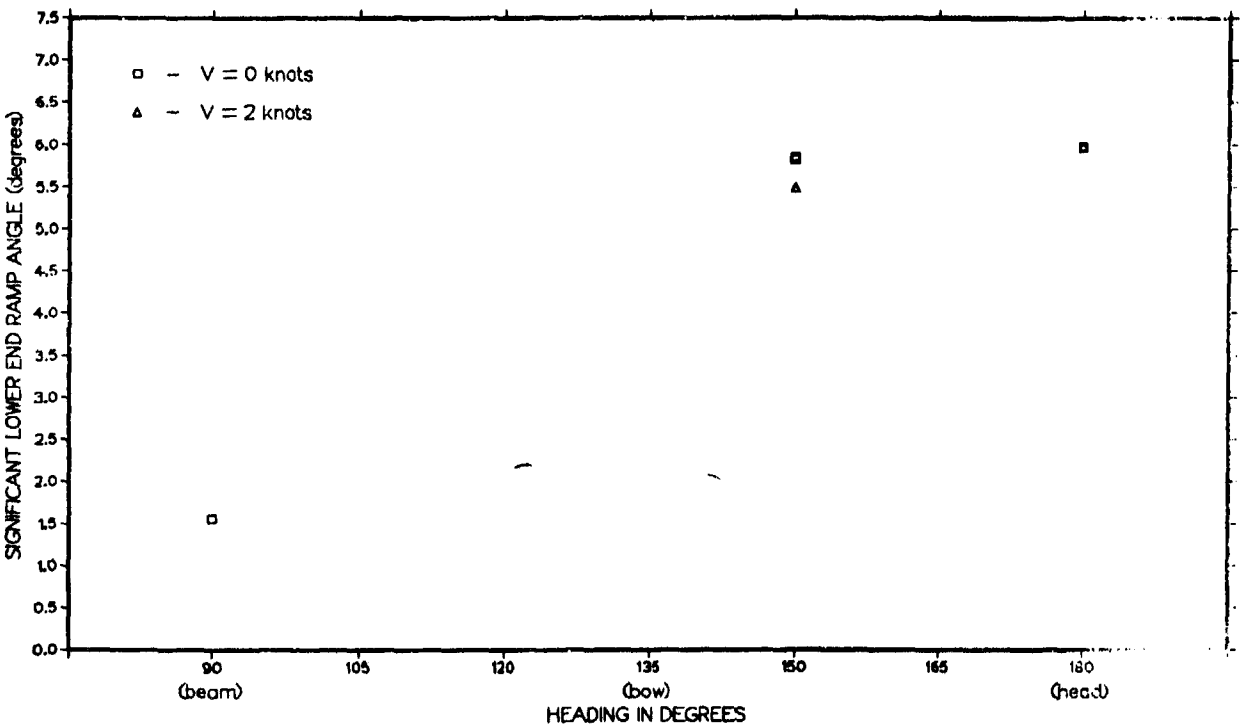

Figure A.19 - Significant Double Amplitude of Relative Angular Displacement at the Lower End of the Off-loading Ramp in Sea State 3 with Swell Superimposed

DTNSRDC ISSUES THREE TYPES OF REPORTS

1. DTNSRDC REPORTS, A FORMAL SERIES, CONTAIN INFORMATION OF PERMANENT TECHNICAL VALUE. THEY CARRY A CONSECUTIVE NUMERICAL IDENTIFICATION REGARDLESS OF THEIR CLASSIFICATION OR THE ORIGINATING DEPARTMENT.

2. DEPARTMENTAL REPORTS, A SEMIFORMAL SERIES, CONTAIN INFORMATION OF A PRELIMINARY, TEMPORARY, OR PROPRIETARY NATURE OR OF LIMITED INTEREST OR SIGNIFICANCE. THEY CARRY A DEPARTMENTAL ALPHANUMERICAL IDENTIFICATION.

3. TECHNICAL MEMORANDA, AN INFORMAL SERIES, CONTAIN TECHNICAL DOCUMENTATION OF LIMITED USE AND INTEREST. THEY ARE PRIMARILY WORKING PAPERS INTENDED FOR INTERNAL USE. THEY CARRY AN IDENTIFYING NUMBER WHICH INDICATES THEIR TYPE AND THE NUMERICAL CODE OF THE ORIGINATING DEPARTMENT. ANY DISTRIBUTION OUTSIDE DTNSRDC MUST BE APPROVED BY THE HEAD OF THE ORIGINATING DEPARTMENT ON A CASE-BY-CASE BASIS.